

AD-A168 618

TOPICAL MEETING ON MICROPHYSICS OF SURFACES BEAMS AND  
ADSORBATES HELD AT. (U) OPTICAL SOCIETY OF AMERICA  
WASHINGTON D C J W QUINN 18 DEC 85 AFOSR-TR-86-0389

1/2

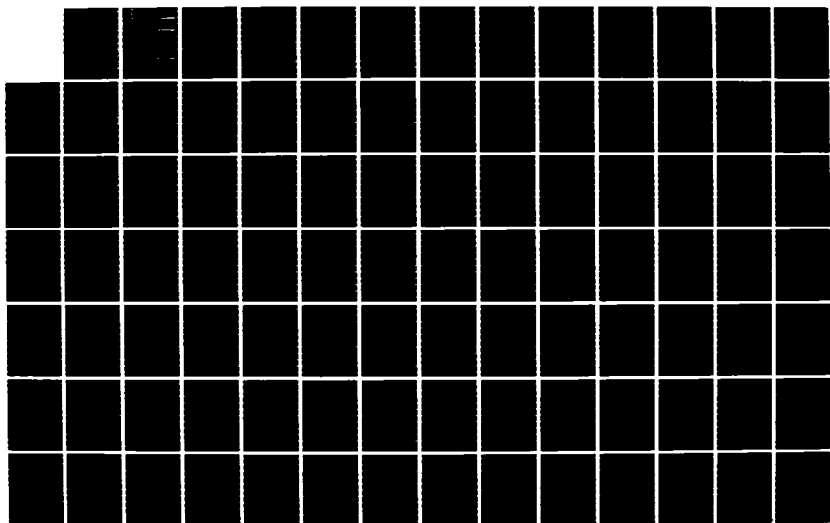
UNCLASSIFIED

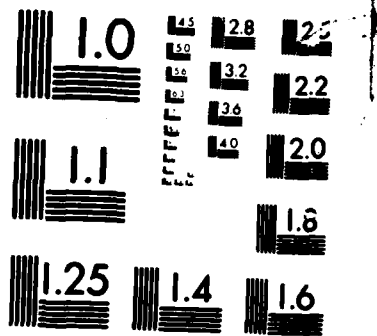
AFOSR-85-0018

F/B

7/3

NL





MICROCOPY CHART

AD-A168 618

AFOSR-TR- 86-0309

21

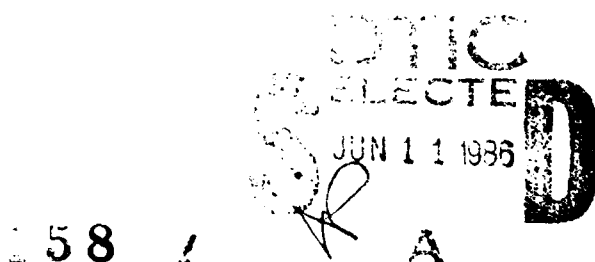
TOPICAL MEETING ON  
**MICROPHYSICS OF SURFACES,  
BEAMS, AND ADSORBATES**

OFFICE FILE COPY

**TECHNICAL  
DIGEST**

SANTA FE, NEW MEXICO  
FEBRUARY 4-6, 1985

Approved for public release;  
distribution unlimited.



58

A

Unclassified

SECURITY CLASSIFICATION OF THIS PAGE

2

## REPORT DOCUMENTATION PAGE

1a. REPORT SECURITY CLASSIFICATION Unclassified		1b. RESTRICTIVE MARKINGS n/a									
2a. SECURITY CLASSIFICATION AUTHORITY		3. DISTRIBUTION/AVAILABILITY OF REPORT Approved for public release; Distribution unlimited									
2b. DECLASSIFICATION/DOWNGRADING SCHEDULE											
4. PERFORMING ORGANIZATION REPORT NUMBER(S)		5. MONITORING ORGANIZATION REPORT NUMBER(S) <b>AFOSR-TR- 86-0309</b>									
6a. NAME OF PERFORMING ORGANIZATION Optical Society of America	6b. OFFICE SYMBOL (if applicable)	7a. NAME OF MONITORING ORGANIZATION AFOSR/NC									
6c. ADDRESS (City, State and ZIP Code) 1816 Jefferson Place, N.W. Washington, D.C. 20036	7b. ADDRESS (City, State and ZIP Code) Bldg. 410 Bolling AFB D.C. 20332										
8a. NAME OF FUNDING/SPONSORING ORGANIZATION AFOSR	8b. OFFICE SYMBOL (if applicable) NC	9. PROCUREMENT INSTRUMENT IDENTIFICATION NUMBER AFOSR-85-0018									
10a. ADDRESS (City, State and ZIP Code) Bldg. 410 Bolling AFB 20332	10. SOURCE OF FUNDING NOS. <table border="1"> <tr> <th>PROGRAM ELEMENT NO.</th> <th>PROJECT NO.</th> <th>TASK NO.</th> <th>WORK UNIT NO.</th> </tr> <tr> <td>61102F</td> <td>2303</td> <td>A2</td> <td></td> </tr> </table>			PROGRAM ELEMENT NO.	PROJECT NO.	TASK NO.	WORK UNIT NO.	61102F	2303	A2	
PROGRAM ELEMENT NO.	PROJECT NO.	TASK NO.	WORK UNIT NO.								
61102F	2303	A2									
11. TITLE (Include Security Classification) Topical Meeting on the		12. PERSONAL AUTHOR(S) Microphysics of Surfaces, Beams, and Adsorbates Quinn, Jarus W.									
13a. TYPE OF REPORT Final	13b. TIME COVERED FROM 01 Nov 84 to 8 Dec 85	14. DATE OF REPORT (Yr. Mo. Day) 85 12 18	15. PAGE COUNT <del>229</del> 120								
16. SUPPLEMENTARY NOTATION <i>Technical Digest</i>											
17. COSATI CODES		18. SUBJECT TERMS (Continue on reverse if necessary and identify by block number)									
FIELD	GROUP	SUB. GR.									
19. ABSTRACT (Continue on reverse if necessary and identify by block number) The Topical Meeting on Microphysics of Surfaces, Beams, and Adsorbates was organized within the interdisciplinary area of molecule/surface interactions induced, or studied, by laser-and ion-beam techniques. Especially emphasized was the molecular physics and electro-magnetism of beam-activated chemical reactions for applications in fabrication of semiconductor devices, in photocatalysis, and in optical recording. Emphasis was on the laser spectroscopy of molecular-collision and reaction processes on surfaces, new sensitive or high-resolution spectroscopies for studies of adsorbates, and optical methods applied to surface characterization.											
20. DISTRIBUTION/AVAILABILITY OF ABSTRACT UNCLASSIFIED/UNLIMITED <input checked="" type="checkbox"/> SAME AS RPT. <input checked="" type="checkbox"/> DTIC USERS <input type="checkbox"/>		21. ABSTRACT SECURITY CLASSIFICATION Unclassified									
22a. NAME OF RESPONSIBLE INDIVIDUAL Francis J. Wodarczyk		22b. TELEPHONE NUMBER (Include Area Code) 767-4963	22c. OFFICE SYMBOL NC								

DTIC  
ELECTRONIC  
JUN 11 1986

# **TOPICAL MEETING ON**

## **MICROPHYSICS OF SURFACES,**

## **BEAMS, AND ADSORBATES**

**A digest of technical papers presented at the Topical Meeting on Microphysics of Surfaces, Beams, and Adsorbates, February 4-6, 1985, Santa Fe, New Mexico.**

*Cosponsored by*

**Air Force Office of Scientific Research**

**American Vacuum Society**

**and**

**Optical Society of America**

*Approved for public release,  
distribution unlimited*

Classification	Approved for
Controlled	ALL
Declassify	BY DATE
Declassify	BY EVENT
Declassify	BY FUNCTION
Declassify	BY LEVEL
Declassify	BY PRIORITY
Declassify	BY SPECIAL
Declassify	BY SPECIAL



## MONDAY, FEBRUARY 4, 1985

### NEW MEXICO ROOM

#### 7:50-8:00 AM OPENING REMARKS

Daniel Ehrlich, *Chairman*  
MIT Lincoln Laboratory

#### 8:00-9:30 AM SESSION I

J. Greene, *President*  
University of Illinois at Urbana

#### 8:00 AM MA1

**Ion-Enhanced Processes in Etching of Silicon**, T. M. Mayer, M. S. Ameen, E. L. Barish, D. J. Vithavage, T. Mizutani, *U. North Carolina*. A case study of the ion-enhanced etching of silicon by chlorine is reviewed as a prototype for a class of ion-enhanced etching reactions. Aspects of reactant absorption, surface modification by ion mixing, product formation, and product removal from the surface are addressed. *(Invited Paper)*

#### 8:30 AM MA2

**Influence of Ion Bombardment on Etching Reactions**, Harold F. Winters, John W. Coburn, *IBM Research Laboratory*. This paper shows how experimental data on the etching of several materials fits into a conceptual framework which is believed to be a general description of a variety of etching reactions. *(Invited Paper)*

#### 9:00 AM MA3

**Study on the Mechanism of Ion-Assisted Etching**, F. H. M. Sanders, *Philips Research Laboratories, The Netherlands*. The reaction of silicon with chlorine under simultaneous exposure to an argon-ion beam has been studied using mass spectrometry combined with time-of-flight techniques. *(Invited Paper)*

### SANTA FE ROOM

#### 9:30-10:00 AM COFFEE BREAK

### NEW MEXICO ROOM

#### 10:00 AM-12:00 M SESSION II

D. Flamm, *President*  
AT&T Bell Laboratories

#### 10:00 AM MB1

**Energy Distributions of Electronically Excited Molecules Produced by Ion Bombardment of Silicon**, R. Walkup, Phaedon Avouris, *IBM T. J. Watson Research Center*. Optical studies and model calculations of energy distributions of molecules produced by ion bombardment of silicon are used to determine the sputtering mechanism.

## MONDAY, FEBRUARY 4, 1985—Continued

#### 10:20 AM MB2

**Mechanistic Studies of Low-Enhanced Etching of Electronic Materials by Modulated-Beam Mass Spectrometry**, M. Balooch, D. R. Olander, W. J. Siekhaus, *U. California, Berkeley*.

#### 10:40 AM MB3

**Simultaneous Exposure of SiO<sub>2</sub> and ThF<sub>4</sub> to XeF<sub>6</sub> and Energetic Electrons**, M. A. Loudiana, J. T. Dickinson, *Washington State U*. The consequences (sorption, desorption) from exposure of thin films of SiO<sub>2</sub> and ThF<sub>4</sub> to gaseous XeF<sub>6</sub> and energetic electrons (100–2000 eV) are examined.

#### 11:00 AM MB4

**Ablation of Organic Polymers by UV and Visible Radiation: A Theoretical Approach**, Barbara J. Garrison, *Pennsylvania State U*; R. Srinivasan, *IBM T. J. Watson Research Center*. Two microscopic models which describe the interaction of UV radiation and visible radiation with organic polymers will be described. The photochemical model for UV radiation predicts cleanly etched pits which exhibit no melting.

#### 11:20 AM MB5

**Laser Interferometry and Laser-Induced Fluorescence Studies of Laser Etching**, R. W. Dreyfus, R. Walkup, J. M. Jasinski, *IBM T. J. Watson Research Center*. We report LIF measurements of energy distributions of atoms and molecules produced during excimer laser ablation. Results are correlated with interferometric measurements of plasma density.

#### 11:40 AM MB6

**Direct-Writing in Self-Developing Resists Using Low-Power, cw, UV Light**, J. E. Bjorkholm, L. Eichner, J. C. White, R. E. Howard, *AT&T Bell Laboratories*; H. G. Craighead, *Bell Communications Research*. Direct writing of micron-sized features in self-developing photoresists is demonstrated using less than 1 mW of cw UV light at 257 nm. No threshold for self-development is observed.

**MONDAY, FEBRUARY 4, 1985—Continued**

**NEW MEXICO ROOM**

**7:30-9:30 PM SESSION III**

*S. Brueck, Presider  
MIT Lincoln Laboratory*

**7:30 PM MC1**

**Raman Characterization of Catalysts**, A. Wokaun, A. Baiker, W. Fluhrl, M. Meier, S. K. Miller, *Swiss Federal Institute of Technology, Switzerland*. Surface-enhanced Raman scattering is emerging as a powerful tool for mechanistic investigations in heterogeneous catalysis as illustrated for reactions of amines on metallic copper catalysts. *(Invited Paper)*

**8:00 PM MC2**

**Surface Raman Spectroscopy Without Enhancement**, Alan Campion, *U. Texas at Austin*. Raman spectroscopy of molecules adsorbed on single crystal surfaces without surface or resonance enhancement and applications in surface science are discussed. *(Invited Paper)*

**8:30 PM MC3**

**Surface Coherent Raman Spectroscopy**, W. M. Hetherington, N. E. Van Wych, E. W. Koenig, Z. Z. Ho, G. I. Stegeman, R. M. Fortenberry, R. Moshrefzadi, *U. Arizona*. Surface coherent Raman scattering has been performed on dielectric surfaces with submonolayer sensitivity using incident and scattered fields in the form of guided waves.

**8:50 PM MC4**

**High-Resolution Electron Energy Loss Spectroscopy of Molecular Bond Weakening on Potassium Promoted Ru(001)**, F. M. Hoffmann, R. A. dePaola, *Exxon Research & Engineering Company*. Vibrational studies reveal drastic differences in molecular bondweakening for adsorbed nitrogen and CO on potassium promoted Ru(001). Differences in molecular structure account for this behavior.

**9:10 PM MC5**

**Photophysical Studies of DAQ on Silica and Aluminum Oxides: a Molecular Probe of Surface Heterogeneity**, J. M. Drake, *Exxon Research & Engineering Company*. The electronic spectroscopic features of 1,4 dihydroxyanthraquinone adsorbed to specific surface sites of silica are strongly perturbed by the polarizable nature of the local surface site environment.

**TUESDAY, FEBRUARY 5, 1985**

**NEW MEXICO ROOM**

**8:00-9:40 AM SESSION IV**

*K. Wittig, Presider  
U. Southern California*

**8:00 AM TuA1**

**Photodesorption and Adsorbate-Surface Interactions Stimulated by Laser Radiation**, T. J. Chuang, *IBM Research Laboratory*. A review is given on laser-stimulated surface processes related to photodesorption, i.e., surface etching and resonantly excited desorption by UV-visible and IR lasers. *(Invited Paper)*

**8:40 AM TuA2**

**Infrared Spectral Electrochemistry of Surface Reactions**, B. Stanley Pons, *U. Utah*. *In-situ* IR vibrational spectroscopy of the electrode/solution interface allows the study of electrode-adsorbed species through several interaction mechanisms. *(Invited Paper)*

**9:20 AM TuA3**

**Pulsed-Laser Atom-Probe Study of H<sub>2</sub>, N<sub>2</sub>, and NH<sub>3</sub> Formation on Metal Surfaces**, T. T. Tsong, C. F. Ai, Wu Liu, *Pennsylvania State U.* Formation of H<sub>2</sub>, N<sub>2</sub>, and NH<sub>3</sub> on ~20 metal surfaces has been studied. Desorption sites can be revealed with atomic resolution by a time gating technique.

**SANTA FE ROOM**

**9:40-10:10 AM COFFEE BREAK**

**NEW MEXICO ROOM**

**10:10 AM-12:10 PM SESSION V**

*L. Brillson, Presider  
Xerox Corporation*

**10:10 AM TuB1**

**Selective Laser-Stimulated Desorption of Molecules by Internal Vibration Excitation**, C. Jedrzejek, *Texas A&M U.* Accounting for anharmonicity of the internal vibration in the LSD internal vibration excitation model produces larger threshold photodesorption rates than in previous theoretical work.

**10:30 AM TuB2**

**Time-Resolved Kinetic Studies of Molecular Decomposition on Ni(100) Using Laser-Induced Desorption**, S. J. Bares, R. B. Hall, *Exxon Research & Engineering Company*. The first application of laser-induced desorption to the study of chemical kinetics on surfaces is reported. Decomposition studies of CH<sub>3</sub>OH and C<sub>2</sub>H<sub>4</sub> are described.

## TUESDAY, FEBRUARY 5, 1985—Continued

10:50 AM TuB3

**Excitation of Interacting Adatoms and Surface-Dressed Bloch Equation**, Jui-teng Lin, *Naval Research Laboratory*. Nonlinear surface-dressed Bloch equation of two-level interacting adatoms is derived from a microscopic Hamiltonian. A proposed experimental setup is analyzed.

11:10 AM TuB4

**Technique for Measuring Surface Diffusion by Laser-Beam-Localized Surface Photochemistry**, H. J. Zeiger, D. J. Ehrlich, *MIT Lincoln Laboratory*; J. Y. Tsao, *Sandia National Laboratories*. A technique has been developed for determining the surface diffusivity of a weakly bound adsorbate by measuring the kinetics of a spatially localized laser-beam-driven surface photoreaction. This technique has been used to determine the surface diffusivity of tetraethyl lead molecules adsorbed on sapphire from data on the deposition of thin films by photolysis of these molecules. The technique should be broadly applicable to the measurement of the surface diffusion of weakly bound or fragile polyatomic molecules.

11:30 AM TuB5

**Characterization of Photochemical Processing**, Masatake Hirose, *Hirosima U., Japan*. Photochemical etching processes of  $\text{SiO}_2$  in  $\text{NF}_3$  plus  $\text{H}_2$  gas and  $\text{GaAs}$  in  $\text{Cl}_2$ , using ArF excimer laser by *in-situ* x-ray photo-electron spectroscopy. (Invited Paper)

## NEW MEXICO ROOM

7:30-9:30 PM SESSION VI

F. Pease, *President*  
*Stanford U.*

7:30 PM TuC1

**Recent Experiments on Photolysis for Low Temperature Epitaxy**, S. J. C. Irvine, J. Giess, J. B. Mullin, G. W. Blackmore, O. D. Dossesr, *Royal Signals and Radar Establishment, U.K.* The epitaxial growth of  $\text{HgTe}$  and related materials is reviewed, with special attention given to surface reactions and assessment of the layer quality. (Invited Paper)

8:00 PM TuC2

**Mechanisms of MOVPE and Routes to a UV-Assisted Process**, J. Haigh, *British Telecom Research Laboratories, U.K.* The potential use of UV for enhancement of MOVPE deposition of III-V compounds is considered from the viewpoint of the mechanisms of MOVPE. (Invited Paper)

## TUESDAY, FEBRUARY 5, 1985—Continued

8:30 PM TuC3

**Studies of Laser Chemical Vapor Deposition Using Surface Sensitive IR Photoacoustic Spectroscopy**, G. S. Higashi, L. J. Rothberg, C. G. Fleming, *AT&T Bell Laboratories*. We report vibrational spectra of surface adsorbates during Al film nucleation on single crystal sapphire substrates stimulated by laser (KrF) photodecomposition of trimethylaluminum.

8:50 PM TuC4

**Laser-Induced Selective Deposition of Micron-size Structures on Silicon by Surface Reduction of Tungsten Hexafluoride**, Y. S. Liu, C. P. Yakymyshyn, H. R. Philipp, H. C. Cole, L. M. Levinson, *General Electric Research & Development Center*. Selective deposition of refractory metal and metal silicide on silicon, induced by a focused argon laser beam, is reported. Micron-size lines with extremely good surface smoothness were observed at a writing speed of 7 cm/sec. Deposition mechanism and properties of fine structures are discussed.

9:10 PM TuC5

**Laser-Initiated Dry Etching of  $\text{SiO}_2$** , Jack O. Chu, George W. Flynn, Peter D. Brewer, Richard M. Osgood, Jr., *Columbia U.* Photochemical etching of thermally grown (masked)  $\text{SiO}_2$  on Si substrates has been achieved by ArF excimer laser photolysis of  $\text{CH}_2\text{CHF}$ . Infrared fluorescence and (high vibrational resolution) diode absorption techniques are employed to study the gas-phase UV-initiated chemical etching of  $\text{SiO}_2$ .

## WEDNESDAY, FEBRUARY 6, 1985

### **NEW MEXICO ROOM**

#### **8:00-9:40 AM SESSION VII**

*P. Liao, Presider*

*Bell Communications Research*

##### **8:00 AM WA1**

**Interface Studies by Optical Second Harmonic Generation,** Y. R. Shen, *UC-Berkeley*. Applications of optical second harmonic generation to studies of molecular adsorption at air/solid, liquid/solid, air/liquid, and vacuum/solid interfaces are discussed. *(Invited Paper)*

##### **8:40 AM WA2**

**Real-Time Monitoring of Surface Reactions on Si(111) by Optical Second Harmonic Generation,** T. F. Heinz, M. M. T. Loy, W. A. Thompson, *IBM T. J. Watson Research Center*. The technique of optical second harmonic generation has been used to study oxidation and Pd-silicide formation on Si(111)-7 x 7 surfaces.

##### **9:00 AM WA3**

**Second Harmonic Generation Studies of Adsorption and Reorientation at Electrode Surfaces,** D. F. Voss, M. Nagumo, L. S. Goldberg, *Naval Research Laboratory*; K. A. Bunding, *Georgetown U.* Second harmonic generation at silver and gold electrodes has been used to study the adsorption and reorientation of organic additives in aqueous solution. Information about both active and nonactive organic species has been obtained using this highly surface-specific technique.

##### **9:20 AM WA4**

**Time-Resolved Vibrational Energy Relaxation of Surface Adsorbates,** E. J. Heilweil, M. P. Casassa, R. R. Cavanagh, J. C. Stephenson, *NBS Center for Chemical Physics*. Measurements of picosecond vibrational population decay of chemisorbed species on colloidal silica and other oxide surfaces in various chemical environments are presented.

### **SANTA FE ROOM**

#### **9:40-10:10 AM COFFEE BREAK**

## WEDNESDAY, FEBRUARY 6, 1985—Continued

### **NEW MEXICO ROOM**

#### **10:10 AM-12:10 PM SESSION VIII**

*K. Kompa, Presider*

##### **10:10 AM WB1**

**Survival of vibrationally excited Nitric Oxide Scattered from LiF(100) Surface: Angular and Velocity Analysis,** J. Misewich, H. Zacharias, M. M. T. Loy, *IBM T. J. Watson Research Center*. We report the first observation of vibrationally excited NO molecules scattered from freshly cleaved LiF(100) surface. Final-state selective angular and velocity distributions are also presented.

##### **10:30 AM WB2**

**Electroreflectance Vibrational Spectroscopy: Theory and Measurement of the Stark Effect of CO on Ni(100),** D. K. Lambert, *General Motors Research Laboratories*. Electroreflectance vibrational spectroscopy (EVS) is used to measure the Stark tuning rate of CO on Ni(100). The Stark effect of adsorbate vibrations is also discussed.

##### **10:50 AM WB3**

**Diffusion and Reaction in Tortuous Structures as Modeled by Fractals,** J. Klafter, J. M. Drake, *Exxon Research & Engineering Company*. We model tortuous structures through the fractal concept and study diffusion and reaction of adsorbates on these structures. Results concerning silica-gel surfaces and Vycor-glass are discussed.

##### **11:10 AM WB4**

**Electronic Spectroscopy and Relaxation Dynamics of Adsorbates on Metal Surfaces,** Phaedon Avouris, *IBM T. J. Watson Research Center*. We present experimental and theoretical results on excited adsorbates on metals. Electronic structure and decay paths are studied, and the implications for surface photoprocesses are discussed.

##### **11:30 PM WB5**

**Molecule Surface Interaction Dynamics by Laser,** Herbert Walther, *Max-Planck-Institut für Quantenoptik, F. R. Germany*. Laser-induced fluorescence and resonance ionization in combination with time-of-flight measurements of molecules scattered from clean surfaces give a new and complete insight into the dynamics of the interaction. *(Invited Paper)*

## WEDNESDAY, FEBRUARY 6, 1985—Continued

### SANTA FE AND CORONADO ROOMS

#### 4:00-5:30 PM POSTER SESSION

##### WC1

**Optical and Electron Probes of the Structure of Surfactant Coated Surfaces.** S. Garoff, R. B. Hall, H. W. Deckman, *Exxon Research & Engineering Company* We have studied the structure of monolayers of adsorbed surfactant molecules and their effect on the wetting properties of the interface. (Poster Paper)

##### WC2

**Above-Bandgap Polarization Anisotropies in Cubic Semiconductors: A Visible-Near-UV Probe of Surfaces.** D. E. Aspnes, *Bell Communications Research* Above-bandgap polarization anisotropies in the near-normal-incidence reflectance spectra of cubic semiconductors show strong contributions from physisorbed molecules, microscopic roughness and anisotropic surface films as well as spatial dispersion in the bulk. (Poster Paper)

##### WC3

**UV-Laser Photodeposition of Patterned Catalyst Films from Adsorbate Mixtures.** D. J. Ehrlich, *MIT Lincoln Laboratory*; J. Y. Tsao, *Sandia National Laboratories*. Efficient catalysts for hydrocarbon polymerization have been prepared photochemically by reaction of mixed  $TiCl_4$  and  $Al_2(CH_3)_6$  adsorbate layers, in the scanned focus of a 257.2-nm laser beam. Monolayer coverages of the photodeposited catalyst have been shown effective for *in situ* patterned polymerization of ethylene and acetylene at room temperature from the vapor-phase organic monomers. Three-micrometer spatial resolution has been obtained in selected-area polymer growth. The chemical kinetics of the mixed-adsorbate reactions and the effects of compositional changes on the catalytic activity of the laser-photodeposited films have been studied. (Poster Paper)

##### WC4

**Chlorine Surface Interaction and Laser-Induced Surface Etching Reactions.** W. Sesselmann, T. J. Chuang, *IBM Research Laboratory*. Laser-induced etching of Si, Ag, and Ni-Fe by chlorine has been studied with ESCA, Auger spectroscopy, and mass spectrometry; reaction mechanisms are discussed. (Poster Paper)

##### WC5

**Mechanism of Trimethylaluminum Chemical Vapor Deposition Studied by Multiphoton Ionization Mass Spectrometric Detection.** D. W. Squire, C. S. Dulcey, M. C. Lin, *Naval Research Laboratory*. Aluminum deposition on a hot substrate surface is studied using multiphoton ionization.  $CH_4$  was detected during deposition. No radical reactions were observed under low-pressure conditions. (Poster Paper)

## WEDNESDAY, FEBRUARY 6, 1985—Continued

##### WC6

**Infrared Laser-Induced Photodesorption and Ultraviolet Laser-Induced Thermal Desorption of Methyl Fluoride from Polycrystalline Copper.** R. Viswanathan, *Beloit College*; I. Hussia, *IBM Research Laboratories*; D. R. Burgess, Jr., P. C. Stair, E. Weitz, *Northwestern U.* Results of  $CO_2$  laser-induced photodesorption and KrF excimer laser-induced thermal desorption of methyl fluoride adsorbed on polycrystalline copper surfaces under UHV are presented. (Poster Paper)

##### WC7

**Quantum Model of Dephasing-Enhanced Laser Desorption.** Jui-teng Lin, *Naval Research Laboratory*; Xi-Yi Huang, Thomas F. George, *U. Rochester*. Laser-induced rates are numerically calculated based on a rate equation which includes the anharmonicity and energy and phase relaxation. A mechanism of dephasing-enhanced desorption is proposed. (Poster Paper)

##### WC8

**Laser-Stimulated Vibrational Excitation of an Adspecies Studied by a Generalized Master Equation.** A. C. Beri, Thomas F. George, *U. Rochester*. Adspecies are shown to absorb energy from a laser and the solid simultaneously for short times. Exact numerical results and two analytic approximations are compared. (Poster Paper)

##### WC9

**Direct Laser Pumping of Adatom-Surface Vibrational Modes.** Merle E. Riley, *Sandia National Laboratories*; Dennis J. Diestler, *Purdue U.* Energy localization in a laser-pumped adatom-surface bond is investigated using exact classical collinear mechanics. Extant theories and physical limitations of the model are discussed. (Poster Paper)

##### WC10

**Second Harmonic Generation Spectroscopy of Molecules Adsorbed on Oxide Surfaces.** N. E. Van Wyck, E. W. Koenig, J. D. Byers, Z. Z. Ho, W. M. Hetherington, *U. Arizona*. Electronic spectra of molecular adsorbate on oxide surfaces have been obtained through the use of the surface-specific technique of second harmonic generation. (Poster Paper)

##### WC11

**Photochemical Deposition of Sn for *In-Situ* Selected Area of Doping of MBE GaAs (001) Epilayers.** Steven P. Kowalczyk, D. L. Miller, *Rockwell International Corporation*. The suitability of tetramethyltin and stannic chloride as tin sources for *in-situ* selected area doping of MBE GaAs was evaluated by XPS and AES studies of their adsorption, desorption, and UV photolysis characteristics. C-V and SIMS were used to characterize the tin incorporation. (Poster Paper)

## **WEDNESDAY, FEBRUARY 6, 1985—Continued**

### **WC12**

**Large Modification of the Surface-Enhanced Raman Scattering of Pyridine on Ag Surfaces by Pd Submonolayers**, T. Lopez-Rios, Y. Gao, *Laboratoire d'Optique des Solides, France*. The Raman scattering of pyridine on quenched or island Ag films is strongly reduced by Pd submonolayer coverages. (Poster Paper)

### **WC13**

**Doppler-Shift Laser Fluorescence Spectroscopy of Sputtered and Evaporated Atoms under Argon Ion Bombardment**, W. Husinsky, G. Betz, I. Grgis, *Technische Universität Wien, Austria*. By DSLFS the energy and state distribution of sputtered and evaporated chromium, zirconium, and calcium atoms has been studied as a function of oxygen coverage. (Poster Paper)

## **SANTE FE AND CORONADO ROOMS**

**5:30-7:30 PM MEXICAN BUFFET**

## **NEW MEXICO ROOM**

**7:30-9:30 PM SESSION X**

*E. Wolfe, Presider  
Cornell University*

### **7:30 PM WD1**

**Atomic-Resolution Dynamics by Electron Microscopy**, David J. Smith, *Arizona State U*. Atomic-level resolution is now directly obtainable with latest electron microscopes: this paper will summarize recent advances and review observations showing atomic (re)arrangements on surfaces. (Invited Paper)

### **8:10 PM WD2**

**Excimer Laser Etching and Oxidation of Silicon**, Y. Horiike, M. Sekine, K. Horioka, T. Arikado, M. Nakase, H. Okano, *Toshiba VLSI Research Center, Japan*. The excimer laser photochemical reactions have been developed for  $n^+$  type poly-Si anisotropic etching, Si selective oxidation, and pattern transfer technologies in LSI processings. (Invited Paper)

### **8:50 PM WD3**

**Effects of Optical Properties on Wet Etching of Semiconductors**, D. V. Podlesnik, H. H. Gilgen, C. J. Chen, R. M. Osgood, Jr., *Columbia U*. We report on the effects of UV illumination in wet etching of Si and GaAs. The formation of surface ripples and drilling of via holes is related to the optical properties of the semiconductors.

## **WEDNESDAY, FEBRUARY 6, 1985—Continued**

### **8:10 PM WD4**

**Transient Nonlinear Laser Heating and Deposition: A Comparison of Theory and Experiment**, J. A. Goldstone, S. D. Allen, *U. Southern California*. Transient temperature profiles and deposition rates are calculated and compared with the results of optically monitored laser chemical vapor deposition experiments.

## **SESSION I**

**J. Greene, *Presider***  
**University of Illinois at Urbana**

## ION ENHANCED PROCESSES IN ETCHING OF SILICON

T. M. Mayer, M. S. Ameen, E. L. Barish,  
D. J. Vitkavage, T. Mizutani

Department of Chemistry  
University of North Carolina  
Chapel Hill, NC 27514

A case study of the ion-assisted etching of silicon by chlorine is presented as a prototype of a class of ion-assisted etching processes. In contrast to the more well studied Si-F system, and other F atom etching reactions, Cl etching processes are much more dependent on energetic ion impact of the surface. We will examine aspects of chlorine adsorption to silicon, sputtering of adsorbed chlorine atoms, incorporation of chlorine into the silicon crystal lattice, and formation and removal of  $\text{SiCl}_x$  etch products. In-situ SIMS, ISS, and modulated beam mass spectrometric measurements, and post etch RBS and XPS analysis of the altered surface are used to examine the dynamics of the etching process and the state of the altered surface layer produced by ion bombardment.

The main features of silicon etching by chlorine appear to be: 1) adsorption of a stable easily sputtered surface Cl layer, which does not in itself promote removal of surface silicon atoms; 2) incorporation of substantial amounts of Cl into the subsurface Si crystal by recoil implantation or enhanced diffusion; 3) substantial damage to the Si crystal lattice caused by energetic ion bombardment. These latter two aspects appear to be the key ingredients in the formation and removal of silicon halides from the surface.

At submonolayer surface coverage, sputtering of Cl atoms occurs with high cross section, and angle of incidence dependence typical of sputtering of adsorbed gases. Contrasts to Si removal yield suggest that surface adsorbed Cl is not effective at promoting removal of Si atoms. Yields of secondary ions  $\text{SiCl}_x^+$ , under these conditions shows that silicon halide formation does indeed occur even at very low surface coverage, but that it is probable due to ion enhanced mixing effects in the first few atomic layers of the crystal rather than surface reactions. Ion bombardment of a chlorinated Si surface is shown to result in substantial lattice damage to the crystal and incorporation of up to 20 atomic % Cl in the first few atomic layers of the crystal. The amount of lattice damage and incorporated Cl are shown to be dependent on the ion impact conditions such as mass, energy and angle of incidence. All of these aspects demonstrate typical ion mixing phenomena in the surface layer of the sample.

The dynamics product liberation from the surface demonstrate that silicon halide species are only weakly bound to the lattice, but require substantial surface alteration to promote their formation. Modulated beam experiments show that under conditions of relatively little surface alteration by ion impact the dominant species removed are the simpler Si, SiCl, Cl. More extensive surface modification promotes the formation of more saturated SiCl<sub>x</sub> species.

The Influence of Ion Bombardment on Etching Reactions, by Harold F. Winters and J. W. Coburn, IBM Research Laboratory, San Jose, California 95193.

**Summary Abstract** Etching involves the interaction of gaseous species (e.g.,  $XeF_2$ ) with a solid surface (e.g., silicon) to produce volatile products (e.g.,  $SiF_4$ (gas)). (For recent review papers on this subject see refs. 1-7.) Moreover this type of reaction is frequently enhanced by bombardment with ions,<sup>8,9</sup> electrons,<sup>8</sup> and photons.<sup>10-12</sup>

It is our opinion that etching is a consequence of three-dimensional compound growth in the surface region and that etch products are generally compounds with a high vapor pressure, *i.e.*, a small binding energy to the surface. The region where a surface compound exists can be rather thin (a few Angstroms) or quite thick, depending upon the specific properties of the solid being etched. Experimental evidence substantiating this point of view will be presented for several systems.

An important question for understanding plasma-assisted etching is, "What surface processes convert reactants to products?" Definitive evidence on this subject is nonexistent and hence the following discussion is somewhat speculative. It is our model<sup>7</sup> that etching (*i.e.*, halide formation) is likely to be analogous to oxide formation (*i.e.*, mechanisms which lead to oxide-growth at surfaces also lead to halide formation, and for halogens subsequently to etching). The major difference between oxidation and halogenation is that *saturated* halides are frequently volatile while most oxides are involatile. The reason for the close analogy is that both halogen and oxygen atoms tend to form negative ions at the surface. The usefulness of the analogy is based on the assumption that phenomena, which are known to occur in the well-studied oxidation reactions, are also likely to occur in etching reactions.

Mott and co-workers have laid the foundation for understanding the growth of thin oxide layers,<sup>13-16</sup> and the reader is referred to Ref. 17 for a recent review. At low temperatures, electrons are able to pass through an oxide film (e.g., by tunneling) to the outer chemisorbed layer and form oxygen anions with metal cations being formed at the metal-oxide interface. The strong electric field generated by this process is able to pull ions through the film. Fehner and Mott<sup>14</sup> propose that the process can best be explained by a place exchange mechanism, *i.e.*, metal and oxygen ions exchange positions in the lattice. Linear kinetics are observed, because the image force (along with other electrostatic forces) pull the negative oxygen ion toward the metal which in turn lowers the activation energy for the process so that it is very small. The change in potential energy due to the image force can approximately equal the strength of a metal-metal bond, providing the distance of separation between the metal and the oxygen is small, *i.e.*, not more than 1-2 monolayers. *For thicker oxides*, logarithmic kinetics are often observed. This stage is dominated by an electric-field-assisted motion of either cations or anions through the oxide layer (see Ref. 17). Finally, it should be noted that growth of thick oxide layers formed by electrochemical<sup>18</sup> or plasma<sup>19</sup> anodization processes are also believed to be controlled by field-assisted mechanisms.

It should be emphasized that oxidation, even for a pure metal, is a highly complex phenomenon which, according to Dearnaley,<sup>20</sup> depends more upon solid-state physical mechanisms than on chemistry. It is influenced by, among other things, mechanical stress, clustering, island formation, nucleation phenomena, motion of anions and cations, and the presence of defects. Etching reactions are likely to be just as complex and also strongly dominated by processes similar to those involved in oxidation.

Ion (or radiation) enhanced etching fits easily into this framework. The mechanism which the present authors now believe is likely to *dominate* this process is analogous to mechanisms operative in oxidation, as summarized above. Place-exchange and more extended motion of cations and/or anions lead to compound formation. These motions are exothermic but activated and hence can be enhanced by the field-assisted mechanisms described in the previous section. The activation energy can also be supplied from the collision cascade induced by ion bombardment, thus enhancing the reaction rate. If the compound which is formed consists of molecules (*i.e.*, saturated halocarbons) which are weakly bound to the surface, then they will be subsequently desorbed into the gas phase, thus producing ion enhanced etching. This process, where *ion bombardment* induces a *chemical reaction* which produces a *weakly bound molecule that desorbs* from the surface, is called *chemical sputtering* by Tu *et al.*<sup>21</sup> Similar ion enhanced reactions have been observed in the growth of oxide layers, except that the products are involatile.<sup>22-25</sup>

In this paper data showing the influence of ion bombardment on the etching of Cu(100) with Cl<sub>2</sub> and the etching Si and W(111) with XeF<sub>2</sub> will be presented. For silicon and tungsten the dominant process which produces ion enhanced etching appears to be chemical sputtering as described above; nevertheless, the influence of lattice damage is significant for W(111) and is also evident for some silicon samples. Ion induced detrappling of gases such as WF<sub>6</sub> and SiF<sub>4</sub> may also occur to some extent. The etching reaction is suppressed by ion bombardment for Cu(100).

1. J.W. Coburn and H.F. Winters, *J. Vac. Sci. Technol.* **16**, 391 (1979).
2. D.L. Flamm and V.M. Donnelly, *Plasma Chem. & Plasma Proc.* **1**, 317 (1981).
3. J.W. Coburn, *Plasma Chem. & Plasma Proc.* **2**, 1 (1982).
4. J.W. Coburn and H.F. Winters, *Ann. Rev. Mater. Sci.* **13**, 91 (1983).
5. H.W. Lehmann and R. Widmer, *J. Vac. Sci. Technol.* **17**, 1177 (1980).
6. C.J. Mogab, *Inst. Phys. Conf. Ser.* **53**, 37 (1980).
7. H.F. Winters, J.W. Coburn and T.J. Chuang, *J. Vac. Sci. Technol.* **B 1** 469 (1983).
8. J.W. Coburn and H.F. Winters, *J. Appl. Phys.* **50** 3189 (1979).
9. T.M. Mayer and R.A. Barker, *J. Vac. Sci. Technol.* **21** 757 (1982).
10. T.J. Chuang, *J. Chem. Phys.* **74**, 1461 (1981).
11. F.A. Houle, *J. Chem. Phys.* **79**, 4237 (1983); *J. Chem. Phys.*, **80**, 4851 (1984).
12. M. Sekine, H. Okano and Y. Horiike, Proc. 1984 Dry Process Symp. Tokyo, Japan., Sept. 19-20, 1983, p. 97.
13. N.F. Mott, *Trans. Faraday Soc.* **43**, 429 (1940).
14. F.P. Fehner and N.F. Mott, *J. Oxidation of Metals* **2**, 59 (1970).
15. N.F. Mott, *Trans. Faraday Soc.* **43**, 429 (1940).
16. N. Cabrera and N.F. Mott, *Rep. Prog. Phys.* **12**, 163 (1949).
17. S.R.J. Saunders, *Sci. Prog. Oxf.* **63**, 163 (1976).
18. D.A. Vermilyea, in *Advances in Electrochemistry and Electrochemical Engineering*, edited by Paul Delahey (Interscience Publishers, New York, 1963). p. 249.
19. J.F. O'Hanlon, *J. Vac. Sci. Technol.* **7**, 330 (1970).
20. G. Dearnaley, *Nuclear Instr. and Meth.* **182-183**, 899 (1981).
21. Y.Y. Tu, T.J. Chuang and H.F. Winters, *Phys. Rev. B* **23**, 823 (1981).
22. W. Wach and K. Wittmaack, *J. Appl. Phys.* **52**, 3341 (1981).
23. W. Reuter and K. Wittmaack, *Appl. Surf. Sci.* **5**, 221 (1980).
24. R. Miranda, J.M. Rojo and M. Salmeron, *Sol. St. Comm.* **35**, 83 (1980).
25. J.C. Pivin, C. Rogues-Carmes, and G. Slodzian, *Int. J. Mass. Spec. and Ion Phys.* **31**, 293 (1979).

## A STUDY INTO THE MECHANISM OF ION-ASSISTED ETCHING

F.H.M.Sanders

Philips Research Laboratories, 5600 JA Eindhoven,  
The Netherlands

During the last few years, the rapidly growing need for ion-assisted, anisotropic etching of a.o. silicon and its compounds for VLSI circuits, has stimulated basic research on the processes underlying the largely empirical etch recipes. Part of the plasma etch process can be simulated in an experiment, where the combined effect of the exposure of a film (Si) to chemically active gases (XeF<sub>2</sub>, Cl<sub>2</sub>, SF<sub>6</sub>), and a low-energy ion beam (Ar<sup>+</sup>) has been investigated. Special attention will be paid to the reaction of Si with Cl<sub>2</sub> alone, Si(Cl<sub>2</sub>), and under simultaneous exposure to an Ar<sup>+</sup> ion beam, Si(Cl<sub>2</sub>,Ar<sup>+</sup>), as a function of the target temperature T, the Ar<sup>+</sup> ion energy E<sub>p</sub>, and the Cl<sub>2</sub> flux  $\phi$ Cl<sub>2</sub>, using mass spectrometry and time-of-flight analysis.

It has been shown that exposure of Si at 300 K to Cl<sub>2</sub> alone does not result in an observable reaction (1). In reference (2) it has been demonstrated that up to about 800 K the thermal reaction, Si(Cl<sub>2</sub>), yields almost exclusively SiCl<sub>4</sub>, see figure 1a-b. Above 800 K, and specifically at 1000 K, see figure 1c, the SiCl<sub>+</sub> and SiCl<sub>2+</sub> signals are drastically enhanced as compared with those of SiCl<sub>4+</sub> and SiCl<sub>3+</sub>, as measured by mass spectrometry. In between 800 and 1000 K the main product changes from SiCl<sub>4</sub> to SiCl<sub>2</sub>.

Figure 1d-e shows the mass spectra of the neutral products from the reaction Si(Cl<sub>2</sub>,Ar<sup>+</sup>) for 1 keV Ar<sup>+</sup> ions and temperatures of 300 and 800 K. Ion beam modulation at 5 Hz discriminates the measured signals against background; the thermal reaction, being continuous, contributes only to this background. The spectra suggest that at 300 K and even at 800 K in the Si(Cl<sub>2</sub>,Ar<sup>+</sup>) process, small SiCl<sub>x</sub> (x=1,2), molecules are emitted preferentially, and they suggest also that the ion-bombardment induced reactions are quite different from the thermal ones. A more quantitative comparison between Si(Cl<sub>2</sub>) at 1000 K and Si(Cl<sub>2</sub>,Ar<sup>+</sup>) at 800 K is only permitted after sorting out the neutral parents of the various products and their kinetic energy distributions.

Time-of-flight distributions of the neutral parents of SiCl<sub>+</sub> and SiCl<sub>2+</sub>, together with the signal dependence of SiCl<sub>x</sub> (x=1,2,3) products on the Cl<sub>2</sub> arrival rate at 300 K, lead to the conclusion that SiCl and SiCl<sub>2</sub> are emitted as such and that the neutral parent of SiCl<sub>+</sub> is mainly the SiCl, and of SiCl<sub>2+</sub> mainly the SiCl<sub>2</sub> molecule.

Studies on the kinetic energy distributions of the neutral products from the Si(Cl<sub>2</sub>,Ar<sup>+</sup>) process, see figure 2, have shown that more than 85% of them have energies above thermal values, and can be well described by a collision cascade like process. So, it appears that the main

fraction of the products emitted in this process results from sputtering and not from stimulation of the thermal reaction path by ion bombardment.

Studies on the influence of  $E_p$ ,  $T$ , and  $\phi_{Cl_2}$  on the time-of-flight distributions of  $SiCl$  and  $SiCl_2$ , as well as of  $Ar$  (first implanted and afterwards resputtered) (3), and the observed large molecular fraction sputtered compared with the atomic fraction, suggest that a modification of the top atomic layers of  $Si$ , from which the products are sputtered, by incorporation of significant quantities of  $Cl$ , plays a dominant part in the reaction mechanism.

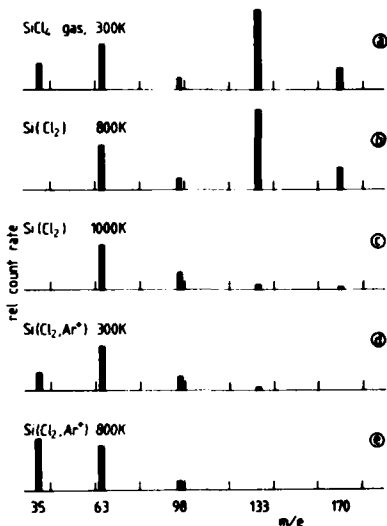


Figure 1.a) Mass spectrum of  $SiCl_4$  gas at 300 K; b) mass spectrum of species emitted in the thermal reaction of  $Si$  with  $Cl_2$  at 800 K ( $\phi_{Cl_2}=5 \times 10^{16} \text{ molec.cm}^{-2}\text{s}^{-1}$ ); c) idem as b) at 1000 K; d) mass spectrum of species emitted from  $Si$  under simultaneous exposure to a  $Cl_2$  beam ( $\phi_{Cl_2}$  see b)), and an  $Ar^+$  ion beam ( $E_p=1 \text{ keV}$ ,  $\phi_{Ar}=4 \times 10^{15} \text{ ionscm}^{-2}\text{s}^{-1}$ ); e) idem like d) at 800 K. All data are normalized to the  $SiCl^+$  signal.

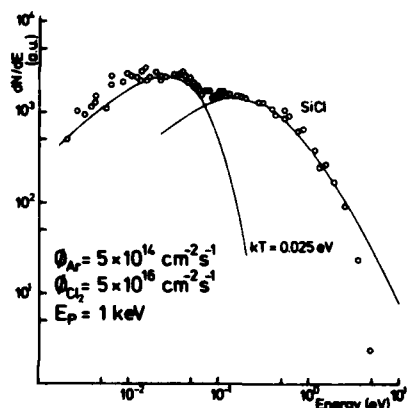


Figure 2. Total fit of the kinetic energy distribution of  $SiCl$  ( $m/e=63$ ) particles for the parameters as given in the figure. At low energy a Maxwell-Boltzmann distribution at 300 K is indicated, while at higher energies, above 0.1 eV, a collision cascade distribution is given with an  $U_0=0.3 \text{ eV}$ .

- 1.T.M.Mayer and R.A.Barker, J.Vac.Sci.Technol.21,757 (1984)
- 2.F.H.M.Sanders, A.W.Kolfschoten, J.Dieleman, R.A.Haring, A. Haring and A.E.de Vries, J.Vac.Sci.Technol.A2(2)487 (1984)
- 3.A.W.Kolfschoten, R.A.Haring, A.Haring and A.E.de Vries, J.Appl.Phys.55(10)3813 (1984)

## **SESSION II**

**D. Flamm, *Presider***  
**AT&T Bell Laboratories**

ENERGY DISTRIBUTIONS OF ELECTRONICALLY EXCITED MOLECULES PRODUCED BY ION BOMBARDMENT OF SILICON

R. Walkup and Ph. Avouris, IBM Thomas J. Watson Research Center, P.O.Box 218, Yorktown Heights, N.Y. 10598

A portion of the flux of sputtered particles produced during ion bombardment of a solid surface consists of molecular fragments. These sputtered molecules are of particular interest because they provide a unique probe of the dynamics of the sputtering process. In addition to center of mass motion away from the surface, the molecular fragments exhibit relative motion of the constituent atoms, e.g. rotations and vibrations. Concurrent measurement of the distribution of energy in these internal modes together with the center of mass kinetic energy enables critical evaluation of sputtering mechanisms.

We report optical measurements of the internal and kinetic energy of the electronically excited molecules  $\text{SiN}(\text{B}^2\Sigma)$  and  $\text{SiH}(\text{A}^2\Delta)$  produced by ion bombardment of silicon. These two species have very different mechanical properties (dissociation energy, mass ratio, etc.), and therefore they may exhibit different collisional sputtering dynamics. The rotational and vibrational energies are obtained by comparing the spectral band intensities and shapes with numerical simulations. A good fit is obtained by using a Boltzmann distribution for both the vibrational and rotational degrees of freedom with effective "temperatures" of  $T_{\text{eff}} = 3500 \pm 500\text{K}$  for  $\text{SiN}(\text{B}^2\Sigma)$ , and  $T_{\text{eff}} = 3000 \pm 500\text{K}$  for  $\text{SiH}(\text{A}^2\Delta)$ . This corresponds to energies of  $kT_{\text{eff}} = 0.30 \pm 0.04\text{eV}$  and  $0.26 \pm 0.04\text{eV}$  for  $\text{SiN}(\text{B}^2\Sigma)$  and  $\text{SiH}(\text{A}^2\Delta)$  respectively. Kinetic energies of the sputtered molecules are obtained by monitoring the optical emission intensity as a function of distance from the surface. We find characteristic kinetic energies of  $E_K = 3.7 \pm 0.7\text{eV}$  for  $\text{SiN}(\text{B}^2\Sigma)$  and  $E_K = 2.3 \pm 0.5\text{eV}$  for  $\text{SiH}(\text{A}^2\Delta)$ . The fact that the kinetic energy of the sputtered molecules is about ten times larger than the internal energy is clear evidence of the non-thermal nature of the particle ejection process.

We compare the experimental observations with an analytical model of the vibrational distribution of sputtered diatomic molecules. Reasonable agreement is obtained and several qualitative conclusions are reached. (1) For the low energy ( $<10\text{eV}$ ) collisions typical of collision cascade sputtering, the collision duration is comparable to or larger than a vibrational period. As a result adjacent atoms generally have a correlated response to a collision, and the probability of vibrational excitation is relatively small. This is in agreement with experimental observations. (2) The bond dissociation energy does not play a major role in limiting the internal energy distributions of sputtered molecules. This is clearly demonstrated by the fact that comparable internal energy distributions have been observed for  $\text{BH}(\text{A}^1\Pi)^1$ ,  $\text{SiH}(\text{A}^2\Delta)$ ,  $\text{CH}(\text{A}^2\Delta)^2$ , and  $\text{SiN}(\text{B}^2\Sigma)$  where the dissociation energies are  $0.55\text{eV}^1$ ,  $0.84\text{eV}^3$ ,  $2.7\text{eV}^4$ , and  $5.1\text{eV}^5$  respectively. (3) Boltzmann-like distributions are calculated from a simple collisional model of vibrational excitation, thus the observation of Boltzmann-like distributions does not imply energy equilibrium for the internal modes of sputtered molecules.

#### References

1. R.Kelley, S.Dzioba, N.H.Tolk, and J.C.Tully, *Surface Science* 102 , 486 (1981)
2. G.E.Thomas and B.R.de Koning, *Chem.Phys.Lett.* 55 , 418 (1978)
3. T.V.R.Rao and S.V.J.Lakshman, *Physica* 56 , 322 (1971)
4. D.R.Childs, *J.Q.S.R.T.* 4 , 283 (1964)
5. H.Bredohl, I.Dubois, Y.Houbrechts, and M.Singh, *Can. J. Phys.* 54 , 680 (1976)

Mechanistic Studies of Low-Enhanced Etching of Electronic  
Materials by Modulated-Beam Mass Spectrometry

M. Balooch, D. R. Olander, and W. J. Siekhaus

University of California

Berkeley, California

**Simultaneous Exposure of  $\text{SiO}_2$  and  $\text{ThF}_4$   
to  $\text{XeF}_2$  and Energetic Electrons\***

M. A. Loudiana and J. T. Dickinson  
Department of Physics  
Washington State University  
Pullman, WA 99164-2814

This study examines the effect of exposing thin films of  $\text{SiO}_2$  and  $\text{ThF}_4$  to gaseous  $\text{XeF}_2$  and energetic electrons. These systems are of interest to VLSI and optical coatings technology. The experiments were done in a stainless steel UHV chamber with Auger Electron Spectroscopy (AES) and Quadrupole Mass Spectroscopy capabilities. Changes in the mass of the thin films was measured with a sensitive, thermally stabilized quartz crystal microbalance. Details of the equipment and procedure are given elsewhere.<sup>1</sup>

When  $\text{ThF}_4$  is exposed to  $\text{XeF}_2$ , microbalance measurements show that 0.7 monolayer of fluorine is adsorbed. When a  $\text{ThF}_4$  film is bombarded by 1 keV electrons in vacuum, electron stimulated processes (including electron stimulated desorption -- ESD) cause it to lose over 27 monolayers of fluorine. The surface composition of a  $\text{ThF}_4$  thin film during electron bombardment was measured with AES. A large loss of fluorine was observed with a corresponding increase in thorium; oxygen and carbon impurities showed a decrease. Microbalance measurements show a sharp increase (a factor of 2) in the electron sputtering yield between 200 and 250 eV. We attribute this increase to the onset of the core-hole Auger decay mechanism, as proposed by Knotek and Feibelman<sup>2</sup> involving the thorium 0-shell.

If a heavily fluorine depleted  $\text{ThF}_4$  film is exposed to  $\text{XeF}_2$  it rapidly regains 6 monolayers of fluorine, also seen in the Auger spectra as an increase in the fluorine Auger peak. When  $\text{XeF}_2$  is present during electron bombardment, the fluorine concentration does not decrease as much as in vacuum. Thus, both uptake and removal of fluorine is happening simultaneously

and that an equilibrium state is reached where fluorine is eventually replaced by  $XeF_2$  at the same rate it is lost by ESD.

When  $SiO_2$  is exposed to  $XeF_2$  it adsorbs 1 monolayer of fluorine.<sup>1</sup> Oxygen is lost from  $SiO_2$  very slowly when it is exposed to energetic electrons in a vacuum.<sup>3</sup> As shown by Coburn and Winters,<sup>4</sup> if  $XeF_2$  is present an electron beam will rapidly etch  $SiO_2$ . We observe in the AES a rapid decrease in the Si Auger signal during electron bombardment in  $XeF_2$ . The rise in oxygen concentration indicates that oxygen removal may be the slowest step in the reaction.

The presence of silver on the surface is observed at large electron doses and is due to the silver substrate reacting with fluorine which has diffused through the  $SiO_2$  film under the influence of electron bombardment. The silver -- fluorine interaction actually results in a net mass gain if sufficiently low energy electrons are used. At sufficiently high energies the removal of  $SiO_2$  saturates at the current densities used in these studies at an electron sputtering yield of 20 AMU/electron.

#### REFERENCES

\* This Work is supported by the Defense Advanced Research Project Agency, ARPA Order No. 3343 under the Office of Naval Research, Contract No. N00014-80-C-0798.

1. M. A. Loudiana, A. Schmid, J. T. Dickinson, and E. J. Ashley, *Surf. Sci.* 141 (1984) 409-416.
2. P. J. Feibelman and M. L. Knotek, *Phys. Rev. B* 18 (1978) 6531-6539.
3. B. Carriere, and B. Lang, *Surf. Sci.* 64 (1977) 209-223.
4. J. W. Coburn and H. F. Winters, *J. Appl. Phys.* 50 (1979) 3189-3196.

**Ablation of Organic Polymers by Ultraviolet and Visible Radiation:**  
**A Theoretical Approach**

Barbara J. Garrison  
The Pennsylvania State University  
Department of Chemistry  
University Park, PA 16802

and

R. Srinivasan  
IBM  
Thomas J. Watson Research Center  
Yorktown Heights, New York 10598

There has been considerable interest recently in the use of laser radiation to remove material from a solid. Of particular interest is the observation that short pulses far-UV (e.g., 193 nm) radiation ablates organic polymers cleanly, i.e., the remaining sample exhibits a precisely defined pit (1-3). It is possible that the radiation could have melted or damaged the remaining sample. Indeed for longer wavelength radiation, e.g. visible light, damaged samples are generally observed (4). Obviously there are at least two distinct processes that can result in ablation of material when it is irradiated by laser light. In the following discussion we will refer to the phenomenon that cleanly etches the material as the photochemical process and the one that melts the sample as the thermal process. We have developed microscopic models for each of the two processes (5). In the photochemical model we assume one photon is directly responsible for dissociating one bond via a transition to an excited electronic state. In the thermal model we assume that the laser energy is absorbed into vibrational modes of the solid.

Microscopic models for photochemical and thermal ablation of polymer films due to pulsed laser radiation are presented. The photochemical model is appropriate for far-UV (e.g., 193 nm) radiation and assumes that the laser light initiates a chemical reaction. The products have a larger specific

volume than the original sample and an explosion occurs. The predictions of the photochemical model are as follows: (1) The reacted material ablates without melting the remainder of the sample. (2) The average perpendicular velocity of the ablated material is 1000-2000 m/s. (3) The angular spread is within 25-30° of normal and peaked in the direction normal to the surface. (4) The material ablates layer by layer.

The thermal model is appropriate for photon energies which are not sufficiently large to dissociate chemical bonds and possibly even cases of UV irradiation of solids. In this case the light is absorbed by vibrational modes in the solid and goes towards heating the sample. The predictions of the thermal model are as follows: (1) The remaining sample is distorted and melted. (2) The angular spread is twice as large as that from the photochemical model. (3) The material does not necessarily ablate layer by layer.

The precise wavelength regime in which the photochemical, thermal or possibly even both processes are operative will undoubtedly depend on the characteristics of individual materials. It is time to make systematic experimental studies in order to quantitatively define these two regimes and to understand their similarities and differences.

1. R. Srinivasan and V. Mayne-Banton, *Appl. Phys. Lett.* 41, 576 (1982); R. Srinivasan and W. J. Leigh, *J. Am. Chem. Soc.* 104, 6784 (1982); R. Srinivasan, *J. Vac. Sci. Tech.* B1, 923 (1983).
2. J. E. Andrew, P. E. Dyer, D. Forster, and P. H. Keys, *Appl. Phys. Lett.* 43, 717 (1983).
3. M. W. Geis, J. N. Randall, T. F. Deutsch, P. D. Graff, K. E. Krohn and L. A. Stern, *Appl. Phys. Lett.* 43, 74 (1983); T. F. Deutsch and M. W. Geis, *J. Appl. Phys.* 54, 7201 (1983).
4. R. Linsker, R. Srinivasan, J. J. Wynne, and D. R. Alonso, *Lasers in Surgery and Medicine* 4, 201 (1984).
5. B. J. Garrison and R. Srinivasan, *Appl. Phys. Lett.* 44, 849 (1984); *ibid*, *Appl. Phys.*, submitted.

**Laser Interferometry and Laser Induced Fluorescence Studies of Laser Etching.** R.W. Dreyfus, R. Walkup and J.M. Jasinski, IBM Thomas J. Watson Research Center, P.O. Box 218, Yorktown Heights, NY 10598.

**SUMMARY:** Excimer laser ablation of solids with laser power densities in the range  $10^6$  to  $10^9$  W/cm<sup>2</sup> is becoming increasingly important in laser processing of materials for microelectronics. The ablation process produces an intense plume of gas phase material which expands rapidly away from the ablated surface. We report on real time interferometric measurements of free electron density and laser induced fluorescence studies of atoms and molecules in the plume, with the objective of understanding the dynamics of material ablation.

A primary concern in studies of laser ablation is whether or not a laser produced plasma is formed above the surface. We have used a Michelson interferometer to measure the index of refraction of the plume of ablated material. Since the refractive index is especially sensitive to the free electron density, this technique provides a direct probe for plasma formation and plasma density. Using this technique, time-resolved measurements of plasma density at a fixed distance (2mm) above the surface of a number of different materials have been made. This provides time-of-flight velocity distributions for the plasma. Threshold energy densities for plasma formation are obtained by measuring the plasma density as a function of laser fluence.

When plasma formation is observed, threshold energies are in the range 0.5-10 J/cm<sup>2</sup> and show remarkably little correlation with simple electronic properties of the material or with optical band gap. The expansion velocity of the laser produced plasma depends primarily on the initial plasma density rather than on the specific properties of the material being ablated. For the specific case of sapphire, the plasma density is  $\sim 10^{16}$  electrons/cm<sup>3</sup> at a fluence of 5 J/cm<sup>2</sup>. The plasma expansion velocity under these conditions is  $\sim 10^6$  cm/sec. Expansion velocities of this magnitude arise from an electrostatic plasma acceleration mechanism, analogous to ambipolar diffusion. The expansion velocity corresponds to ion kinetic energies in the range of 10 eV. This kinetic energy can be transferred to neutrals by ion neutral collisions and/or charge transfer reactions. Collisional coupling of ion and neutral motion should be strong since the density of ions in the plasma is large ( $\sim 10^{16}$  cm<sup>-3</sup>) and the degree of ionization is high ( $\gtrsim 10\%$ ).

Energy distributions for ground state atoms and molecules in the plume have been obtained by laser induced fluorescence studies. A narrow band dye laser probes specific species 2 cm above the surface 0.1 to 100  $\mu$ sec after the ablating laser pulse. Time-of-flight velocity distributions obtained in this way for Al and AlO produced in the ablation of sapphire are shown in Figure 1. These data can be fit to Boltzmann distributions giving average kinetic energies of  $13.3 \pm 0.6$  eV for Al and  $0.61 \pm 0.03$  eV for AlO. The high kinetic energy of the aluminum atoms results from resonant charge transfer reactions with fast aluminum ions, as noted above. Laser

induced fluorescence spectra of diatomics such as AlO also provide information on internal energy distributions. We find that the rotational and vibrational energies of AlO are  $\sim 0.1$  eV, substantially less than the translational energy. This may be indicative of a relatively low surface temperature.

RWD acknowledges many helpful discussions with Ph. Avouris, R. Kelly, and J. Rothenberg

Figure 1. Velocity distributions of Al and AlO formed during ablation of  $\text{Al}_2\text{O}_3$ . The solid lines are calculated curves assuming a Boltzmann distribution.

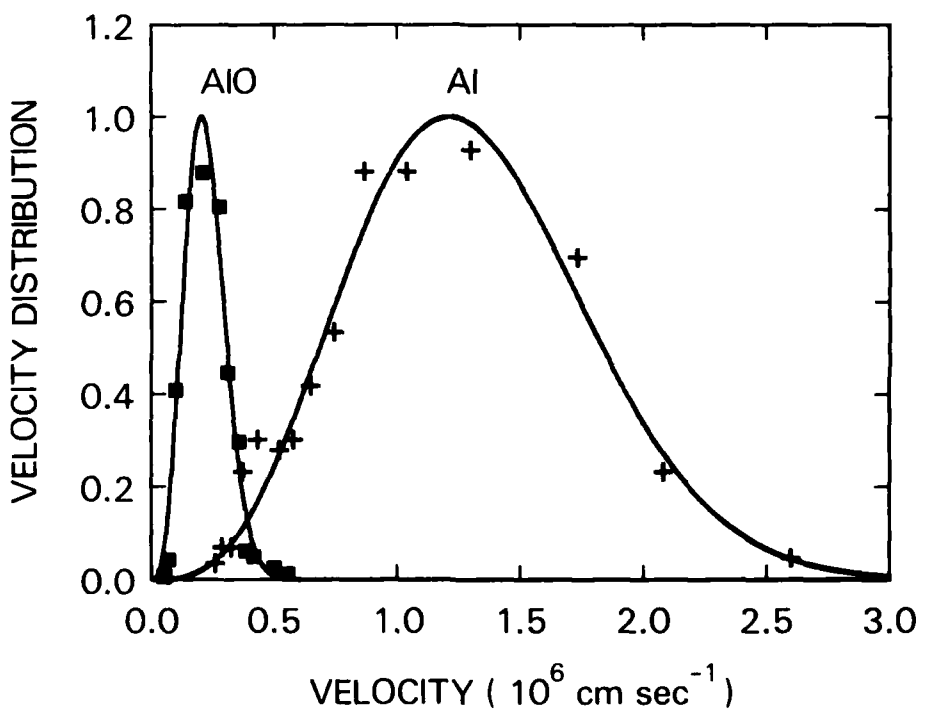


Table I. Summary of Translational and Internal Energies for Al and AlO ablated from  $\text{Al}_2\text{O}_3$ .

	AlO	Al
$E_{\text{trans}}$	0.6 eV	13 eV
$E_{\text{rot}}$	$\sim 0.1$ eV	-
$E_{\text{vib}}$	$\sim 0.1$ eV	-

**Direct-writing in self-developing resists using  
low-power, cw, ultraviolet light**

by

**J. E. Bjorkholm, L. Eichner, J. C. White, and R. E. Howard**

**AT&T Bell Laboratories**

**Holmdel, NJ 07733**

and

**H. G. Craighead**

**Bell Communications Research**

**Holmdel, NJ 07733**

**SUMMARY**

"Direct-write" technologies for the laser processing of semiconductors use sharply focused laser beams to induce localized chemical reactions at semiconductor surfaces. Though these processes are slow compared with conventional optical printing, they are of scientific interest and they appear promising for applications involving the customizing, repairing, and testing of integrated circuits. There also has been interest in "self-developing" photoresists; these are materials that ablate during exposure to optical radiation. The use of a self-developing resist eliminates the need for a development step following exposure.

In this talk we describe the first direct-writing of micron-sized features in self-developing resists. The direct writing is carried out using less than 1 mW of UV light at 257 nm focused to a spot size of about 1.5  $\mu\text{m}$  on thin films of polymeric photoresists deposited on a variety of substrates. Most of our work was carried out with poly(methylmethacrylate) (PMMA), although similar results have been obtained with other resists. The substrate is scanned under the light beam to create patterns in the resist. Completely ablated grooves having widths of 1.5  $\mu\text{m}$  have been fabricated at scan speeds of up to 120  $\mu\text{m/sec.}$

Previous work on self-developing photoresists has been carried out by irradiating relatively large surface areas with both cw and pulsed light sources. The peak power levels used were much greater than those employed here, ranging from about a factor of ten for the cw cases to many orders of magnitude greater for the pulsed cases. Nonetheless, because of the small focal spots used here, our exposures were much larger than those of the preceding work. For an incident power of 1 mW the peak intensity is on the order of about  $10^4 \text{ W/cm}^2$ , corresponding to an incident energy density of about  $2 \times 10^3 \text{ J/cm}^2$  for a typical scan speed of  $10 \mu\text{m/sec}$ .

Important features of our observations are that there are no energy density or intensity thresholds for ablation and that the depth of the ablated groove is determined by the deposited energy density, independent of the deposition rate. In other words, the self-developing or ablation process is reciprocal. Clearly the ablation process is not thermal in origin. These observations are consistent with the preceding cw work; however, all of the pulsed observations have reported the existence of a distinct threshold for ablation. This indicates that different physical mechanisms are responsible for ablation in cw and pulsed conditions.

We have further observed that the cw ablation process in PMMA is a form of photo-initiated oxidation. Irradiation of PMMA in vacuum or in an inert environment only results in a slight localized shrinkage of the thin film. Ablation is observed only in the presence of oxygen. The ablation rate is roughly proportional to the oxygen partial pressure for partial pressures of less than 100 torr and it saturates above several hundred torr.

Reactive-ion etching of silicon substrates through patterned PMMA films has yielded good results. For example,  $1.5 \mu\text{m}$  wide grooves were written in  $160 \text{ nm}$  thick PMMA films deposited on silicon. After reactive-ion etching with  $\text{SF}_6$ , these grooves were transferred into the substrate; they were about  $320 \text{ nm}$  deep,  $1.5 \mu\text{m}$  wide at the surface, and their profile mirrored the profile of the groove in the PMMA.

## **SESSION III**

**S. Brueck, *Presider***  
**MIT Lincoln Laboratory**

Raman Characterization of Catalysts

A. Wokaun\*, A. Baiker†, W. Fluhr\*, M. Meier\*, and S.K. Miller†

Physical Chemistry Laboratory\*

and

Department of Industrial and Engineering Chemistry†  
Swiss Federal Institute of Technology  
ETH Zentrum, CH 8092 Zurich, Switzerland

The use of surface enhanced Raman scattering as a tool for the elucidation of reaction mechanisms in heterogeneous catalysis is investigated. The following information is desired:

- identification of the molecular species adsorbed at the surface, even if present in low concentrations; this includes reactants, major and side products;
- type and geometry of bonding to the surface;
- detection of intermediates which exist only as surface species.

Vibrational spectroscopy, being highly molecule specific, is suitable to answer these questions. Applications of Raman scattering in catalysis have previously been impeded by low sensitivity. Surface enhancement, which is intrinsically strongest for the first adsorbed molecular layer, makes Raman scattering comparable in sensitivity to electron energy loss spectroscopy in UHV. Compared to transmission IR spectroscopy, Raman scattering is particularly attractive for catalyst characterization due to its independence of a transparent support. It gives easy access to bands in the low wavenumber region, corresponding to motions of the adsorbate relative to the surface.

Reactions of amines, such as dehydroamination and disproportionation, on metallic copper catalysts have been chosen as systems of current

interest, and of a complexity which is typical for catalytic processes of industrial relevance. Activity and selectivity of the copper catalysts are strongly influenced by the adsorption and desorption behavior of the reactant and product amines. Thus as a first step the adsorption of *m*-toluidine on Cu is being studied.

Surface enhanced Raman spectra of toluidine on Cu have been recorded; they exhibit significant frequency shifts compared to the spectrum of the neat liquid, as well as additional bands. Raman spectra of two model compounds were compared with the surface spectrum: In lithium toluidide, a covalent bond between nitrogen and the metal atom is formed; in the toluidinium ion an electron acceptor ( $H^+$ ) is attached to the nitrogen lone pair. Interpretation was aided by a normal coordinate analysis of the frequency shifts. The data allow a clearcut decision between two models put forth for the bonding of toluidine to the surface.

Further work includes the study of reactant and product amine adsorption at elevated temperatures, and *in situ* spectroscopic characterization of copper surfaces during dehydroamination reactions. Progress along these lines is reported, and the scope of the technique is asserted.

The successful use of enhanced Raman scattering in reaction environments hinges on the preparation of metallic surfaces which are both Raman active and catalytically active. A simple etching procedure for producing such substrates is described. The surfaces consist of relatively large ( $\approx 1000 \text{ \AA}$ ) particles and protrusions, which are randomly placed and close enough to each other to be strongly interacting.

Theoretical advances in the modeling of such a surface are reported. A theory of dipolar interactions between arbitrarily sized particles on a surface is outlined, which provides guidelines for maximizing the molecule - independent electromagnetic enhancement contribution.

SURFACE RAMAN SPECTROSCOPY WITHOUT ENHANCEMENT

Alan Campion  
Department of Chemistry  
University of Texas at Austin

I will describe recent experiments that demonstrate our ability to observe Raman scattering from molecules adsorbed on single crystal surfaces without requiring either surface or resonance enhancement. I will discuss the details of the experimental method, relevant selection rules, information obtainable from the angular distribution of the scattered radiation and some implications of our experiments regarding the mechanism of surface-enhanced Raman scattering. To illustrate the versatility of our method, examples will include studies of molecules adsorbed on metal and semiconductor surfaces in ultrahigh vacuum, in the presence of reactive gases at high pressures and in the electrochemical environment.

## Surface Coherent Raman Spectroscopy

W. M. Hetherington, N. E. Van Wyck, E. W. Koenig and Z. Z. Ho  
Department of Chemistry, University of Arizona, Tucson, Arizona 85721

G. I. Stegeman, R. M. Fortenberry and R. Moshrefzadi  
Optical Sciences Center, University of Arizona, Tucson, Arizona 85721

Surface coherent Raman scattering (SCRS) is a powerful technique for obtaining vibrational Raman spectra of surface species with submonolayer sensitivity. This sensitivity is achieved by using incident and scattered fields in the form of guided waves. A planar optical waveguide ( $1 \mu\text{m}$ ) of a transparent oxide is deposited upon a silica substrate. Dye laser beams of frequencies  $\omega_1$  and  $\omega_2$  are coupled into the waveguide via coupling prisms in optical contact with the surface. The allowed TE and TM modes (electric field and magnetic field in the plane of the surface, respectively) for guided waves are characterized by a discrete set of wavevectors which depend upon the indices of refraction and the film thickness. The guided wave fields extend beyond the film into the surrounding media, and hence nonlinear interactions such as coherent anti-Stokes Raman Scattering (CARS) can occur on the surface of a waveguide. The field distribution functions exhibit an exponentially decaying evanescent tail outside the film.

Coherent Raman Scattering processes, such as CARS where  $\omega_3 = 2\omega_1 - \omega_2$ , occur within the film and in both the upper and lower interfacial regions. The achievement of phase-matching, where  $k_3 = 2k_1 - k_2$ , leads to a very efficient generation of the CARS signal because the propagation distance can be 1 cm in the film and because high power densities are easily attained when the film is only  $1 \mu\text{m}$  thick.

In order to detect a CARS signal only from the surface of the optical waveguide, the contribution to the signal from the third order susceptibility,  $\chi^{(3)}$ , of the film itself can be removed by an interference effect based upon a thoughtful choice of the TE modes for the fields at the three frequencies for a particular film thickness. This interference effect has been observed experimentally and has enabled the observation of CARS spectra of molecules adsorbed on oxide waveguides.

Under high vacuum and ambient atmospheric environments, a variety of molecules have been allowed to adsorb onto the surface of ZnO and Nb<sub>2</sub>O<sub>5</sub> optical waveguides. CARS spectra have been observed with 2 cm<sup>-1</sup> resolution over the range of 700 to 1300 cm<sup>-1</sup> using two dye laser pulses from a synchronously pumped laser system.

This initial investigation of surface coherent Raman scattering demonstrates the submonolayer sensitivity, the wide range of accessible frequencies, the cancellation of the bulk film signal and the environmental flexibility of this type of spectroscopy, and it strongly suggests that SCRS is an excellent way of studying the structure, chemistry and dynamics of surfaces.

High Resolution Electron Energy Loss  
Spectroscopy of Molecular Bond Weakening  
on Potassium Promoted Ru(001)

by

F. M. Hoffmann and R. A. dePaola  
Exxon Research and Engineering Company  
Corporate Research Science Labs  
Route 22 East - Clinton Township  
Annandale, New Jersey 08801

The adsorption of molecular nitrogen and carbon monoxide on potassium promoted Ru(001) has been investigated with vibrational spectroscopy, thermal desorption, LEED and work function measurements. For carbon monoxide, small precoverages of potassium result in anomalously weak C-O bonds which manifest themselves in large C-O stretch frequency shifts ( $600$  to  $1400\text{ cm}^{-1}$ ) and an increase in vibrational overtone anharmonicities[1]. Facile C-O bond-breaking was observed by isotopic scrambling in thermal desorption experiments. Both vibrational and thermokinetic data as well as analogies to metalcarbonyls[2] and molecularly adsorbed oxygen on Pt(111) [3] suggest a side-on bonding mode of the molecule with substantial weakening and lengthening of the C-O bond.

In contrast, the molecular adsorption of nitrogen is not significantly affected by alkali promotion of the Ru(001) surface. Both on the clean and potassium promoted surface molecular nitrogen adsorbs only weakly ( $T_{des} \sim 100K$ ) with N-N stretching frequencies of  $2260$ - $2200\text{ cm}^{-1}$  for clean Ru(001), and  $2160$ - $2130\text{ cm}^{-1}$  for small potassium precoverages ( $\theta_k < 0.10$ ). Higher potassium precoverages ( $\theta_k < 0.10$ ) completely suppress adsorption of molecular nitrogen at  $90K$ . The difference in the molecular adsorption behavior of nitrogen and carbon monoxide must be explained with the different molecular structure of these molecules[4,5]. The ability of carbon monoxide to form strong  $5\sigma$  donor

bonds with the metal surface results in synergetic  $2\pi^*$ -backdonation which can be promoted by alkali adsorption. In contrast, nitrogen forms weaker donor bonds and therefore shows a reduced ability for alkali promoted backdonation.

References

- [1] F. M. Hoffmann and R. A. dePaola, Phys. Rev. Letters 52 (1984) 1697.
- [2] W. A. Herrmann, H. Biersack, M. L. Ziegler, K. Weidenhammer, R. Siegel and D. Rehder, J. Am. Chem. Soc. 103 (1981) 1692.
- [3] J. Stöhr, J. Gland, W. Eberhardt, D. Outka, R. J. Madix, F. Sette, R. J. Koestner, U. Doebler, Phys. Rev. Lett. 51 (1983) 2414.
- [4] K. Hermann, P. S. Bagus, C. R. Brundle and D. Menzel, Phys. Rev. B24 (1981) 7025.
- [5] C. M. Kao and R. P. Messmer, Phys. Rev. B., submitted.

Photophysical Studies of DAQ on Silica and  
Aluminum Oxides. A Molecular Probe of Surface Heterogeneity

J. M. Drake

Exxon Research and Engineering Company  
Corporate Research-Science Laboratories  
Clinton Township - Route 22 East  
Annandale, New Jersey 08801

The optical features of organic molecules adsorbed to the surface of oxides, such as silica and alumina, can be strongly perturbed by the chemical properties of the surface adsorption sites. The topography of the surface as it relates to the fractal dimension and its relation to the nature and distribution of surface sites is important information if we are to be able to understand the photophysics and photochemistry of surface bound molecules. The work we report here is for the molecule 1,4 dihydroxyanthraquinone (DAQ, Quinizarin). This molecule provides striking evidence of how the surface of silica gel modifies the optical features of DAQ in different ways depending on the nature of the surface adsorption site.

The direction of our work with DAQ is to develop an understanding of the relationship between the spectroscopic changes (compared to homogeneous solution) observed for the surface bound molecule and the chemical and physical nature of surface adsorption sites. We chose DAQ because of the range of chemical behavior it exhibits. As a site specific molecular probe of surfaces, DAQ interacts with the surface through: hydrogen bonding, charge transfer and proton transfer. The features of the hydrogen bonding between the surface and DAQ are studied by the technique of photochemical hole burning (PHB). This is a very unique form of site selective surface photochemistry, which for DAQ is based on a phototautomerization reaction. We have been successful in doing PHB of DAQ on selected silica surfaces.

The charge transfer and proton transfer interactions, both the intramolecular and intermolecular processes, are studied using optical techniques. We use the absorption, fluorescence and fluorescence lifetime features of surface bound DAQ to interrogate the polarizable nature of the local surface site environment. The broad structureless inhomogeneously broadened absorption feature of the total ensemble of surface bound molecules is separated into two subsets, those DAQ molecules which are chemisorbed to sites which result in quenched fluorescence and those adsorbed to sites which allow the molecule to continue to fluoresce. Those which fluoresce, can be subdivided further into those which are weakly adsorbed and therefore exhibit fluorescence features similar to homogeneous solution and those which are adsorbed forming a strong complex with the surface. The DAQ molecules which form a surface complex exhibit strongly perturbed fluorescence features.

The dynamics of the excited state proton transfer reaction are modeled using fluorescence lifetime data obtained for each of the surface bound forms of DAQ. Time resolved fluorescence spectra are taken to understand the apparent shifts in the fluorescence spectra of DAQ in different surface environments. The resulting spectroscopic and dynamic data demonstrate the usefulness of optical techniques in probing the chemical nature of heterogeneous oxide surfaces.

## **SESSION IV**

**C. Wittig, *Presider***  
**University of Southern California**

**PHOTODESORPTION AND ADSORBATE-SURFACE INTERACTIONS  
STIMULATED BY LASER RADIATION**

T. J. Chuang  
IBM Research Laboratory  
5600 Cottle Road  
San Jose, California 95193

**Summary:** Laser photons can interact with a gas-solid system to promote heterogeneous reactions and to stimulate desorption. Two classes of photon-enhanced surface processes have been extensively investigated in recent years. The first one involves laser-induced adsorbate-surface reaction and desorption resulting in the chemical etching of the solid. The examples include the halogen reactions with silicon and metals affected by ultraviolet and visible photons. Recent time-resolved mass spectrometric studies in conjunction with ESCA, Auger spectroscopy and thermal desorption measurements have revealed interesting surface reaction dynamics and etching mechanisms. The second one involves infrared laser photodesorption initiated by excitation of internal molecular vibrations. Recent studies of the desorption phenomenon for molecules adsorbed on both dielectric and metal surfaces excited by the infrared radiation will be discussed. The photo-excitation process, including both single and multiple photon absorption and the various vibrational energy transfer and relaxation processes related to photodesorption, will be examined with particular emphasis on assessing the quantum and thermally-assisted effects. A review on both classes of laser-stimulated surface processes will be given.

## Infrared Spectral Electrochemistry of Surface Reactions

B. Stanley PONS, Department of Chemistry, University of Utah, Salt Lake City, Utah 84112

In situ infrared vibrational spectroscopy of the electrode/solution interface has established itself as an efficient and informative method for study of the orientation and structure of adsorbed species. The method is growing rapidly in popularity due to its ease in implementation. Very high sensitivities (approximately  $10^{-6}$  absorbance) is attained with relatively simple instrumentation and by simple single external specular reflection. A range of related experimental techniques and their application has led to study of problems of wide electrochemical and general interest including:

- a) The detection and identification in aqueous and non-aqueous solvents of the potential dependent populations of solvent, simple ions, and organic solutes both in the adsorbed state and free in the double layer using a wide range of metallic and non-metallic electrode materials including well-defined single crystal surfaces.
- b) The investigation of the orientation, surface bonding, and intermolecular interaction of adsorbed species and the effects of electrode potential on these parameters.
- c) The identification and kinetics of reaction of adsorbed and non-adsorbed reaction intermediates such as radical anions and cations.

In addition to the generally recognized surface selection rules governing the interaction of polarized infrared radiation with adsorbed species at metal surfaces, other factors contribute to observed changes in the vibrational spectra of adsorbed species from the free species. The first is the fact that adsorption of a species at a surface results in a symmetry change. Translational, and at least some of the rotational degrees of freedom are removed, and thus new vibrational modes will appear. The new adsorbant/adsorbent complex will have reduced symmetry. Consideration of the new spectra along with possible models

of adsorption onto the two dimensional lattice has been made by several workers, and can lead to a wealth of new information regarding the adsorbed state. The second factor is the response of the oscillating dipole in the presence of strong ( $> 10^6$  V/M) electric fields present in the electrical double layer. Induced dipole moments into polarizable modes result in infrared activation of those modes. This electrochemical Stark effect is characterized by a quadratic dependence of the intensity of the band with electric field strength. Related to this is the vibronic coupling of easily polarizable modes in charge transfer complexes to the free electron in the surface leading once more to infrared activation of those modes, and enhanced intensities.

Normal surface selection rule behavior is observed in the electroadsoption of molecules near the point of zero charge. The isomeric difluorobenzenes, for example, are observed to lie flat on a platinum surface. Out-of-plane ring modes are thus observed. When the molecular plane is forced up at an angle to the surface by various means, the in plane modes, then having non-zero values of the dipole derivative, are observed in the spectra. Anthracene, at potentials further removed from the point of zero charge, exhibits the electrochemical Stark effect, and tetracyanoethylene, when forced to adsorb at a platinum electrode, is observed to exhibit strong vibronic coupling with the surface electrons, leading to vibronic activation of normally Raman active bands.

Pulsed-Laser Atom-Probe Study of  $H_3$ ,  $N_3$  and  $NH_3$  Formation on Metal Surfaces

T. T. Tsong, C. F. Ai and Wu Liu

Physics Department, The Pennsylvania State University  
University Park, Pennsylvania 16802

The surface field must play an important role in the reactivity of a surface. This effect can be probed in field ion emission experiments. First, the applied field in these experiments is an adjustable parameter and it is of the same order of magnitude as the surface field. Second, the size of a field ion emitter resembles well a dispersed catalytically active metallic particle. We report here a study of surface catalyzed formation of  $H_3$ ,  $N_3$  and  $NH_3$  on various crystal planes of about 20 transition metals using pulsed-laser stimulated field desorption technique. In pulsed-laser stimulated field desorption, adsorbed surface species are first thermally desorbed by pulsed-laser heating of the surface. They are subsequently field ionized and detected.

Two atom-probes have been used in this study. One is the high resolution pulsed-laser time-of-flight atom-probe where desorbed ions from a small area of a few atomic-sites from a chosen crystal plane can be detected one by one. The other is the pulsed-laser imaging atom-probe where desorbed ions from the entire emitter surface are detected all at once. Using a time gating technique, however, the adsorption sites of various species can be revealed with atomic spatial resolution.

In the presence of hydrogen, nitrogen, or nitrogen-hydrogen mixed gas, the pulsed-laser atom-probe mass spectrum may contain  $H_3$ ,  $N_3$  or  $NH_3$ . The species are found to desorb from sites of rough surfaces such as the high index planes and the misplaced metal atoms by the chemisorption process. We have studied the material specificity, the surface site specificity, and the temperature and field dependence of the reactivity of the surface in the formation of  $H_3$ ,  $N_3$  and  $NH_3$  on various surfaces of about 20 transition metals. The experimental results obtained and the conclusions drawn from this study will be discussed. Principles and capabilities of these new instruments will also be described.

Work supported by DOE.

## **SESSION V**

**L. Brillson, *President*  
Xerox Corporation**

## Selective Laser-stimulated Desorption of Molecules by Internal Vibration Excitation

C. Jedrzejek

Department of Physics, Texas A&M University, College Station, TX 77843

A model of photodesorption due to a laser resonantly coupled to an internal vibration mode of the adsorbed molecule is considered. Contrary to works of Gortel, Kreuzer and collaborators<sup>1,2</sup> the model accounts for an anharmonicity of the internal vibration, broadening of energy levels of a zero-order Hamiltonian, and partly for multiphonon nature of the resonant heating mechanism. The importance of these features of the model was earlier demonstrated by the author and coworkers for thermal desorption<sup>3</sup> and laser-stimulated desorption (LSD) through the excitation of the surface bond.<sup>4</sup>

Detailed numerical calculation of the photodesorption rates as a function of a laser intensity is presented for a multilevel system of  $\text{CH}_3\text{F}$  on  $\text{NaCl}$  and compared with experimental data of Heidberg *et al.*<sup>5</sup>. Whereas the Gortel *et al.*<sup>1</sup> assumption of the harmonic oscillator for the internal vibration produced much too low necessary laser fluences for LSD, our results (the threshold intensities are  $\sim 10^5 - 10^6 \text{ W cm}^{-2}$ ) are in closer agreement with experiment. Several other model systems<sup>6-8</sup> are qualitatively discussed. More satisfactory correlation of LSD theoretical models with the existing experimental data would require clear-cut determination of important input parameters such as an adsorbate-substrate surface potential, anharmonicity and broadening of internal vibrational levels and the substrate temperature rise upon laser irradiation.

1. Z. W. Gortel, H. J. Kreuzer, P. Piercy, and R. Teshima, Phys. Rev. B **27**, 5066 (1983); Phys. Rev. B **28**, 2119 (1983).
2. Z. W. Gortel and H. J. Kreuzer, Phys. Rev. B **29**, 6926 (1984).
3. S. Efrima, C. Jedrzejek, K. F. Freed, E. Hood, and H. Metiu, J. Chem. Phys. **79**, 2436 (1983); E. Hood, C. Jedrzejek, H. Metiu, and K. F. Freed, J. Chem. Phys. (to be published).
4. C. Jedrzejek, K. F. Freed, S. Efrima, and H. Metiu, Surf. Sci. **109**, 191 (1981).
5. J. Heidberg, H. Stein, and E. Riehl, Phys. Rev. Letters **49**, 666 (1982); Surf. Sci. **126**, 183 (1983).
6. T. J. Chuang, Surf. Sci. Rept. **3**, 1 (1983).
7. F. G. Celli, M. P. Cacasa, and K. C. Janda, Surf. Sci. **141**, 169 (1984).
8. J. Lin and T. F. George, J. Chem. Phys. **72**, 2554 (1980); Surf. Sci. **100**, 381 (1980); J. Phys. Chem. **84**, 2957 (1980).

**Time Resolved Kinetic Studies of Molecular Decomposition  
on Ni(100) using Laser Induced Desorption**

S. J. Bares and R. B. Hall

Corporate Research Laboratory  
Exxon Research and Engineering  
Route 22 East, Annandale N.J. 08801

Laser induced desorption (LID) of surface bound species is rapidly developing into an important technique for studying the dynamics of the adsorbate-substrate bond. We report here the first application of this new technique to time resolved studies of reaction kinetics on a clean metal surface. In particular, measurements of decomposition rates of methanol to form the methoxy intermediate and hydrogen are described. Surprisingly, the decomposition curves cannot be interpreted assuming a simple first order rate expression; rather, a pseudo-second order rate law is invoked to explain the data. Additional insight into the methanol decomposition reaction is obtained from studies of the reaction rate dependence on the initial concentration of methanol. Preliminary results using this technique to study the decomposition of ethylene on Ni(100) will also be discussed and compared to the methanol results.

A conventional ultra-high vacuum apparatus equipped with AES,  $\text{Ar}^+$  ion sputtering, and mass spectrometer is used for these studies and has been described elsewhere.<sup>(1)</sup> Methanol ( $\text{CH}_3\text{OH}$ ) was adsorbed onto the cooled ( $< 110\text{K}$ ) Ni crystal by ambient exposure. Radiation from a q-switched Nd-YAG laser is used to desorb methanol molecules which are monitored by the mass spectrometer. By scanning the focussed laser across the Ni(100) crystal, approximately 100 independent samplings of the methanol surface coverage can be obtained.

In figure (1) we show the evolution in time of the methanol LID signal following a rapid ( 6 sec.) transition in temperature from 100 K to various reaction temperatures. At doses of methanol below saturation, app.  $4 \times 10^{14} \text{ cm}^{-2}$ , less than 10 % is lost due to thermal desorption<sup>(1)</sup>. The results of figure (1) show that a simple unimolecular rate law is not obeyed. However, the data is well represented by a second order rate expression; ie.  $d[\text{CH}_3\text{OH}]/dt = k(T)[\text{CH}_3\text{OH}]^2$ , for which a plot of  $[\text{CH}_3\text{OH}]^{-1}$  vs. time is linear with slope equal to  $k(T)$ . We calculate an energy barrier to reaction of

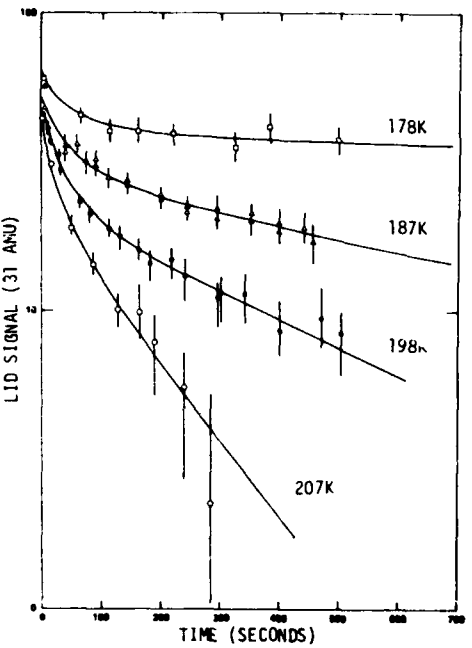


Figure 1.  
Methanol loss at various  
substrate temperatures measured  
by laser induced desorption.  
Methanol coverage =  $3.0 \times 10^{14}$   
 $\text{cm}^{-2}$ .

$8.5 \pm 0.5$  kcal/mole and pre-exponential factor equal to  $1 \times 10^{-7} \text{cm}^2/\text{sec}$ . Further studies show that decreasing the initial concentration of adsorbed methanol on the surface results in a dramatic increase in the rate of decomposition. We propose a simple model that quantitatively accounts for the observed decomposition rates:

$$-d \frac{[\text{CH}_3\text{OH}]}{dt} = [\text{CH}_3\text{OH}(t)] \cdot [S_d(t)] k_m(T) \quad (1)$$

where  $k_m$  is the two dimensional encounter frequency of  $\text{CH}_3\text{OH}$  with active sites,  $S_d$ . Note that at saturation coverage the number of adsorbed methanol molecules and active sites are approximately equal yielding the second order dependence observed in figure (1).

Preliminary studies on the decomposition of ethylene ( $\text{C}_2\text{H}_4$ ) on  $\text{Ni}(100)$  have also been performed using LID. Decomposition occurs at temperatures near 160 K with curves suggesting a unimolecular decomposition process with an activation energy of about 5 kcal/mole. Significantly higher temperatures are required to decompose  $\text{C}_2\text{D}_4$  (30 K). This isotope effect, which was not observed in methanol, will be explored in further studies.

1. R.B. Hall and A.M. De Santolo, Surf. Sci. 137, (1984), 421.

EXCITATION OF INTERACTING ADATOMS AND SURFACE-DRESSED BLOCHEQUATION

Jui-teng Lin, U.S. Naval Research Laboratory, code 6540,  
Washington, D.C. 20375 USA

The influence of a solid surface on the electronic excitation of a group of two-level adatoms and the associated power spectrum is investigated by means of a nonlinear surface-dressed Bloch equation. In the presence of a surface at a distance from the adatom which is comparable to the optical wavelength, the energy transfer dynamics is inflenced by the following factors: (i) nonradiative energy relaxation of the excited adatom via electron-phonon coupling, (ii) radiative spontaneous decay and stimulated emission caused by both the applied field and the reflected field, (iii) the oscillatory behavior of the adatom lifetime due to the interference between the applied and reflected field, (iv) the reflectivity and refraction index of the surface, (v) dipole dephasing caused by the surface phonons and plasmons, and (vi) interaction among the adatoms.

From a microscopic Hamiltonian, represented in a second-quantization form including the above described effects, and employing the many-body technique for the multiphonon coupling<sup>1</sup>, we obtain a set of nonlinear-coupled, surface-dressed Bloch equation(SBE)

$$\dot{S} = -i\Delta_{\text{eff}}S + (2cJ)WS - i\Omega W/2 \quad (1)$$

$$\dot{W} = -2\Gamma'(W-1) - (2cJ)S^2 - i\Omega(S-S^*). \quad (2)$$

Where  $S$  is the ensemble-averaged collective dipole for the interacting adatoms, assuming identical and initially populated at the ground states;  $\Delta_{\text{eff}} = \Delta - i\Gamma$  with  $\Delta = \omega_0 - \omega$  is the detuning and  $\Gamma$  is the total damping factor of the dipole;  $\Gamma' = \Gamma - \gamma_2$  is the pure energy relaxation rate, with  $\gamma_2$  being the phonon-induced dephasing factor;  $\Omega$  is the Rabi frequency

and  $c$  is the coverage (number of adsorbed atoms/area) the adatom; finally,  $J=J_1+J_2$ , with  $J_1$  being the direct dipole-dipole coupling constant and  $J_2$ , the *indirect* phonon-induced coupling among the adatoms. Note that the above SBE reduces to that of a single adatom when  $cJ=0$ , i.e., at very low coverage and/or non-interacting many-adatom system.<sup>2,3</sup> We note that at the resonance condition, the steady-state population inversion,  $W$ , is given by a cubic equation and bistability occurs when the coupling strength  $2cJ$  is greater than a threshold value,  $16P$ . This collective excitation effect caused by the direct and the indirect (phonon-mediated) interactions among the adatoms can not be found in our previously studied single adatom system.<sup>2</sup>

Other salient features of the above SBE which are significantly different from that of the ordinary surface-free Bloch equation are summarized as follows: (i) the distance and dipole orientation dependence of the energy ( $T_1$ ) and phase ( $T_2$ ) damping factors; (ii) the population-dependent dephasing factor of the dipole, second term in Eq.(1); (iii) temperature dependence of the effective frequency ( $\Delta_{\text{eff}}$ ), the direct dipole-dipole coupling ( $J_1$ ) and the phonon-mediated coupling among the adatoms ( $J_2$ ).

The energy transfer dynamics will be studied via the numerical solution of SBE and the nonlinear power spectrum for both weak field and strong field will be analyzed at various system parameters such as laser polarization, adatom concentration, adatom distance and orientations of the transition dipole. Finally, the critical parameters involved in a proposed experimental setup in which two-level atoms adsorbed on an interface system, e.g., fatty acid coated metal surface will be discussed.

---

1. J. Lin and T.F. George, *J. Phys. Chem.* 84, 2957 (1980).
2. J. Lin, X. Huang and T.F. George, *Solid. Sta. Commun.* 47, 63 (1983).
3. X. Huang, J. Lin and T.F. George, *J. Chem. Phys.* 80, 893 (1984).

Technique for Measuring Surface Diffusion by  
Laser-Beam-Localized Surface Photochemistry\*

H. J. Zeiger, J. Y. Tsao,\*\* and D. J. Ehrlich  
Lincoln Laboratory, Massachusetts Institute of Technology  
Lexington, Massachusetts 02173-0073

Summary

The surface migration of adsorbed species is a fundamental kinetic step in most surface chemical reactions, e.g., those involved in heterogeneous catalysis, thin-film growth, and etching. Consequently, numerous techniques have been developed over the years for measuring surface-migration rates. Most of these techniques, however, are only applicable to strongly bound or robust adsorbates, such as atoms and some diatomic molecules, since they involve subjecting the surface to extreme environmental conditions, such as large electric fields or electron bombardment. An ultrahigh vacuum is usually also a requirement.

Because the majority of technologically important surface chemical reactions involve at some stage weakly bound or fragile polyatomic molecules, it is of interest to develop techniques for measuring surface-migration rates of these molecules. In this paper we describe such a technique and report its application to a study of the surface migration of tetraethyl lead (TEL) adsorbed on sapphire. The technique is based on the use of a tightly focused UV laser beam to drive a highly spatially localized photoreaction, in this case the photolysis of TEL, in an adsorbed molecular layer. This reaction creates a particle sink to which parent molecules diffuse, allowing the reaction to continue. The rate at which the reaction proceeds is used as a sensitive measure of the surface-diffusion rate of the parent molecules. In the present study the reaction rate was found by measuring the absorption of the laser beam by the films deposited by TEL photolysis.

In order to obtain a general picture of surface transport near a beam-localized reaction zone and to extract parameter values from the experimental results for deposition, a general mathematical model based on the Green's function technique was formulated. The calculation assumes a uniform initial molecular coverage, which is not necessarily at equilibrium with the molecular concentration present in the gas phase at the time the laser is switched on. Replenishment of the reacting molecules takes place both by diffusion along the surface and by transport from the gas phase. The analytic expressions generated were evaluated numerically to obtain the deposition rate as a function of radial position with respect to the center of the laser spot and as a function of time for various rates of photolysis. In particular, in the high-illumination limit the radial distributions of the deposit thickness (see Fig. 1) and deposition rate are shown to deviate appreciably from the UV-beam profile.

---

\*This work was sponsored by the Department of the Air Force, in part under a specific program supported by the Air Force Office of Scientific Research, by the Defense Advanced Research Projects Agency and by the Army Research Office.

\*\*Present address: Sandia National Laboratories, Albuquerque, NM 87185.

Finally, the analysis was used to extract parameter values for the specific case of TEL adsorbed on a sapphire surface. The value obtained for the room-temperature surface diffusivity is  $7 \times 10^{-7} \text{ cm}^2/\text{s}$ . The analysis also gives the room-temperature rate and activation energy of TEL desorption, at  $\sim 1$  monolayer coverage, as  $k_{\text{des}} = 7 \times 10^{-3}/\text{s}$  and  $E_{\text{des}} = 0.13 \text{ eV}$ , respectively. The new measurement technique should be broadly applicable to studies, impractical by ultrahigh-vacuum techniques, of the surface kinetics for similar fragile and weakly bound molecules.

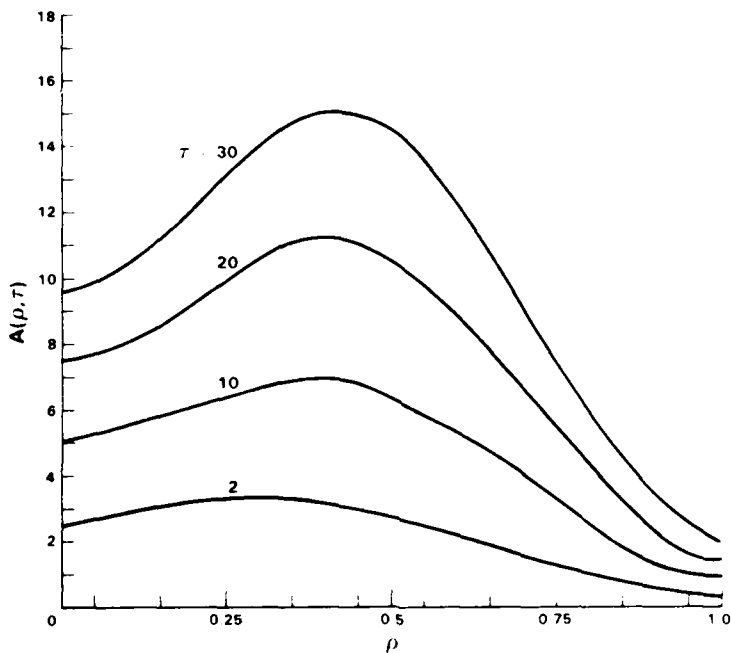


Fig. 1. Transverse profiles of the thickness,  $A(p, \tau)$ , of a deposit produced by photolysis of adsorbed parent molecules transported by surface diffusion into a laser-beam-localized reaction zone. The parameter  $p$  is the normalized radial distance from the beam center;  $\tau$  is the normalized time after the beam is switched on. The laser beam has a Gaussian width of  $p = 0.5$ .

**Characterization of Photochemical Processing**

**Masatake Hirose**

**HIROSHIMA University**

**Tokyo, Japan**

Photochemical etching processes of  $\text{SiO}_2$  in  $\text{NF}_3$  plus  $\text{H}_2$  gas and  
 $\text{GaAs}$  in  $\text{Cl}_2$  using ArF excimer laser by in-situ x-ray photo-electron  
spectroscopy.

## **SESSION VI**

**F. Pease, *Presider***  
**Stanford University**

## Recent Experiments on Photolysis for Low Temperature Epitaxy

S J C IRVINE, J GIESS, J B MULLIN, G W BLACKMORE and O D DOSSER  
Royal Signals and Radar Establishment, St Andrews Road, Great Malvern  
Worcs. WR14 3PS, UK.

The infrared detector material  $\text{Cd}_{x}\text{Hg}_{1-x}\text{Te}$  (CMT) has become the most widely used narrow gap semiconductor for photon detection, despite problems such as high volatility of Hg, high interdiffusion coefficient for Hg and Cd, fast dopant diffusion and large segregation coefficients from the melt. The key to overcoming these difficulties lies with low temperature growth of epitaxial CMT and low temperatures for device processing. Photochemical deposition offers an elegant solution to these problems by removing the need for heat to dissociate metal-organics on the substrate. This review will concentrate on the conditions needed for epitaxial growth of these materials at temperatures below 300°C, more than 100°C below temperatures required for the pyrolytic growth process.

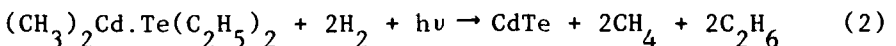
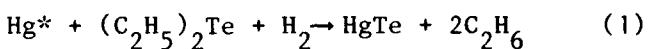
The preferred reactant materials for HgTe epitaxy by the pyrolytic route are  $(\text{C}_2\text{H}_5)_2\text{Te}$  and Hg vapours in a  $\text{H}_2$  carrier gas.  $(\text{C}_2\text{H}_5)_2\text{Te}$  does not readily photodissociate to yield Te in a region of high UV intensity when using a flow process, an alternative photochemical process is therefore needed if this metal-organic is to be used. A surface selective photochemical reaction is necessary for epitaxial growth at low temperatures, where a high supersaturation of the elements in the vapour leads to homogeneous nucleation and dust formation. In the case of HgTe epitaxy a surface photosensitisation reaction can be promoted by generating a high Hg vapour pressure which will yield a high surface coverage in Hg. Selective excitation of the absorbed Hg using a high pressure Hg arc lamp can lead to dissociation of  $(\text{C}_2\text{H}_5)_2\text{Te}$  by interaction with excited Hg decaying to the ground state.

Epitaxial layers of HgTe have been grown over the temperature range 200°C to 300°C and their crystalline quality has been assessed. Also, results on surface quality and surface/layer interface sharpness will be presented.

The absence of a vapour phase photochemical reaction releasing Te from  $(\text{C}_2\text{H}_5)_2\text{Te}$  is an advantage as it enables the surface reaction to proceed without particles of Te or HgTe forming in the vapour. However, CdTe does form readily from a vapour phase reaction when using the metal-organics  $(\text{CH}_3)_2\text{Cd}$  and  $(\text{C}_2\text{H}_5)_2\text{Te}$ , probably from UV absorption by the adduct  $(\text{CH}_3)_2\text{Cd} \cdot \text{Te}(\text{C}_2\text{H}_5)_2$ . Here the homogeneous nucleation problem is more severe than

say for Cd, CdTe is very stable and therefore equilibrium vapour pressures are very low; eg at 250°C Cd pressure over CdTe is  $\sim 10^{-12}$  atm compared with  $\sim 10^{-5}$  atm over pure Cd. Some results showing the effects of this homogeneous nucleation will be given and contrasted with the high quality HgTe films grown by photosensitisation.

In order to suppress this vapour phase reaction, the metal-organic precursors could be replaced by metal-organics not absorbing in the UV which can then be dissociated by Hg photosensitisation. An alternative approach is to modify the carrier gas which can be a reactive constituent. For the photosensitisation reaction to grow HgTe and for the vapour phase photochemical reactions we have:



By replacing hydrogen with an inert carrier gas, radicals such as  $\text{CH}_3$  and  $\text{C}_2\text{H}_5$  will have longer life-times in the vapour and can recombine with the metal-organic molecules; in the case of CdTe, avoiding vapour phase nucleation.

Growth experiments on HgTe growth using an inert carrier gas have shown that the surface reaction is largely unaffected. However, a dramatic reduction in vapour phase nucleation is observed for CMT and CdTe growth when an inert carrier gas is used. The quality of CMT and CdTe films grown using an inert gas will be discussed together with SIMS results on the abruptness of heterostructure interfaces.

## THE MECHANISMS OF III-V MOVPE AND ROUTES TO A UV-ASSISTED PROCESS.

J. Haigh, British Telecom Research Laboratories, Ipswich IP5 7RE, UK

The epitaxial growth of III-V compounds by co-pyrolysis of Group III metal alkyls and Group V hydrides constitutes one application of the well-known technique of MOVPE (metallo-organic vapour phase epitaxy). Recently interest has been aroused in the possibility of photolytic enhancement of the process. Encouraging results have been reported [1,2] with GaAs. Photolysis and pyrolysis, at least in the case of the simpler metallo-organics, lead to rather similar products, and this implies that the initial stages are chemically similar and potentially compatible. The motivation for developing a photolytic/pyrolytic process derives primarily from the high spatial resolution of photon fluxes compared with conductive or radiative heat sources.

In order to develop such a technique more needs to be known about the mechanism of the pyrolytic process, in particular with regard to its relationship to other epitaxial deposition processes. It has recently been shown [3] that III-V MOVPE does not proceed via gas-phase production of Group III metal atoms from the alkyls. Since there are three metal-carbon bonds in, for example, the MOVPE precursor  $\text{In}(\text{CH}_3)_3$ , this implies that breaking of the third metal-carbon bond occurs on the semiconductor surface, and thus the surface stage of the process is qualitatively different from that in, for example, molecular beam epitaxy. However it leaves open the question of whether the first and second of the three metal-carbon bonds break on the surface or in the gas phase. By contrast, complete gas-phase pyrolysis of the group V precursors, the hydrides  $\text{PH}_3$  and  $\text{AsH}_3$ , producing species such as  $\text{P}_4$ ,  $\text{P}_2$ ,  $\text{As}_4$  or  $\text{As}_2$ , seems to occur or at least be permissible in an optimised system.

Under the range of conditions where MOVPE is reaction-kinetics limited surface processes appear to be the rate-determining factor [4]. Different surfaces show distinct differences in their ability to catalyse group III - carbon bond-breaking [5,6]. These differences undoubtedly reflect differences in ability to bond the electron-deficient Group III and electron-rich Group V species. Recently thermal desorption studies have begun to yield information on the relative strengths of such surface bonding.

A role for uv in MOVPE enhancement could in principle exist in three areas.

- 1) To modulate the extent of gas-phase bond-breaking, by direct photolysis.
- 2) To modulate the rate of surface metal-carbon bond-breaking.
- 3) To modulate the rate of surface atomic migration and crystal lattice formation, by direct surface electron-hole pair creation.

The limited evidence available does not yet enable clear distinctions to be made between these hypothetical processes. It is important to identify which of them is the most beneficial, since this governs the choice of uv wavelength and of the experimental configuration.

#### REFERENCES

1. I. A. Frolov, D. L. Druz', P. B. Boldyrevskii and E. B. Sokolov, Izv. Akad. Nauk S. S. S. R. Neorg. Mat. 13, 1977, 906.
2. N. Putz, H. Heinecke, G. Arens, M. Heyen, H. Luth and P. Balk, presented at Second Int. Conf. on MOVPE, Sheffield 1984.
3. J. Haigh and S. O'Brien, J. Crystal Growth 67, 1984, 75.
4. D. H. Reep and S. K. Ghandhi, J. Electrochem. Soc. 130, 1983, 675.
5. M. G. Jacko and S. J. W. Price, Can. J. Chem. 42, 1964, 1198.
6. J. Haigh and S. O'Brien, J. Crystal Growth to be published.

Studies of Laser Chemical Vapor Deposition  
Using Surface Sensitive Infrared Photoacoustic Spectroscopy

G. S. Higashi, L. J. Rothberg and C. G. Fleming  
AT&T Bell Laboratories, Murray Hill, NJ 07974

We report vibrational spectra of surface adsorbates during KrF laser assisted chemical vapor deposition (CVD) of Al films from trimethylaluminum (TMA) on single crystal sapphire substrates. The pulsed optoacoustic technique used has submonolayer sensitivity to O-H and C-H infrared active stretching vibrations and allows studies of the interactions between adsorbed H<sub>2</sub>O and TMA on surfaces prior to deposition. It also provides information about film composition during the early stages of laser stimulated growth. In addition, because surface Al-CH<sub>3</sub> groups can be observed directly, the role of surface phase photochemistry in laser CVD can be investigated.

Tunable pulsed infrared radiation (between 2800 and 3800 cm<sup>-1</sup>, bandwidth <1 cm<sup>-1</sup>) is passed through a sapphire substrate upon which a piezoceramic transducer is edge bonded. The laser radiation absorbed by the sample is converted into heat and the corresponding thermal expansion generates acoustic waves which are monitored by the voltage transient across the piezoelectric. Since the substrate is transparent at these wavelengths, acoustic signals monitored by the transducer originate from energy absorbed by surface adsorbates.

Fig. 1a plots the normalized acoustic signal intensity (or infrared absorbance) versus laser frequency for a sample which was acid etched, baked, dosed with water and finally exposed to multiple flushes of TMA. The feature around 2960 cm<sup>-1</sup> is an absorption peak associated with the asymmetric C-H stretching mode of Al(CH<sub>3</sub>)<sub>x</sub> at about a monolayer coverage as gauged by an adsorption isotherm of TMA taken using infrared adsorbances. The sharp peak at 3300 cm<sup>-1</sup> does not participate in surface chemistry and is probably due to O-H stretching vibrations of subsurface hydrogen. The very broad peak (~400 cm<sup>-1</sup> wide) at ~3500 cm<sup>-1</sup> reflects "hydrogen bonded" O-H stretching vibrations from a little less than a monolayer of adsorbed water. Approximately this same water coverage was present prior to TMA dosing, surprising in light of the explosive reaction between vapors of TMA and H<sub>2</sub>O. Since water is a common surface contaminant, a surface with coexisting water and organometallic species may be typical of a starting surface for laser CVD.

We initiate film growth (Fig. 1b-d) by illuminating the sample with KrF (248 nm) laser radiation in the presence of 250 mtorr of TMA. The surface vibrational spectra in scans b through d show the result of successive irradiations and three trends are observed. A large increase in the Al-CH<sub>3</sub> content occurs, a broad background absorption begins to grow, and the surface water content is reduced. The broad background absorption most likely indicates that we are beginning to form a metallic film. We infer from the high surface methyl content that the film is probably composed of Al/Al(CH<sub>3</sub>)<sub>x</sub> clusters. Unsaturated Al in the clusters would be highly reactive and may be responsible for gettering the surface hydroxyl groups.

To explore the role that surface phase photodecomposition plays in the film growth process, a sample chamber was evacuated (<10<sup>-6</sup> torr) after recording

the spectrum of Fig. 1d and the sample was irradiated with 110,000 KrF laser pulses of  $\sim 15 \text{ mJ/cm}^2$ . No change in the spectrum due to irradiation is observed, indicating that at 248 nm one photon desorption of methyl groups occurs with cross-section less than  $\sim 10^{-22} \text{ cm}^2$ .

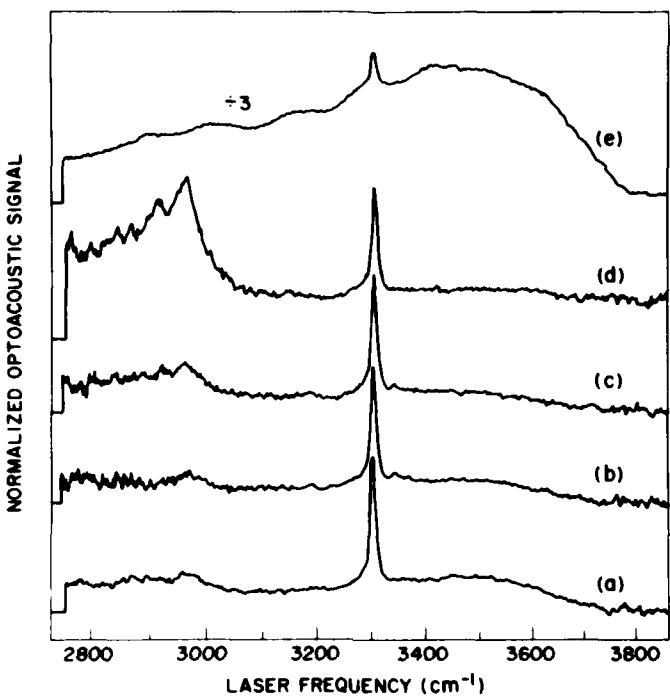


Fig. 1(a) Sample acid etched, baked at 140°C for 3 hrs., exposed to 250 mtorr of water and finally to 5 flushes of TMA at 250 mtorr.

Irradiated at 248 nm under 250 mtorr of TMA for  
 (b) 3,000 pulses at  $2 \text{ mJ/cm}^2$   
 (c) 45,000 pulses at  $5-10 \text{ mJ/cm}^2$   
 (d) 150,000 pulses at  $10-20 \text{ mJ/cm}^2$   
 (e) Dosed with 250 mtorr of water following (d).

Note that extreme left portion of scans indicates level of zero absorption.

Subsequent exposure of this sample to water vapor (Fig. 1e) illustrates two important points. First, the huge increase in water absorption reflects the high surface area of the film and, second, the disappearance of the C-H feature confirms its having been ascribed to species with Al-C bonds.

We have demonstrated monolayer sensitivity to O-H or C-H carrying molecular species using a pulsed optoacoustic technique. Surface chemistry has been studied prior to and during KrF laser CVD of Al from TMA. Surprisingly, we observe that adsorbed  $\text{Al}(\text{CH}_3)_x$  and  $\text{H}_2\text{O}$  coexist on our surfaces prior to deposition. We also find that KrF laser stimulated desorption of surface methyl groups does not play a major role in our Al film growth. The growth apparently proceeds via cluster formation originating with gas phase photo-decomposition of TMA.

**Laser-Induced Selective Deposition of Micron-size Structures on  
Silicon by Surface Reduction of Tungsten Hexafluoride**

Y.S. Liu, C.P. Yakymyshyn, H.R. Philipp,  
H.C. Cole and L.M. Levinson,

General Electric Research and Development Center  
Schenectady, New York, 12301

Selective deposition of refractory metal and metal silicide on silicon induced by a focussed Argon laser beam is reported. Micron-size lines with extremely good surface smoothness were observed at a writing speed of 7 cm/sec. Deposition mechanism and properties of fine structures are discussed.

Recently, Ehrlich and Tsao (1) have reported the fabrication of 0.2  $\mu$ m poli-Si lines by pyrolytically depositing polysilicon in  $SiCl_4/H_2$  vapor using an Argon laser beam. Since the rate of chemical reactions depends nonlinearly upon the local temperature, the line-width drawn was significantly narrower than the laser beam size. This result was significant in demonstrating the feasibility of writing sub-micron structures with a laser beam using the nonreciprocal nature of the laser-microchemical processing technique. The writing speed of this specific technique was, however, very slow.

In this study, micron-size (About 1 micron has been achieved to date.) lines were selectively deposited on silicon using a focussed Argon laser with a beam spot size of about 20 microns. Deposition was induced by surface reduction of tungsten hexafluoride on silicon. The nonlinearity exhibited by localization of the chemical reaction significantly reduced the feature dimension of deposited lines from the focussed laser spot size. At a writing speed 7 cm/sec, which was limited by the translating stage used in the study, fine line structures with excellent surface smoothness were obtained. This finding has demonstrated, for the first time, the feasibility of writing structures of micron dimension at a high speed with a laser beam.

The chemical pathway for tungsten deposition, as reported in several previous studies, is believed to be initiated via surface-reduction of tungsten hexafluoride by silicon at a temperature of about 350 C. Higher temperature leads to the formation of tungsten silicide. In thermal CVD, hydrogen is used for reducing tungsten hexafluoride to form thicker metal film. (2) Consequently, tungsten hexafluoride and silicon offer an interesting system for studying both surface- and gas- phase reaction kinetics which are frequently observed under a laser-induced chemical vapor deposition condition. Furthermore, selective deposition of the refractory metal has drawn increasing interest for its future applications in VLSI technology.

In this paper, we will examine the mechanism which leads to the formation of micron size structures. By using a reflectivity measurement technique, equipped with a scanning laser beam with a spatial resolution of microns, the surface reflectivity of fine lines deposited was measured and compared with morphology examined with Nomarski micrographs and SEM. In addition, the structure and composition of the deposited lines were analysed using a scanning Auger spectrometer. Formation of tungsten silicide was observed and results will be discussed.

REFERENCE:

1. D.J. Ehrlich and J.Y. Tsao, *Applied Physics Letters*, Vol.44, p. 267, (1984)
2. T.Moriya, S.Shima, Y.Hazuki, M.Chiba, and M.Kashiwagi, *Intern. Elect. Devices Meeting (IEDM)*, Technical Digest, p.550, (1983)

Laser-Initiated Dry Etching of  $\text{SiO}_2$ 

Jack O. Chu, George W. Flynn, Peter D. Brewer, and Richard M. Osgood, Jr.

Columbia Radiation Laboratory and

Departments of Chemistry and Electrical Engineering

Columbia University, New York, N. Y. 10027

In general photochemical (drying etching) process of thin films based on (UV) laser-initiated chemistry is difficult to investigate both mechanistically and kinetically. Some of the most important questions are concerned with the photo-formation of the reactive species and their (reactive) chemical interaction with the surface. The UV-laser assisted etching of  $\text{SiO}_2$  from photolysis of  $\text{CH}_2\text{CHF}$  is quite attractive for mechanistic studies of the etching process because of the relative simple (in-situ) application of IR (time-resolved) fluorescence and absorption techniques to monitor both the HF etchant and the  $\text{SiF}_4$  products within the gas-surface system. The strong oscillator and absorption strength of the HF molecules makes it possible to monitor its photo-production and follow the subsequent etching reaction with the  $\text{SiO}_2$  surface. Moreover, high resolution and sensitive diode laser absorption probes can be used to investigate the surface products ( $\text{SiF}_4$ ,  $\text{SiF}_3$ ,  $\text{SiF}_2$  and  $\text{SiF}$ ) in the gas phase.

Photochemical etching of masked  $\text{SiO}_2$  films has been performed under two laser-substrate configuration with the incident laser beam being parallel (indirect) or perpendicular (direct) to the sample surface. The indirect configuration serves mainly to probe the photochemical interaction of pure gas-phase photodissociation with the surface. Using this orientation we have measured the etched depth as a function of laser energy density. This plot (see Fig. 1) essentially exhibits a linear dependence with laser power. In the direct-orientation processing, the etched depth shows a faster etch rate as a function of energy density (as expected from a geometric consideration), and a linear dependence with the  $\text{CH}_2\text{CHF}$  pressure.

Infrared emission from HF molecules has been directly observed following 193nm photoelimination of  $\text{CH}_2\text{CHF}$  in both the absence<sup>(1)</sup> and presence of the  $\text{SiO}_2$  surface.

(1) M.J. Berry and G.C. Pimentel, *J. Chem. Phys.* 51, 2274 (1969)

\*Work supported by the Joint Services Electronics Program (U.S. Army, U.S. Navy, and U.S. Air Force) under contract DAAG29-82-K-0080. Equipment support provided (to G. W. F.) under NSF grant CHE8023747 and D.O.E. contract DE-AC02-78ER04940.

## **SESSION VII**

**P. Liao, *Presider***  
**Bell Communications Research**

**INTERFACE STUDIES BY OPTICAL SECOND HARMONIC GENERATION**

Y. R. Shen

Department of Physics  
University of California  
Berkeley, California 94720

and

Materials and Molecular Research Division  
Lawrence Berkeley Laboratory  
Berkeley, California 94720

Optical second harmonic generation has recently been shown to be an effective probe for surface studies. Its surface specificity derives from the fact that the process is generally forbidden in a bulk with inversion symmetry but always allowed at a surface or interface. As an optical technique, the method has the advantages of being non-destructive, capable of ultrafast time resolution, and applicable to interfaces between condensed media. We consider here only applications of the method to studies of molecular adsorption at interfaces.

Molecular adsorption at an interface modifies the surface nonlinearity in two ways: the adsorbed molecular layer can be nonlinear, and the interaction between the molecules and the substrate can effect a change in the surface nonlinearity. The first mechanism often dominates when the adsorbed molecules are large and highly nonlinear. We describe a few experiments in which second harmonic generation is used to study adsorption of large organic molecules at air/solid, liquid/solid, and air/liquid interfaces. It is seen that with this technique, the adsorption isotherm, the symmetry of molecular arrangement, the orientation of molecular adsorbates, and the orientational phase transition can all be measured. Spectroscopic information about the adsorbates can also be

obtained. The second mechanism often dominates in the case of chemisorption of small molecules on metals and semiconductors. We take CO adsorption on transition metals and oxidation of silicon as examples. The experiments carried out in ultrahigh vacuum show that the technique can be used to monitor the time development of adsorption and desorption, and is sensitive to adsorption on different surface sites. Since second harmonic generation detects molecules left on the surface, it acts as a complimentary technique to thermal desorption spectroscopy for surface analysis. Other possible applications and extensions of the technique will be discussed.

**Real-time Monitoring of Surface Reactions on Si(111) by Optical Second-Harmonic Generation**

T. F. Heinz, M.M.T. Loy, and W. A. Thompson  
IBM T.J. Watson Research Center, Yorktown Heights, NY 10598

The sensitivity of optical second-harmonic generation (SHG) to atomic and molecular monolayers absorbed on surfaces of centrosymmetric media has now been well established.<sup>1</sup> Recent work has also demonstrated the dependence of the SHG process on the ordering and symmetry of the surface region.<sup>2</sup> In this paper, we apply the surface SHG technique to follow in real time some widely studied and technologically important reactions occurring on clean, well-defined Si(111)-7x7 surfaces. We discuss here both the oxidation of the Si surface and the formation of thin layers of disordered and epitaxial Pd silicide.

Our experiments were conducted in a standard vac-ion pumped ultrahigh vacuum chamber at a base pressure of better than  $10^{-10}$  Torr. Laser excitation was provided at  $1.06\mu\text{m}$  by a Q-switched Nd:YAG laser producing 8 ns pulses at a 10 Hz repetition rate. For the measurements reported here, the reflected SH signal was collected with pump radiation striking the sample at normal incidence and polarized along the [011] direction in the surface plane. The pump energy was held to  $< 10$  mJ/pulse in a 1mm-diameter spot, which was found to be sufficiently low to avoid any laser-induced changes in the sample. The Si(111)-7x7 surfaces, prepared by annealing silicon surfaces cleaved *in situ*, were exposed to oxygen leaked into the chamber and Pd atoms evaporated from a resistively heated filament.

The data in Fig. 1 show the effect of exposure of the Si(111)-7x7 surface to O<sub>2</sub>. The SH signal (polarized along the [211] direction) is displayed as a function of elapsed time or, equivalently, of exposure in Langmuirs since the measurement was taken with O<sub>2</sub> at  $10^{-6}$  Torr. The SH signal stabilizes at a very low level after an exposure of  $\cong 200$  Langmuirs, as expected for the oxidation of the Si surface at room temperature. In Fig. 2, we present the corresponding results for Pd deposition. With the aid of a quartz crystal monitor, we determined that the rate of Pd mass deposition was 0.04 Å/sec. The SH signal is again seen to fall sharply as the surface layer of the sample is modified during the deposition of 2-3 monolayers of Pd. The second part of the Figure shows the SH intensity during an annealing cycle after the Pd deposition has been stopped. The annealing process consisted of heating the sample from room temperature to 400 C and then maintaining the sample at that temperature. Note sudden increase in the SH signal to roughly 20% of the value for the clean Si(111)-7x7 surface.

For the normally incident pump radiation used in these measurements, the surface can contribute to the SHG only if it lacks a center of inversion in the plane. Consequently, a completely disordered surface would not exhibit any nonlinear response. The dramatic decrease in the SH intensity observed during oxygen exposure (Fig. 1) is expected since the oxidation process is known to disrupt the surface structure severely. The weak residual SH signal remaining after oxidation can be attributed to the magnetic-dipole and electric-quadrupole terms in the bulk Si.<sup>3</sup> As indicated by the dotted curve in the Figure, we can fit the observed SH signal quite well by assuming Langmuir adsorption kinetics and a surface nonlinear susceptibility proportional to the area of the unreacted portion of the surface. From this analysis we can deduce a sticking coefficient for O<sub>2</sub> on the Si(111)-7x7 surface.

The decrease in the SH intensity during Pd deposition can also be understood as the result of a disordering of the surface. It is known, however, that an epitaxial  $Pd_2Si$  layer can be formed by a mild thermal annealing.<sup>4</sup> We associate the abrupt rise in the SH signal observed upon heating the sample with the creation of such an ordered silicide layer. These data constitute what we believe is the first direct time-resolved measurement of thermally driven surface ordering in silicides. We have also obtained results on the symmetry of the annealed silicide layer by means of an analysis of the polarization dependence of the SH radiation.

In conclusion, we have utilized the SHG technique to study reactions at the surface of Si(111)-7x7. Oxidation of the surface and the presence of Pd (both in ordered and disordered phases) can be detected with monolayer sensitivity. This optical method is nondestructive and should be applicable in a wide variety of environments. As we have demonstrate here, the technique is particularly well-suited for real-time measurements.

This work was supported in part by the U.S. Office of Naval Research.

#### References

1. H. W. K. Tom *et al.*, Phys. Rev. Lett. **52**, 348 (1984).
2. T. F. Heinz and M. M. T. Loy, to be published.
3. H. W. K. Tom, T. F. Heinz, and Y. R. Shen, Phys. Rev. Lett. **51**, 1983 (1983).
4. S. Okada, K. Oura, T. Hanawa, and K. Satoh, Surface Sci. **97**, 88 (1980).

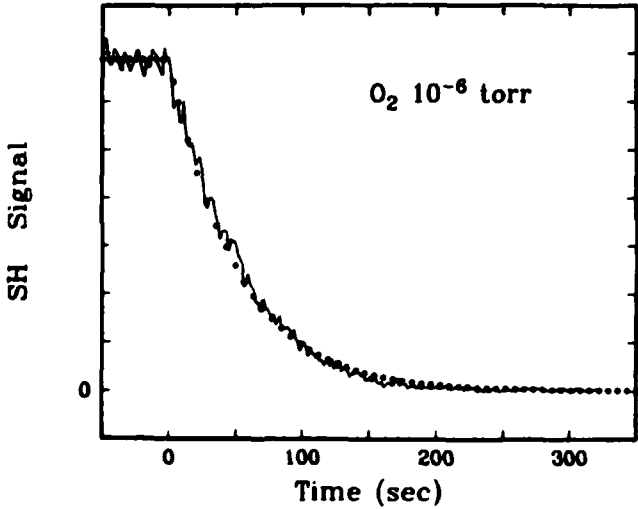


Fig. 1

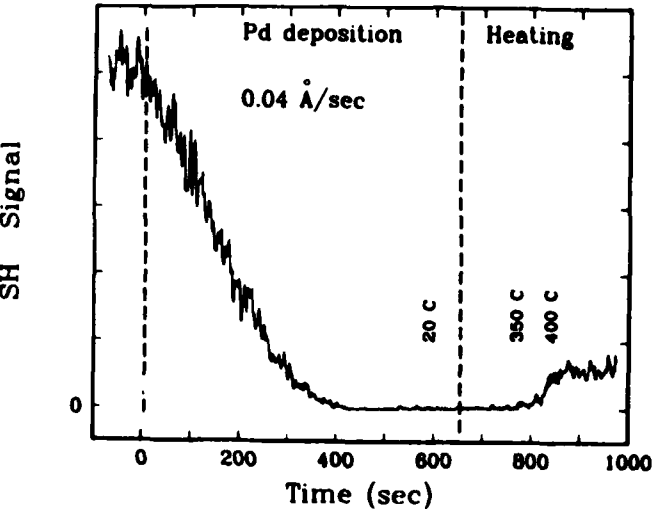


Fig. 2

**Figure 1** SH signal from the Si(111)-7x7 surface as a function of exposure time to  $O_2$  at  $10^{-6}$  Torr. The dotted curve is a theoretical fit based on Langmuir kinetics.

**Figure 2** SH signal during the evaporation of Pd and the subsequent thermal annealing cycle.

## Second Harmonic Generation Studies of Adsorption and Reorientation at Electrode Surfaces

D.F. Voss, K.A. Bunding, M. Nagumo, and L.S. Goldberg  
Naval Research Laboratory, Washington, DC 20375

Second harmonic generation at surfaces (SSHG) has recently been the subject of increasing interest among researchers who require a probe of interfacial phenomena that is both surface-specific and can be utilized in condensed phase studies (see [1] and references therein). SSHG belongs to a larger class of second order nonlinear optical processes that includes optical rectification, sum and difference frequency mixing, and the Pockles effect, all of which are symmetry forbidden in isotropic media (at least in the electric dipole approximation [1]). At an interface between dissimilar media the isotropy which may be present in the bulk material is disturbed, and processes such as second harmonic generation can occur. This property is attractive for probing surface phenomena because only very weak electric quadrupole and magnetic dipole signals are generated in the bulk material. Furthermore, SSHG is an optical effect and requires only transparency of the media at the fundamental and harmonic wavelength, rather than the more stringent condition of ultrahigh vacuum imposed by electron and ion probes.

For these reasons several groups have been employing SSHG for investigations of phenomena occurring at electrode surfaces [1-3] which show contributions from surface charge density, adsorbate coverage, and orientation. All of the systems studied to date have involved either inorganic electrolyte constituents or non electroactive organic species. We report observations of SSHG of 4,4'-bipyridine (bipy) on silver and gold electrodes [4] in sulfate solution, in which irreversible electrochemistry occurs, and in perchlorate/phosphate buffer, in which reversible electrochemistry is seen. Formation of different electrochemical species and adsorbate reorientation is manifested in the SSHG polarization dependence.

In our experimental configuration the 1.06  $\mu\text{m}$  output of a CW mode-locked Nd:YAG laser is focussed onto the working electrode at 45 degrees incidence angle. The 532 nm second harmonic signal is collected with f/1 optics and detected with a photomultiplier. The fundamental beam is chopped and the SSHG signal sent to a lock-in amplifier to improve the signal to noise ratio. The fundamental beam polarization is adjustable and the SSHG signal polarization is analyzed before entering the PMT. The electrochemical cell is the standard three electrode configuration with the working electrode maintained under potentiostatic control at all times (voltage referenced to an Ag/AgCl electrode in 3M KCl solution). The cell solution is bubbled with inert gas before a voltage scan to remove dissolved oxygen and the cell is covered with the gas during a scan to keep the solution deaerated.

SSHG signals from both evaporated and mechanically polished bulk electrodes were investigated. The SSHG signal from the smooth evaporated gold and silver electrodes was polarized parallel to the plane of incidence (P-polarization) and yielded very little signal polarized perpendicular to the plane of incidence (S-polarization), as expected [1]. The mechanically polished electrodes (0.3  $\mu\text{m}$  alumina), however, generated a substantial amount of depolarized SSHG, indicating a high degree of roughness. We are attempting to correlate the depolarization ratio with the polishing procedure to better control the surface preparation.

An example of SSHG signals in the presence of an electroactive species

(bipy) on mechanically polished silver is shown in Fig. 1. 10 mM of bipy was dissolved in 0.1 M sodium sulfate, yielding the cyclic voltammogram in Fig. 1A. The scan was started at -0.5 V (vs. Ag/AgCl) and swept at 10 mV/sec between -1.2 V and 0.0 V. On the cathodic sweep reduction of the bipy is seen [4] at -1.2 V, while the anodic sweep shows a complex irreversible oxidation between -0.7 V and -0.4 V. The corresponding SSHG signals for different input laser polarizations are shown in Figs. 1B (P-polarization) and 1C (S-polarization). The signal is maximum at -0.6 V in both cases (possibly indicating adsorption of the organic species at the potential of zero charge) during the cathodic sweep and decreases to a minimum at -1.1 V at the onset of the first one-electron reduction of the bipy. During the anodic sweep the signal is diminished but shows an interesting polarization dependence, possibly a voltage dependent reorientation of the adsorbate or formation of different electrochemical species on the electrode.

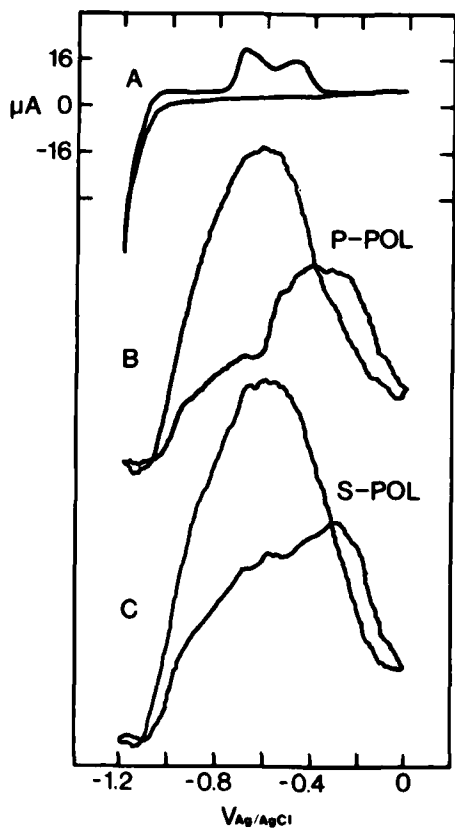


Fig. 1. A: Cyclic voltammogram of 10 mM bipy in sulfate on Ag. B: SSHG signal for P-polarized input. C: SSHG signal for S-polarized input.

1. Y.R. Shen, The Principles of Nonlinear Optics, Wiley, 1984
2. G.L. Richmond (1984) Chem. Phys. Lett. 106, 26-29
3. R.M. Corn et. al. (1984) Chem. Phys. Lett. 106, 30-35
4. T.M. Cotton et. al. (1984) Chem. Phys. Lett. 106, 491-497

Time-Resolved Vibrational Energy Relaxation  
of Surface Adsorbates

E. J. Heilweil, M. P. Casassa, R. R. Cavanagh, and J. C. Stephenson

Molecular Spectroscopy Division  
Physics Building - Room B268  
National Bureau of Standards  
Gaithersburg, MD 20899

Many chemical and physical processes that occur at solid interfaces may be better understood from the measurement of energy flow within adsorbate and substrate vibrational modes. In order for a chemical transformation to occur along a reaction coordinate, for example, specific molecular bond vibrational excitation followed by dissociation and reformation is required. With the advent of ultrashort optical pulse technology, we are now in a position to directly monitor the ultrafast kinetics of energy decay of vibrational modes in condensed-phase molecular systems. While such measurements have been conducted for gas and liquid phase systems, there have been no previous reports of measurements of energy relaxation in chemically relevant surface species. We have thus undertaken a course of research to directly investigate the vibrational relaxation dynamics of molecules adsorbed on high surface area metal oxides.

An infrared pump/probe method using tunable picosecond pulses has been used to measure the vibrational population decay rates ( $T_1^{-1}$ ) of ground electronic state  $v=1$  vibrational modes. Our initial measurements were conducted on the surface hydroxyl group (-OH) bound to colloidal fumed silica (120Å diameter particles with  $200 \text{ m}^2/\text{gm}$  surface area) dispersed in liquid  $\text{CCl}_4$  at room temperature.<sup>1</sup> Such samples exhibit strong infrared absorptions in the  $3000\text{-}4000 \text{ cm}^{-1}$  region which arise from the isolated  $\text{SiOH}$  group ( $3691 \text{ cm}^{-1}$  with  $50 \text{ cm}^{-1}$  FWHM) and molecular physisorbed water ( $\sim 3400 \text{ cm}^{-1}$ ). The surface hydroxyl  $v=0\rightarrow 1$  transition was excited with a strong IR pulse which transferred about 10% of the population to the  $v=1$  level. As the population relaxes, the transient increase in sample transmission ( $T$ ) returns to its steady-state value ( $T_0$ ). The transmission of a second weak IR pulse as a function of time is therefore a measure of the  $v=1$   $T_1$  lifetime. It was found that the  $v=1$  population for isolated surface OH groups on silica in  $\text{CCl}_4$  decays exponentially with a characteristic lifetime of  $T_1 = 150 \text{ ps}$ , or roughly  $10^4$  vibrational periods.

The above experiment measures only the  $v=1$   $T_1$  lifetime of the highly anharmonic OH oscillator on the silica surface. It does not ascertain where the energy flows or by what mechanism(s). Studies of OH on silica in vacuum (pressed disk), with coadsorbates and in various organic solvents have also been performed. Additional measurements of the  $-\text{SiOD}$ ,  $-\text{SiNH}_2$  and  $-\text{SiOCH}_3$  species and of  $\text{BCl}_3$  (-BOH) modified silica have revealed that the dominant relaxation pathway is most likely through local vibrational modes of the adjacent surface subunit (the  $\text{SiO}_4$  tetrahedron).

While the precise mechanism for surface vibrational relaxation of these systems is unclear at present, it appears that the presently known  $T_1$  lifetimes for surface species on silica may have chemical importance. It will be argued that vibrational energy, which apparently remains localized for periods longer than molecular reorientation and gas or liquid phase reactant diffusion can become available for surface reaction.

Supported in part by the Air Force Office of Scientific Research.

---

<sup>1</sup>E. J. Heilweil, M. P. Casassa, R. R. Cavanagh, and J. C. Stephenson, *J. Chem. Phys.*, 81, (6) 1984.

## **SESSION VIII**

**K. Kompa, *Presider*  
Max Planck Institute**

## Survival of vibrationally-excited Nitric Oxide Scattered from LiF(100) Surface: Angular and Velocity Analysis

J. Misewich, H. Zacharias, and M. M. T. Loy  
IBM T.J. Watson Research Center, Yorktown Heights, NY.

The role of internal energy in the scattering of molecular beams from surfaces has recently attracted much attention.<sup>1-3</sup> Most of these experiments however are confined to the scattering of molecules distributed over the lowest few rotational levels of the ground vibrational state. In the experiments presented here, laser spectroscopic techniques are utilized to perform state-to-state molecular beam scattering experiments. Two laser beams intersect the molecular beam: tunable infrared laser radiation excites the incident molecular beam to a single vibrational-rotational state then tunable ultraviolet laser radiation state-selectively probes the molecular beam through two photon resonance enhanced ionization. The beam of vibrationally excited molecules is well defined in time allowing the direct determination of velocity distributions for a laser-selected state by taking time-of-flight spectra at various probe laser positions. We report here the angular and velocity distribution of vibrationally excited molecules that we have observed surviving the collision with a freshly cleaved LiF(100) surface.

The apparatus used in this experiment has been described previously.<sup>4</sup> Briefly, a supersonic expansion beam of 10% NO seeded in Helium (total backing pressure 450 torr) is collimated by a skimmer. The molecular beam is crossed by tunable infrared radiation produced by difference frequency mixing in a lithium iodate crystal of  $\sim 590$  nm output of a Nd:YAG-pumped dye laser and 532 nm second harmonic of the Nd:YAG fundamental. The intra-red is tuned to the  $R_{11}(J''=1/2)$  line at  $1876.076 \text{ cm}^{-1}$  to populate a single rotational state ( $v'=1, J'=3/2, \Omega'=1/2$ ). Resonantly enhanced ionization via the  $X \rightarrow A \gamma(0-0)$  and  $\gamma(1-1)$  bands was used to state specifically detect the NO molecules. The tunable UV (224 nm) was produced by frequency doubling the output of a XeCl excimer pumped dye laser in potassium pentaborate.

LiF(100) was prepared for this experiment by making a fresh cleave just prior to pumpdown of the vacuum system. In a SIMS investigation of air cleaved and vacuum cleaved LiF surfaces, Estel et. al.<sup>5</sup> have shown that LiF cleaved in air and then mounted in a vacuum system and pumped down exhibit only contaminations far below the monolayer regime.

Figures 1 and 2 show the ionization signal as a function of the delay time between the IR excitation pulse and the UV probe pulse. Both laser pulses are on the order of a few nanoseconds; the microsecond time scale of the experiment is determined by the overlap of the laser and molecular beams. As shown in figure 1, this arrangement produces an effective molecular beam pulse of about 2 microseconds FWHM. This allows for direct velocity analysis of the incident and scattered molecular beams by simply taking time-of-flight spectra at different probe laser positions. An analysis of time of flight data indicates an incident velocity of  $1.42 \times 10^5 \text{ cm/sec}$  and a scattered radial velocity at the specular angle (45 deg) of  $1.1 \times 10^5 \text{ cm/sec}$ . Further, the angular distribution was found to be narrow and specular as illustrated in figure 3. These angular and velocity distributions indicated that the magnitude of the component of momentum parallel to the surface decreased by 30%, about the same amount as that of the normal component. Thus, the simple cube model clearly cannot describe this process.

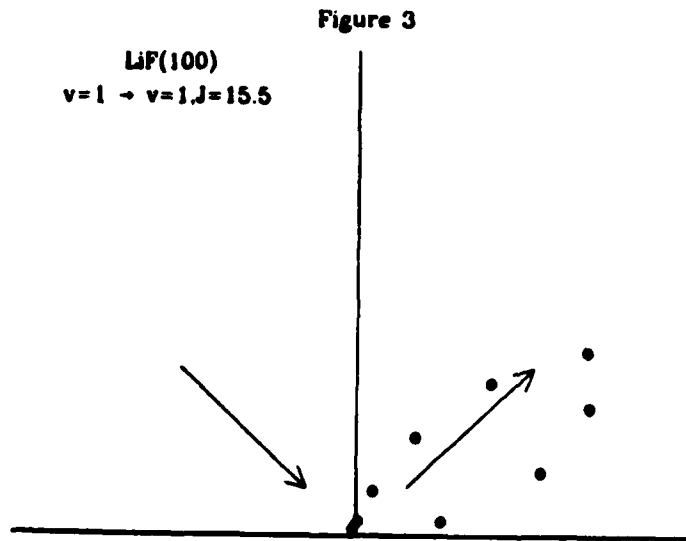
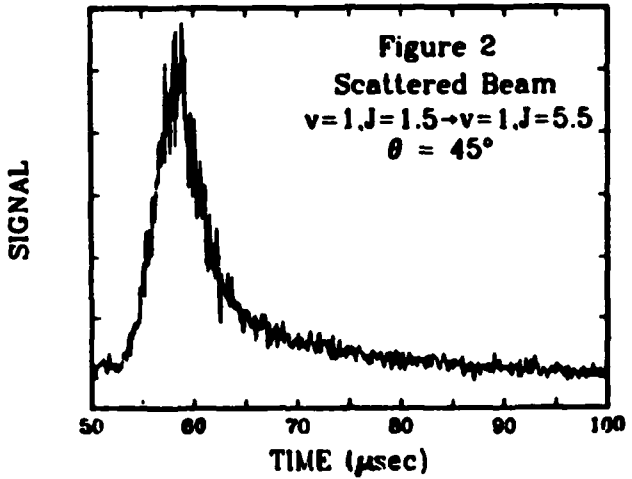
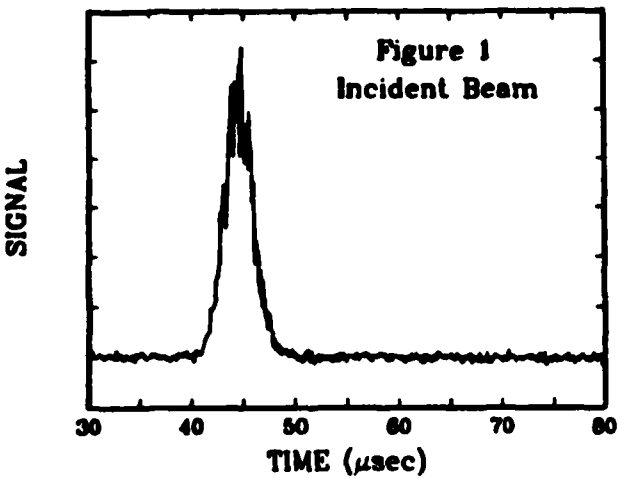
The importance of using freshly cleaved LiF(100) surfaces is dramatized in experiments previously reported in which polished LiF was used.<sup>4</sup> In those experiments, no vibrationally excited molecules were seen in the scattered beam implying that perhaps impurities left over from the polish led to trapping of vibrationally excited molecules and deactivation.

UV spectra were taken at fixed time delay with the IR on and the IR off, the difference of which was analyzed to give the rotational distribution for  $v=1$  to  $v=1$  scattering. Analysis of these data should yield the survival probability for the vibrationally excited NO molecules scattering from the LiF surface.

This work was supported in part by the Office of Naval Research.

#### References

1. G.D. Kubiak, et. al., *J. Chem. Phys.* **79**, 5163 (1983)
2. A. W. Kleyn, A. C. Luntz, and D. J. Auerbach, *Surf. Sci.* **117**, 33 (1982).
3. J. Segner, et. al., *Surf. Sci.* **131**, 273 (1983).
4. H. Zacharias, M. M. T. Loy, and P. A. Roland, *Phys. Rev. Letts.* **49**, 1790 (1982).
5. J. Estel, et. al., *Surf. Sci.* **54** 393 (1976)



**Electroreflectance Vibrational Spectroscopy:  
Theory and Measurement of the Stark Effect of CO on Ni[100]**

D. K. Lambert  
Physics Department  
General Motors Research Laboratories  
Warren, Michigan 48090-9055

Electroreflectance vibrational spectroscopy<sup>1-4</sup> (EVS) is an infrared technique for obtaining extremely high resolution spectra of adsorbed species. Light from a tunable infrared diode laser is reflected from an adsorbate covered surface to a detector. The reflected light is modulated by using a large electric field to shift adsorbate vibrational frequency - the Stark effect. Sensitivity to fractional modulation as low as  $2 \times 10^{-8}$  Hz<sup>-1/2</sup>, near the shot noise limit, is obtained. The high sensitivity and zero background nature of EVS also allow absolute measurements of the Stark tuning rate to be made.

Measurement of the Stark tuning rate of adsorbed species allows frequency shifts observed in vibrational spectra due to changes in microscopic electric field to be interpreted. One example of such a shift is seen<sup>5,6</sup> with CO on the Pt to aqueous electrolyte interface as the potential difference between the electrode and electrolyte is varied. The observed shift can be quantitatively predicted<sup>7</sup> from the measured Stark tuning rate for CO on Ni[110], the differential capacitance of the interface, and the dielectric constant of oriented water molecules at the interface. Similar shifts are also observed<sup>8</sup> with surface enhanced Raman scattering. Microscopic electric fields at the solid-vacuum interface are also large enough<sup>9</sup> to significantly influence vibrational spectra.

In the talk, recently obtained EVS spectra of CO on Ni[100] will be presented together with a measurement of the Stark tuning rate of CO on this surface. Recent improvements in the system we use to obtain EVS spectra will be described. The theory of EVS and the vibrational Stark effect will also be discussed, including the effect of the vibration not being oriented along the surface normal and estimates of the vibrational Stark effect for H on Ni[100] and O on Pt[111],  $1.2 \times 10^{-7}$  and  $2.4 \times 10^{-7}$  cm<sup>-1</sup>/(V/cm) respectively.

REFERENCES

1. D. K. Lambert, J. Electron Spectroscopy 30, 59 (1983).
2. D. K. Lambert, Phys. Rev. Lett. 50, 2106 (1983).
3. D. K. Lambert, in Tunable Diode Laser Development and Spectroscopy Applications, edited by Wayne Lo (SPIE, Bellingham, Washington, 1983), pp. 158-164
4. D. K. Lambert, U. S. Patent No. 4 446 719, (8 May 1984).
5. K. Kunitatsu, J. Electroanal. Chemistry 145, 219 (1983).
6. B. Beden, A. Bewick, and C. Lamy, J. Electroanal. Chemistry 148, 147 (1983).
7. D. K. Lambert, Sol. St. Comm. 51, 297 (1984).
8. J. Billman and A. Otto, Surf. Sci. 138, 1 (1984).
9. S. Efrima and H. Metiu, Surf Sci. 109, 109 (1981).

DIFFUSION AND REACTION IN TORTUOUS  
STRUCTURES AS MODELLED BY FRACTALS

J. Klafter and J. M. Drake

Exxon Research and Engineering Company  
Route 22 East - Clinton Township  
Annandale, New Jersey 08801

It has been recently suggested that many structures in nature have fractal geometries: polymers<sup>1</sup>, diffusion limited aggregates<sup>2</sup>, sandstones<sup>3</sup>, Vycor glasses<sup>4</sup> and various irregular surfaces<sup>5</sup>. Avnir et al.<sup>5,6</sup> have demonstrated that for porous surfaces the concept of surface area is not meaningful. The area as measured by molecular adsorption changes with the size of the adsorbate molecules (the yardsticks). It has been proposed<sup>5,6</sup> that many porous surfaces are characterized by their fractal dimension  $d$  in a way which relates the number of adsorbed molecules to their cross sectional areas (yardstick sizes),  $\sigma$ ,

$$n \propto \sigma^{-d/2}, d > 2. \quad (1)$$

There have been only a few works<sup>7-9</sup> which study the dynamics of molecules adsorbed in Vycor glasses and on porous silica gels. However no attempt has been made to relate the observations to a geometrical parameter. Interestingly enough both porous Vycor and porous silica gel have been proposed as fractal systems.<sup>4,5</sup>

In this presentation we introduce the fractal concept as a model for tortuous, porous structures and study theoretically and experimentally diffusion and reaction of molecules restricted to move on fractal structures. We show that the geometry drastically affects the transport and kinetic properties of the molecules.<sup>11,12</sup> We consider two limiting cases:

(1) Direct reaction between a donor molecule and acceptor molecules on a fractal structure which might apply for electronic energy transfer among the adsorbates. This reaction depends on the fractal dimension  $d$ . Direct transfer among adsorbates in porous Vycor has been recently interpreted in terms of this model.<sup>4</sup> (2) Indirect process in which the molecules (or excitations) diffuse along the structure. Here both the molecules and the reaction depend on the spectral dimension  $d$ , which describes the connectedness of the tortuous structure.

We present results on the properties of excited adsorbates on silica-gel surfaces<sup>12</sup> and in Vycor glasses and discuss the effects of the geometrical restriction in terms of the fractal model.

#### References

1. B. B. Mandelbrot, *The Fractal Geometry of Nature* (Freeman, San Francisco, 1982).
2. D. A. Weitz and M. Oliveria, *Phys. Rev. Lett.* 50 (1983) 839.
3. A. J. Katz and A. H. Thompson, submitted to *Phys. Rev. Lett.*
4. U. Even, K. Rademan, J. Jortner, N. Manor and R. Reisfeld, *Phys. Rev. Lett.* 52 (1984) 2164.
5. D. Avnir, D. Farin and P. Pfeifer, *J. Chem. Phys.* 79 (1983) 3566.
6. P. Pfeifer, D. Avnir and D. Farin, *J. Stat. Phys.* 36, Sept. 1984.
7. P. deMayo, *Pure Appl. Chem.* 54 (1982) 1623.
8. P. deMayo, L. V. Natarajan and W. R. Ware, *Chem. Phys. Lett.* 107 (1984) 187.
9. R. K. Baur, P. deMayo, W. R. Ware and K. C. Wu, *J. Phys. Chem.* 86 (1982) 3781.
10. J. Klafter, A. Blumen and G. Zumofen, *J. Stat. Phys.* 36, 533 (1984).
11. J. Klafter and A. Blumen, *J. Chem. Phys.* 80 875 (1984).
12. J. M. Drake and J. Klafter, *J. of Lumin.* (in press).

## Electronic Spectroscopy and Relaxation Dynamics of Adsorbates on Metal Surfaces

Phaedon Avouris

IBM T. J. Waston Research Center  
P.O. Box 218  
Yorktown Heights, NY 10598

Information on the nature and non-radiative decay of electronically excited states of adsorbates is essential for the microscopic understanding of a variety of surface dynamical processes.

Here we present spectroscopic results, obtained by electron energy loss and optical techniques, on the valence<sup>(1)</sup> and core<sup>(2)</sup> excitations of adsorbates on metals. The observed changes in the excitation energies of intraadsorbate transitions are explained in terms of electronic structure changes induced by the interaction with the substrate. Ab-initio<sup>(3)</sup> and model Hamiltonian calculations<sup>(4)</sup> are used to deduce these changes. Thus, a satisfactory description is obtained for a wide variety of adsorption systems ranging from physisorbed noble gases to chemisorbed CO. Particular emphasis is placed on the excitations of chemisorbed CO since this system has long been considered as a prototype in chemisorption studies. Thus, it is shown that unlike previous suggestions, the low-lying excitations of chemisorbed CO are not all of a charge-transfer nature and that the intramolecular valence excitations are within  $\pm 0.5\text{eV}$  of the corresponding free CO excitations. A similar behavior is seen in the spectra of other adsorbates. A simple, general interpretation is provided for these surprising results. We also demonstrate, by studying the electronic excitations of aromatic hydrocarbons on transition metals, that the excitations of the free molecule do not always have a direct analogue in the adsorbed phase.<sup>(1,6)</sup> This observation has significant implications in the analysis of optical processes such as surface enhanced Raman.

Besides the modified intraadsorbate excitations, new excitations of a charge-transfer nature develop upon adsorption. Such excitations are documented in the case of aromatic hydrocarbons on both noble and transition metals.<sup>(1,6)</sup>

In addition to the spectral shifts and intensity changes, the adsorbate spectral bands are strongly broadened (dumped) by the interaction with the substrate.<sup>(7)</sup> Three different decay mechanisms are considered: (A) Field coupling of the adsorbate and substrate excitations; (B) excited adsorbate  $\rightarrow$  substrate resonance electron transfer; and (C) auger decay. The range of applicability and strength of these decay mechanisms are discussed, and comparison is made with observed spectral lineshapes. It is concluded that, in general, non-radiative decay at metal surfaces is  $\sim 10^5\text{-}10^6$  times faster than

radiative decay, yielding lifetimes in the range of  $10^{-14}$ - $10^{-15}$  sec. The implications of the fast non-radiative decay, ground state charge transfer, and metallic screening on the photochemistry and photodesorption of adsorbates is discussed.

1. Ph. Avouris, N.J. DiNardo and J.E. Demuth, *J. Chem. Phys.* 80, 491 (1984); Ph. Avouris and J.E. Demuth, *J. Chem. Phys.* 75, 4783 (1981).
2. Y. Jugnet, F. J. Himpel, Ph. Avouris and E.E. Koch, *Phys. Rev. Lett.* 53, 198 (1984).
3. P.S. Bagus, A.R. Rossi and Ph. Avouris, *Phys. Rev. B*, to be published.
4. B.N.J. Persson and Ph. Avouris, *J. Chem. Phys.* 79, 5156 (1983).
5. Ph. Avouris and J.E. Demuth, *Surface Sci.*, to be published.
6. N.J. DiNardo, Ph. Avouris and J.E. Demuth, *J. Chem. Phys.* 81, 2169 (1984).
7. Ph. Avouris in "Dyanmics on Surfaces," B. Pullman et al, editors (Reidel, Dordrecht, Holland, 1984); Ph. Avouris and B.N.J. Person, *J. Phys. Chem.* 88, 837 (1984).

Study of Molecule Surface Interaction Dynamics by Laser

Herbert Walther

Max-Planck-Institut für Quantenoptik and  
Sektion Physik der Universität München,  
D-8046 Garching, Fed. Rep. of Germany

During the last decade atomic and molecular beam techniques have been of great help for investigating the dynamics of atom or molecule-surface interaction. As long as atoms are involved in the interaction process, the measurements of angular and velocity distributions provide sufficient insight. When molecules are scattered, however, additional information on changes of the internal energy is necessary. Recently, the laser-induced fluorescence method and resonance ionization in combination with time-of-flight measurements were successfully used to determine the influence of surface interaction on the energy distribution between translational, rotational, vibrational and electronic excitation (see references [1,2] for a survey on the published work). The laser experiments lead to a complete description of the dynamics of the molecule-surface interaction.

In the talk the scattering of NO molecules from different solid-state surfaces performed in our laboratory is discussed in detail [1,2,3]. In the experiments a supersonic beam of NO molecules was scattered from clean and well-characterized surfaces (mainly pyrographite and platinum). The scattered molecules were investigated by laser-induced fluorescence in order to determine the distribution of the energy among the different internal degrees of freedom. The resonance ionization and time-of-flight measurements give the state selective and scattering angle dependent translational energy.

The NO/Pt system shows trapping/desorption behaviour for all surface temperatures  $T_s$ , with full rotational accommodation at low  $T_s$  and incomplete rotational accommodation at higher  $T_s$ . This behaviour together with the complete velocity accommodation for the whole temperature range investigated (100 K - 800 K) can be explained by the long residence time of the molecules on the surface and the desorption of the molecules from the state of a hindered rotor (fixed on the surface) to that of a free rotor. At lower  $T_s$  the surface is covered with NO molecules, leading to scattering of the incoming particles at the relatively low precursor potential. This process does not result in trapping of the molecules but nevertheless leads to a long residence time and to full rotational and translational accommodation.

The NO/graphite system at sufficiently low surface temperatures (< 300 K) can be characterized by two scattering channels. One leads to scattered molecules in a lobular angular distribution, peaked near the direction for specular reflection, with a mean velocity slightly smaller than the velocity of the incoming beam; the other yields diffusively scattered molecules in a cosine angular distribution with a much lower mean velocity. The rotational temperatures  $T_{rot}$  derived from the Boltzmann-like rotational energy distributions of these two groups of scattered molecules are slightly different but close to the surface temperature. The rotational and translational energies are not in thermal equilibrium. At high  $T_s$  the diffusively scattered part

disappears and  $T_{rot}$  becomes smaller than  $T_s$ . There is a net momentum transfer to the molecules scattered in the normal direction, and at sufficiently high surface temperatures the molecules can gain a net translational energy from the surface in the quasi-specular direction.

To summarize the results on the overall energy balance for the NO/graphite system, it is found that the diffusively scattered NO molecules gain some rotational energy, but transfer much more translational energy to the surface, so that the energy balance is highly negative. For the specularly scattered molecules, the energy loss and gain are nearly balanced at low surface temperatures, but with increasing  $T_s$  the translational energy of the scattered molecules increases while the rotational energy stays constant, resulting in a substantial energy transfer from the surface to the scattered NO molecules.

- [1] F. Frenkel, J. Häger, W. Krieger, H. Walther, G. Ertl, J. Segner, and W. Vielhaber, *Chem. Phys. Lett.* 90, 225 (1982).
- [2] J. Segner, H. Robota, W. Vielhaber, G. Ertl, F. Frenkel, J. Häger, W. Krieger, H. Walther, *Surface Sciences* 131, 273 (1983).
- [3] J. Häger, Y.R. Shen, H. Walther, *Proceedings of the International Conference on Laser Processing and Diagnostics*, Linz, July 15-19, 1984, Springer, Berlin, Heidelberg, New York.

# **POSTER SESSION**

Optical and Electron Probes of the Structure  
of Surfactant Coated Surfaces

by

S. Garoff, R. B. Hall, D. W. Deckman  
Exxon Research and Engineering Co.  
Route 22 East - Clinton Township  
Annandale, New Jersey 08801

The absorption of a monolayer of amphiphilic or surfactant molecules onto a surface can dramatically affect a number of the macroscopic properties of that surface. These properties, such as wetting by a fluid, lubrication of the solid, or chemical reactions of the surface, are of fundamental as well as technological importance. Our studies have focussed on the molecular scale structure of these monolayers and have attempted to probe how the structure depends on the deposition process used to absorb the monolayers. Further, by studying the molecular aspects of surfactant coated surfaces, we hope to gain insight into the nature of wetting and the other macroscopic phenomena which are profoundly affected by the presence of the surfactant monolayer.

Our studies have centered on three aspects of the molecular structure of the surfactant monolayers: coverage, molecular conformation, and long range order. We have begun to examine how these three structural properties affect the wetting of the interface. In our UHV studies, we have found that the low energy nature of these hydrocarbon surfaces makes ex-situ dosing of the surfactant entirely compatible with UHV probing of the surface composition. Using Auger spectroscopy, we have determined the number of hexadecyl mercaptan ( $C_{16}H_{33}-SH$ ) molecules which adsorb on a silver surface. For this system, the surface/head group bond dominates the tail/tail interaction in the adsorption process. At low surfactant coverages, the surface is wet by both polar and nonpolar fluids. At higher coverages, the

surface rejects both types of fluids. In addition, we have obtained vibrational spectra of the adsorbed molecules using surface-enhanced Raman scattering. From this measurement, we have learned that in the presence of air or nonwetting fluid overayers the adsorbed surfactant layer exhibits molecular conformation similar to that in the solid, bulk material. However, conformational changes occur in the alkyl chain of the adsorbed molecules when they are contacted by fluid overayers that wet the surface. Finally, transmission electron diffraction has revealed long-range order in Langmuir-Blodgett monolayers of barium stearate on carbon substrates. These monolayers are poorly crystalline and collapse to bulk crystallites of the salt under electron bombardment.

Above-Bandgap Polarization Anisotropies in Cubic Semiconductors: A Visible-Near uv Probe of Surfaces

D. E. Aspnes

Bell Communications Research, Inc., Murray Hill, N.J. 07974

Recent work on the 0.5 eV below-bandgap surface state on 2x1-<111> Si cleaved in ultrahigh vacuum showed strong polarization anisotropy in near-normal incidence absorptance and reflectance measurements.<sup>1,2</sup> The present work describes the first experiments undertaken to systematically study anisotropies in the above-bandgap reflectance of cubic semiconductors. An experimentally simple configuration is used, wherein the sample is rotated while being illuminated with near-normal-incidence linearly polarized light and the second harmonic of the mechanical rotation frequency in the reflected beam is phase-sensitively detected and determined as a function of photon energy.

Surprisingly large anisotropies, of the order of 1% in the relative reflectance differences, are observed. Owing to the approximately isotropic nature of the optical properties of the bulk material, these anisotropies are found to be particularly sensitive to surface conditions. Contributions from physisorbed molecules, microscopic roughness,

anisotropic surface films and oxides, surface asperities, and spatial dispersion effects in the bulk can all be identified.

The bromination of clean  $\langle 110 \rangle$  Ge surfaces by 3 vol. % Br in methanol produces an anisotropic optical absorption band overlapping exactly the absorption band of molecular  $\text{Br}_2$ . The sign of the reflectance change shows that the physisorbed Br must lie predominantly perpendicular to  $\langle 110 \rangle$ , with oscillator strength apparently enhanced by the presence of the surface. Oxide growth and removal on  $\langle 110 \rangle$  Si and Ge surfaces and on  $\langle 001 \rangle$  GaAs and GaP surfaces causes large changes in the anisotropy spectra which are not yet understood. The predominant bulk process contributing to the reflectance anisotropy for  $\langle 110 \rangle$  surfaces is identified as fourth-rank spatial dispersion describable by a perturbation approach and found to be strongly enhanced relative to previously measured below-bandgap anisotropies due to vanishing denominators in the perturbation expansion.

When completely understood, polarization anisotropy measurements may be an important means of obtaining information about surfaces of cubic materials under non-uhv conditions.

-----

<sup>1</sup>P. Chiaradia, A Cricenti, S. Selci, and G. Chiarotti, Phys. Rev. Lett. 52, 1145 (1984).

<sup>2</sup>M. Olmstead and N. Amer, Phys. Rev. Lett. 52, 1148 (1984).

## UV-Laser Photodeposition of Patterned Catalyst Films from Adsorbate Mixtures\*

D. J. Ehrlich and J. Y. Tsao\*\*  
Lincoln Laboratory, Massachusetts Institute of Technology  
Lexington, Massachusetts 02173-0073

It has been demonstrated in recent studies that laser-induced photochemical modifications of surface properties can be used in combination with nonlinear kinetics and interfacial chemistry for maskless patterning of thin films by selected-area growth.<sup>1-3</sup> With one exception,<sup>3</sup> these new techniques have relied on photochemical lowering of surface-tension barriers to physical condensation, e.g., prenucleation; laser-modification of chemical surface properties will have practical advantages over the use of physical barriers, particularly on surfaces with previously defined structures and crystalline defects.<sup>1</sup> In this paper we describe a study in which chemical catalysts have been prepared by local photochemical reaction under UV-laser irradiation. Thin (monolayer) films of these laser-deposited surface agents are shown to predispose surfaces to "spontaneous" polymerization of ethylene or acetylene on exposure to these monomer vapors. The UV-laser deposition reaction for preparation of these catalysts involves a greater-than-unity-order reaction in a mixed-component adsorbed layer of  $TiCl_4$  and  $Al_2(CH_3)_6$ . The method is far more efficient than direct radiation-driven polymerization, and is of particular interest as a method for the patterning of easily oxidized polymers, many of which are difficult or impossible to pattern by lithographic methods.

The laser-deposited materials of this study are closely related to the Ziegler-Natta catalysts employed widely in the manufacture of high-molecular-weight polymers from hydrocarbon solution. The active agent in these catalysts is a Ti-halide/metal-alkyl complex. In the present application, laser

photochemistry in room-temperature adsorbates is used to prepare similar catalysts, as films, in substitution for the conventional preparation by bulk reaction in solution at elevated temperature. The chemical kinetics of catalyst formation have been studied by real-time optical transmission and quartz-crystal microbalance methods, both of which are sensitive to submonolayer coverages.

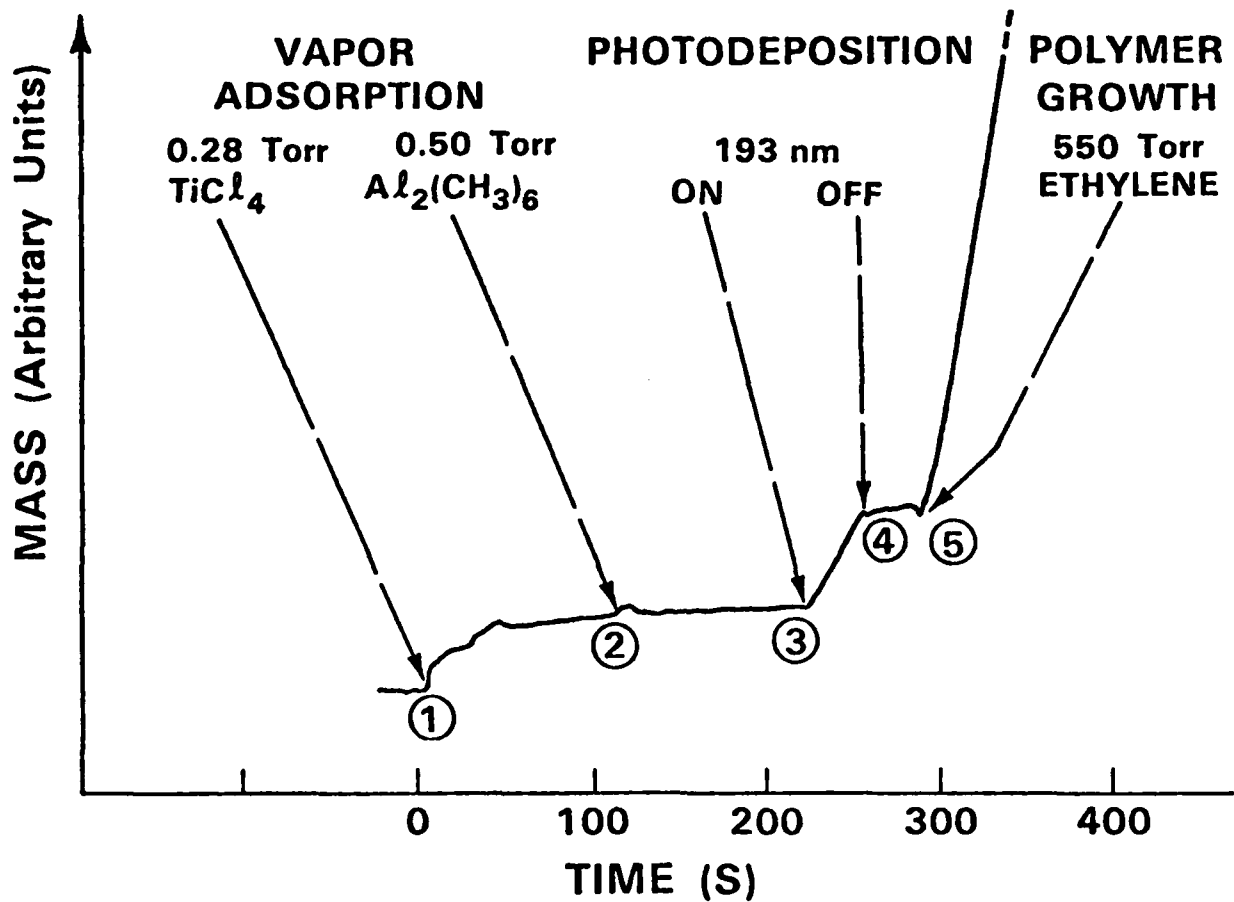


Fig. 1 Quartz-crystal microbalance trace showing adsorption of  $TiCl_4$  and  $Al_2(CH_3)_6$  (at times 1 and 2, respectively) on a well-pumped hydroxylated surface, followed by 193-nm excimer-laser deposition (between 3 and 4) and polyethylene growth (from 5 to later times).

#### References

1. J. Y. Tsao and D. J. Ehrlich, *J. Cryst. Growth* (to be published, Vol 68, 1984), 1984), and references therein.
2. C. Arnone, V. Daneu and S. Riva-Sanseverino, *Appl. Phys. Lett.* 37, 1012 (1980); D. J. Ehrlich, R. M. Osgood, Jr. and T. F. Deutsch, *Appl. Phys. Lett.* 38, 946 (1981).
3. J. Y. Tsao and D. J. Ehrlich, *Appl. Phys. Lett.* 45, 617 (1984).

\*This work was sponsored by the Department of the Air Force, in part under a specific program supported by the Air Force Office of Scientific Research, by the Defense Advanced Research Projects Agency and by the Army Research Office.

\*\*Present address: Sandia National Laboratories, Albuquerque, NM 87175

**Chlorine Surface Interactions and Laser Induced  
Surface Etching Reactions**

W. Sesselmann and T.J. Chuang

IBM Research Laboratory, K33/281

5600 Cottle Road, San Jose, CA 95193

It is by now quite well established that photon beams, in particular lasers, can be used to induce or enhance chemical reactions between a gas and a solid surface [1]. Also, recent advances in applications of lasers to perform chemical etching and vapor deposition have raised firm expectation that the laser technique may have significant impact on processing materials for microelectronics [2]. In laser induced chemical etching of solids, the fundamental surface processes include the reaction between the adsorbate and substrate and the vaporization of product species. In order to better understand the radiation-gas-surface interaction mechanisms, we have carried out experiments with ESCA and Auger depth profiling, and time-resolved mass spectrometry in conjunction with laser irradiation of solid surfaces. Specifically, we have investigated Si/Cl<sub>2</sub>, Ni-Fe/Cl<sub>2</sub>, and Ag/Cl<sub>2</sub> systems.

The behavior of chlorine-surface interactions for these metal and semiconductor systems can be divided into two classes. For Si and Ni-Fe alloys exposed to Cl<sub>2</sub>, chemisorption is followed by formation of passivated surface layers and for Ag/Cl<sub>2</sub> chlorine diffuses into the bulk of the solid. Thus, it is quite interesting to study and compare the laser etching behavior of these systems. Our experiments show that etching can occur by uv and visible laser irradiation of the solid surfaces. However, the mechanisms for the photo-enhanced reactions can be quite

different for different systems. For Si excitation of electrons and holes by photons with higher than band gap energy can be important. A distinct difference in etching rates for n-type and p-type Si is observed using uv-radiation. For metals chlorine diffusion and chloride formation to weaken the metal-metal bond is crucial for the kinetics of the radiation-assisted etching processes. The etch rate dependence of Ni-Fe alloys as a function of Fe concentration has been studied. The observed etch rate apparently increases with Fe concentration, although the proportionality seems to be slightly sublinear.

The chlorine adsorption and diffusion behavior on Ag has been investigated by ESCA and Auger depth profiling for various chlorine exposure times and pressures up to 1Torr. The chlorinated surface layer may be represented as  $\text{AgCl}_x$  with  $x$  being less than 1. Apparently, as long as Ag is present under the surface layer, Ag can diffuse through the  $\text{AgCl}$ -containing layer to the surface for further reaction with chlorine from the gas phase. In spite of the incomplete surface chlorination exposure of the surface to uv or visible radiation results in efficient etching of the metal. This means, while surface chlorination is essential for laser etching to take place at pulse intensities of about  $10\text{MW/cm}^2$ , complete  $\text{AgCl}$  formation is not necessary. Based on our time-resolved mass spectrometry experiments it is suggested that also non-thermal radiation effects may be important in laser induced etching reactions.

- [1] T.J. Chuang, *Surface Sci. Reports* **3**, 1 (1983).
- [2] T.J. Chuang, *J. Vac. Sci. Technol.* **21**, 798 (1982); *Mat. Res. Soc. Symp. Proc.* **17**, 45 (1983).

Mechanism of Trimethylaluminum Chemical Vapor Deposition  
Studied by Multiphoton Ionization Mass Spectrometric  
Detection

D.W. Squire, C.S. Dulcey, and M.C. Lin

Chemistry Division, Naval Research Laboratory,  
Washington, DC 20375-5000

Recent mechanistic studies of organometallic chemical vapor deposition (MOCVD) have suggested that organometallic cleavage and organic radical recombination take place on or above the heated substrate.<sup>1</sup> We have employed the method of multiphoton ionization (MPI) in conjunction with conventional mass spectrometry to probe radical<sup>2</sup> as well as stable products to elucidate the mechanisms of CVD processes.

In the apparatus used, a diffuse beam of trimethylaluminum (TMA), diluted 1:100 in helium, flowed through a 0.127 mm nozzle and impinged on a heated copper substrate 10 mm away. Products and unreacted TMA were deflected into (30 mm downstream) the ionization region of a quadrupole mass spectrometer modified for either electron or photon ionization.<sup>2</sup> The surface was held at 45° to both reactant beam and quadrupole axis. Overall chamber pressure was maintained at  $2.0 \times 10^{-6}$  Torr. Electron ionization was used to identify products formed in the reaction and also to check the MPI results. MPI signals were generated by doubling the output of a Nd:YAG laser pumped dye laser and focusing the resultant beam with a 50 mm f.l. lens into the ionization region. Oxazine 720 laser dye (doubled) produces the wavelength region from 330-335 nm, probing the two photon

resonant  $0^0$  band of the methyl radical 3p Rydberg transition.<sup>3</sup> At these wavelengths, TMA is photolyzed and the aluminum non-resonantly ionized.<sup>4</sup> Therefore, the principal laser products seen are methyl and aluminum ions.

As the temperature rose above 350° C, the methyl radical peak at 333.4 nm began to appear and mass 27 ( $\text{Al}^+$ ), the product of non-resonant ionization of scattered TMA, was found to be the only other laser produced mass peak of any significance.

Electron ionization was used to probe for methane or ethane production from possible radical reactions on the surface. A methane background was present as an impurity in the TMA but no change in methane signal level was observed. Most importantly, no ethane could be detected under all conditions studied. Accordingly, no recombination of the methyl radicals on the surface appears to take place and no products other than the methyl radical could be detected.

#### References

1. P.D. Dapkus, Ann. Rev. Mat. Sci., 12, 243 (1982).
2. T.G. DiGiuseppe, J.W. Hudgens, and M.C. Lin, Chem. Phys. Lett., 82, 267 (1981).
3. J.W. Hudgens, T.G. DiGiuseppe, and M.C. Lin, J. Chem. Phys., 79, 571 (1983).
4. S.A. Mitchell and P.A. Hackett, J. Chem. Phys., 79, 4815).

Infrared Laser-induced Photodesorption and Ultraviolet Laser-induced Thermal Desorption of Methyl Fluoride from Polycrystalline Copper

R. Viswanathan<sup>a</sup>, I. Hussla<sup>b</sup>, D.R. Burgess, Jr., P.C. Stair, and E. Weitz,  
Department of Chemistry, Northwestern University, Evanston, IL 60201.

a. Permanent Address : Department of Chemistry, Beloit College,  
Beloit, WI 53511

b. Present Address : K-33/281, IBM Research Laboratory, San Jose,  
CA 95193

Laser-induced desorption of methyl fluoride from a polycrystalline copper surface has been achieved by either direct excitation of the  $\nu_3$  vibrational mode of adsorbed methyl fluoride using a pulsed CO<sub>2</sub> laser at 10  $\mu$  or via heating of the copper substrate using a KrF excimer laser operating at 248 nm. We have previously demonstrated that at ultraviolet wavelengths, the reflectivity of copper is low enough that the KrF laser pulse of  $\approx$  200 mJ deposits enough energy into the surface to desorb CO from either single crystal (100) or polycrystalline copper [1]. Time-of-flight (TOF) spectra have been characterized with respect to the CO translational velocity as a function of laser power density and CO coverage [2]. In the present work, preliminary results of such measurements are presented for the CH<sub>3</sub>F-Cu system.

Copper is highly reflective in the 10  $\mu$  spectral region. Thus, CO<sub>2</sub> laser radiation does not effectively heat the copper substrate and the laser is not efficient at desorbing molecules thermally from the copper surface. However, when the CO<sub>2</sub> laser output is tuned to the

AD-R168 618

TOPICAL MEETING ON MICROPHYSICS OF SURFACES RENNS AND  
ADSORBATES HELD AT. (U) OPTICAL SOCIETY OF AMERICA  
WASHINGTON D C J W QUINN 18 DEC 85 AFOSR-TR-85-0289

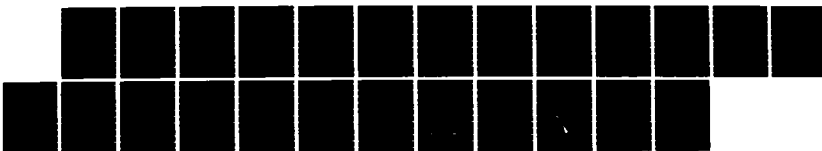
2/2

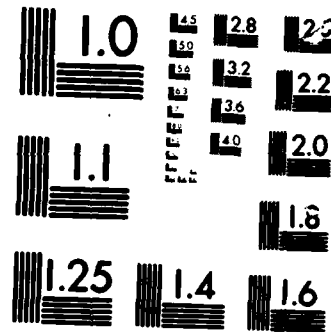
UNCLASSIFIED

AFOSR-85-0018

F/8 7/5

ML





MICROCOM<sup>®</sup>

CHART

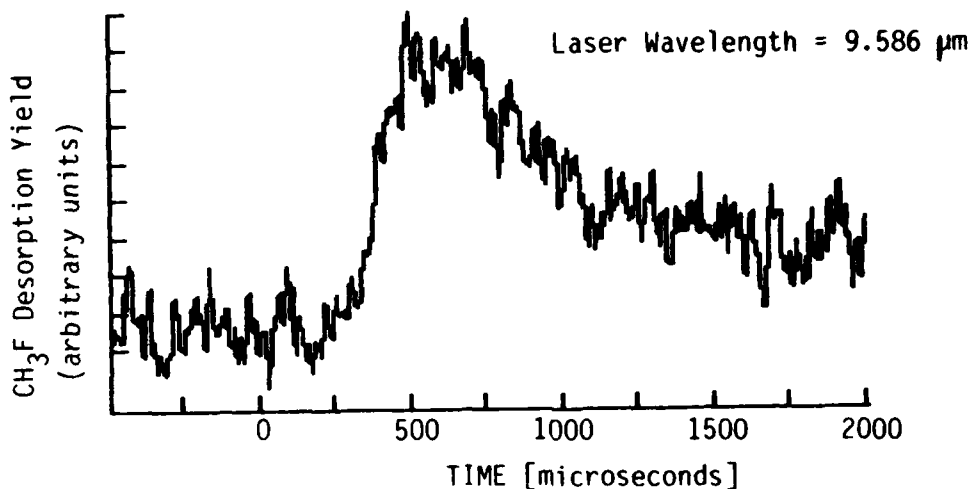


**FIGURE 1** : Photodesorption of  $\text{CH}_3\text{F}$  from a polycrystalline copper surface by a pulsed  $\text{CO}_2$  laser.

frequency of the  $\nu_3$  mode of adsorbed  $\text{CH}_3\text{F}$ , desorption results (Figure 1). Preliminary results indicate that selective desorption of  $\text{CH}_3\text{F}$  can also be achieved in a mixed  $\text{CO}/\text{CH}_3\text{F}$  adsorbate system. The implication of these results will be discussed, specifically in the context of results for two other systems -  $\text{CH}_3\text{F}-\text{NaCl}$  and  $\text{NH}_3-\text{Cu}(100)$  - that have recently been reported [3,4].

Acknowledgements: We would like to thank the Office of Naval Research for support of this work under ONR contract No. N00014-79-C-0794. One of us (I.H.) would like to thank the Deutsche Forshungsgemeinschaft for granting fellowship Hu 339/1-1.

#### References

1. D.R. Burgess, Jr., R. Viswanathan, I. Hussla, P.C. Stair, and E. Weitz, *J. Chem. Phys.* 79, 5200 (1983).
2. I. Hussla, R. Viswanathan, D.R. Burgess, Jr., P.C. Stair and E. Weitz, *Rev. Sci. Instrum.* (in press).
3. J. Heidberg, H. Stein, and E. Riehl, *Phys. Rev. Lett.* 49, 666 (1982).
4. T.J. Chuang and I. Hussla, *Phys. Rev. Lett.* 52, 2045 (1984).

Quantum Model of Dephasing-Enhanced Laser Desorption

Jui-teng Lin

Laser Physics Branch, Optical Sciences Division, Naval Research Laboratory  
Washington, D.C. 20375

Xi-Yi Huang and Thomas F. George

Department of Chemistry, University of Rochester  
Rochester, New York 14627Summary

Existing theories of laser-induced and/or phonon-assisted desorption are based upon one-dimensional (1D) surface potential analyses, which include a truncated harmonic potential (THP), 1D Morse potential (1MP) and master equation treatment with multiphonon transitions [1]. One of the severe limitations of these models is that any two-dimensional (2D) features of the excited adspecies are completely ignored, causing some unrealistic results. For example, THP overestimates the transition rate, while the rate is underestimated by 1MP. In the present paper, we propose a qualitatively correct physical model which is able to effectively take into account the 2D features by introducing a dephasing factor into an anharmonic master equation.

The dephasing effects of a realistic adspecies-surface system, which are usually absent in 1D models, may be caused by the following proposed mechanisms [2]: (i) dephasing of the active dipole of the adspecies; (ii) intramolecular mode-mode coupling; (iii) fluctuations of the conformation of the adspecies; (iv) vibrational motion and rotational relaxation within the vibrational manifold; (v) lateral motion or migration-induced collisional broadening; and (vi) phonon-dispersion-induced broadening.

In a heat-bath model, attention is focused on the active mode (AM) of the adspecies, and a master equation describing the vibrational distribution of the AM is usually investigated. In our new model, which is particularly appropriate for admolecules with very fast intramolecular relaxation, all the intramolecular vibrational modes are treated on an equal footing. The rate equation describing the probability of the adspecies (as a whole) absorbing  $n$  photons is given by [3]

$$\dot{P}_n = \gamma_1 [(n+1)P_{n+1} - nP_n] + 2\gamma_R^2(t) \left\{ \frac{n(P_{n-1} - P_n)}{\Gamma^2 + [2\epsilon(n-1) - \Delta]^2} + \frac{(n+1)(P_{n+1} - P_n)}{\Gamma^2 + (2\epsilon n - \Delta)^2} \right\},$$

where  $\gamma_R(t)$  is the Rabi frequency,  $\Gamma = \gamma_1/2 + \gamma_2$ ,  $\gamma_1$  and  $\gamma_2$  are the energy- and phase-relaxation rates, and  $\Delta$  and  $\epsilon$  are the laser detuning and anharmonicity of the admolecule-surface potential. In the above equation, we have used the Markovian approximation for the phonon relaxation and the Born approximation for the density matrix. However, several features of this equation should be noted: (i) it reduces to the usual master equation only when  $\gamma_2 = \infty$  (random-phase approximation), i.e., our rate equation preserves the partially coherent phase of the off-diagonal density matrix; (ii) the absorption cross section is saturated at the high excited states due to the anharmonicity; (iii) the energy-relaxation rate ( $\gamma_1$ ) describes the actual energy flow from the excited admolecule to the surface phonons, while the phase-relaxation rate ( $\gamma_2$ ) only changes the intramolecular phases without changing their energy populations. Furthermore, we note that in the multiphonon treatment, transitions beyond the nearest level (NL) are usually not required in photon-induced desorption where dipole (NL) transitions dominate. The multiphonon relaxation of the excited admolecule is governed by  $\gamma_1$ , which is generally strongly temperature dependent.

We are interested in the desorption rate constant,  $k_D$ , for a first-order desorption process, which may be related to the mean first-passage time,  $\bar{t}$ , by  $k_D = 1/\bar{t}$ . Using the equation of the previous page, we can calculate  $\bar{t}$  (and  $k_D$ ) from

$$\bar{t} = \sum_{n=0}^{n^*} \int_0^{\infty} dt P_n(t),$$

where  $n^*$  is the desorption threshold number of photons absorbed by the admolecule.

The numerical results are shown in Fig. 1 for the effect of anharmonicity and in Fig. 2 for the effect of dephasing. It is seen that the desorption rate constant is a decreasing function of the anharmonicity and reaches a constant value where the admolecule-surface potential is highly anharmonic and the excitation is very low, i.e.,  $P_n(t) \approx 0$  for  $n \neq 0$ . The dephasing-enhanced desorption is shown in Fig. 2 in which there is an optimum value of  $\gamma_2$ . This may be realized by the fact that the dephasing relaxation tends to compensate the anharmonicity "bottleneck" effect. In conclusion, we remark that the phase-relaxation rate ( $\gamma_2$ ) may compete with the energy-relaxation rate ( $\gamma_1$ ) and tends to diminish the detuning and anharmonicity. In a complete random-phase treatment, i.e.,  $\gamma_2 = \infty$ , the desorption rate is underestimated. The proposed dephasing effects due to the 2D features of the adspecies-surface system which enhance the desorption rate may provide, at least, a qualitatively correct physical model.

This research was supported by ONR and AFOSR.

- [1] M. S. Slutsky and T. F. George, *Chem. Phys. Lett.* 57, 474 (1978); C. Jedrzejek, K. F. Freed, S. Efrima and H. Metiu, *Surf. Sci.* 109, 191 (1981).
- [2] J. Lin and T. F. George, *J. Chem. Phys.* 72, 2554 (1980).
- [3] J. Lin and T. F. George, *Chem. Phys. Lett.* 66, 5 (1979); X. Y. Huang, T. F. George, J. M. Yuan and L. M. Narducci, *J. Phys. Chem.*, submitted.

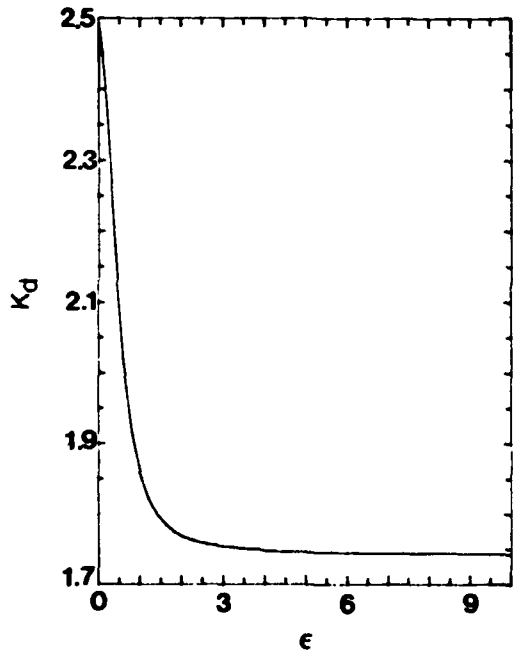


Fig. 1. Typical plot of  $k_d$  vs  $\epsilon$ .

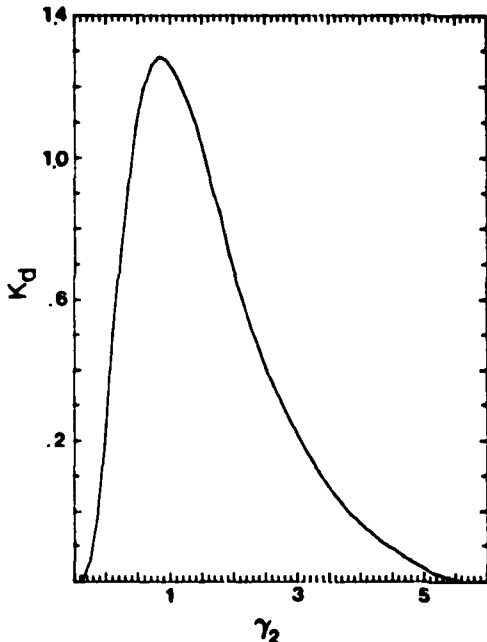


Fig. 2. Typical plot of  $k_d$  vs  $\gamma_2$ .

**Laser-Stimulated Vibrational Excitation of an Adspecies Studied by a Generalized Master Equation.**

A. C. Beri and Thomas F. George, Department of Chemistry,  
University of Rochester, Rochester, New York 14627, USA

**Introduction**

Recent attempts to clearly demarcate selective and nonselective effects in the IR-laser-stimulated vibrational excitation of an atom or molecule adsorbed on a solid surface<sup>1</sup> have included a number of model studies<sup>2</sup> and a few that have examined the detailed nature of the individual quantum states of the adsorption potential.<sup>3,4</sup> The presence of at least four time scales in such dynamical studies (experiment, laser, phonon, adbond) leads to difficulties in applying approximations such as the Markovian approximation (MA) which neglects memory effects in the generalized master equation (GME) describing the excitation. Use of the MA leads to the Pauli master equation (PME) which is easier to solve than the exact GME, and is therefore almost universally employed, but to our knowledge no realistic comparison has been made of the GME and the PME. We present below our results of the exact GME and the PME and find that for the few cases considered the two are drastically different in an (arbitrary) time range related to a time parameter  $\tau$  necessary to force the MA in the first place. In the asymptotic (long time) limit the solutions can be made to converge. We also present the results of an approximation which gives results (for any time range) which are almost as good as those of the exact GME, but which are as easy to obtain as those of the PME.

**Theoretical Formulation and Results**

In a quantum statistical formulation of the Heisenberg (or equivalently, Liouville) equations of motion of a many-body system, the process of projecting out the degrees of freedom of the "irrelevant" system(s) (phonons, laser) leads to a GME, i.e. a Volterra-type integrodifferential equation (VTE) for the projected density matrix of the relevant system (the vibrational eigenstates of the adspecies/solid potential, the adbond)

$$P_S(t) = \sum_{S=0}^t dt [K_{SS}(t-t')P_S(t') - K_{S'S}(t-t')P_S(t')] \quad (1)$$

Here  $P_S(t)$  is the diagonal matrix element of the projected density operator in the basis representing the adbond subspace (in our case the wave functions representing eigenstates of the effective potential between the adatom and the solid), and the memory kernels  $K_{SS}(t-t')$  involve time correlations between the motions of different lattice atoms and an analogous term originating from the laser field. This VTE is derived from the GME by invoking the Born and random-phase approximations.

The memory kernel can, via an appropriate partitioning of the Hamiltonian, be separated into two subkernels due to the phonons and the laser, respectively. The exact form of the former precludes analytic solutions of the VTE. We have found it possible, however, to obtain numerical solutions of Eq. (1) using an iterative technique, but only for times of the order of a few periods of the phonon kernel. The results for three levels ( $S=0,1,3$ ) of an effective Morse potential seen by a mass 16 species on germanium (with  $\omega_{10}$  equal to  $\omega_D$ , the Debye frequency, and  $\omega_{31}$  equal to  $\omega_L$ , the laser frequency) are shown in Fig. 1. We see that in the transient region, this arrangement leads to absorption of energy by the adbond from the laser and phonon fields at the same time. The populations of levels 1 and 3 actually cross at about 2 ps, a pattern which can be expected to continue and lead to an eventual steady state.

We now consider two approximate solutions of Eq. (1). The phonon kernel is oscillatory with an amplitude which falls off quite rapidly in time. The laser part, on the other hand, is constant. We approximate the phonon kernel as a delta function and write

$$K_{SS}(t-t') = \Omega_{SS} \delta(t-t') + k_{SS} \quad (2)$$

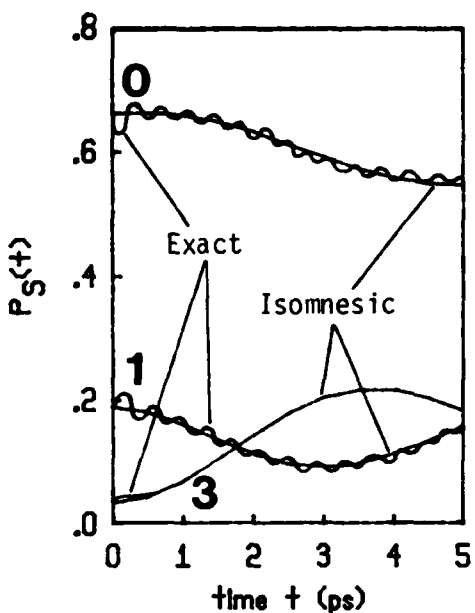


Fig. 1. Population of levels 0, 1 and 3 of a laser-pumped abond as a function of time obtained via the exact and isomnesic GME.

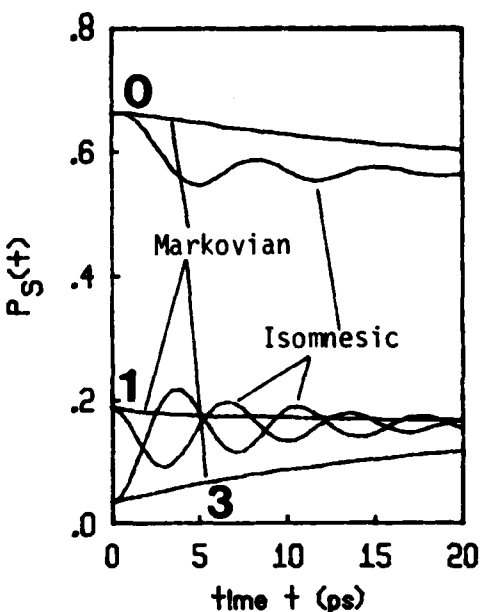


Fig. 2. Population profile of the system of Fig. 1 obtained with the isomnesic and Markovian approximations

where  $\Omega$  and  $k$  are constants. The first (phonon-) term is Markovian-like, but the second (laser-) term represents a constant memory. The resulting "isomnesic" approximation gives closed-form solutions of Eq. (1) for arbitrary times. The agreement between these and the exact results (Fig. 1) is excellent, with the population crossings and flip-floppings reproduced accurately. The Markovian approximation can only be applied if we introduce a parameter  $\tau$  such that  $k_{S\bar{S}} = k_0 \tau \delta(t-t')$ . The resulting population profiles then depend on the value of  $\tau$ . We obtain essentially monotonic behavior with the MA, in contrast with the oscillatory patterns obtained otherwise. The steady-state values in the MA can be made to approach the exact steady-state values if  $\tau$  is chosen to be much smaller than the equilibration time.

In conclusion, we have shown that the dynamical behavior of the laser/abond/phonon system can be studied in detail for arbitrary times by using the isomnesic approximation, and that in the transient region, interesting and unexpected patterns of energy transfer emerge which could have an important bearing on our understanding of ultrafast laser-stimulated surface processes.

This work was supported by AFOSR and ONR.

1. T. J. Chuang, *Surf. Sci. Rep.* **3**, 1 (1983); T. F. George, A. C. Beri, K. S. Lam and J. Lin, "Laser Photochemistry," in *Laser Applications*, Vol. 5, ed. by J. F. Ready and R. K. Erf (Academic Press, New York, 1984).
2. Z. W. Gortel, H. J. Kreuzer, P. Piercy and R. Teshima, *Phys. Rev. B* **27**, 5066 (1983); **28**, 2119 (1983); J. Lin, A. C. Beri, M. Hutchinson, W. C. Murphy and T. F. George, *Phys. Lett.* **79A**, 233 (1980).
3. C. Jedrzejek, K. F. Freed, S. Efrima and H. Metiu, *Surf. Sci.* **109**, 191 (1981).
4. A. C. Beri and T. F. George, *J. Chem. Phys.* **78**, 4288 (1983) and to be published.

## Direct Laser Pumping of Adatom-Surface Vibrational Modes

Merle E. Riley  
Sandia National Laboratories  
Albuquerque, NM 87185

Dennis J. Diestler  
Purdue University  
West Lafayette, IN 47907

## SUMMARY

The interaction of laser radiation with chemical species adsorbed on solid surfaces is a process of relevance to vibrationally activated desorption and other reactive processes. For desorption, photons can either excite an internal mode of the adsorbate, A, forming  $A^*$  which can convert to translational motion and removal, or the photons can directly excite the adspecies-surface bond A-S above the dissociation limit. In both cases the important competing process is vibrational deactivation due to the coupling with the modes of the solid lattice. The central question is the amount of energy that can be localized in the surface bond at a given laser intensity.

Murphy and George [1] (MG) introduced a classical one-dimensional (1D) model for laser-pumped adatom-surface bonds in which the adatom of mass  $m_a$  is bound by a harmonic bond of force constant  $k'$  to the end atom of an atomic, harmonic, 1D lattice with masses and force constant  $m$  and  $k$ . The classical laser field is coupled into the system by a transfer of charge  $q$  between the adatom and the end atom. MG calculate, at steady state, the intensity required to maintain a given surface bond energy when the laser is in resonance with that bond. Goodman [2] reexamined the MG model, but found a different result for the ratio of bond energy to applied intensity. Goodman proved that the minimal intensity vanishes under appropriate conditions, which means that an arbitrarily weak laser would eventually cause desorption.

We have examined the MG model and discovered: (1) the different result of Goodman is due to a modified definition of surface bond energy, (2) the minimal intensity vanishes exactly as predicted by Goodman, (3) the condition for vanishing is easily stated, and (4) the harmonic bond assumption precludes applying the model to dissociation.

As the MG model assumes the lattice is initially cold, the response of the semi-infinite lattice can be solved exactly by Laplace transforms, Green's functions, or the Zwanzig approach. Transients are ignored and the steady-state solution to the coupled system, consisting of applied field, adatom, and lattice, is found explicitly. The result is conveniently expressed as a dimensionless ratio of the applied laser intensity  $I$  to a quantity  $I_0$  containing the average

excitation energy  $E$  of the surface bond,

$$I_0 = 2ce_0k'E/q^2.$$

Obviously the degree of excitation depends linearly on the applied intensity.  $e_0$  is vacuum permittivity and  $c$  the speed of light.  $I/I_0$  is a function of dimensionless system parameters: the ratio of the laser frequency  $w_L$  to the lattice Debye frequency  $w_D$ , the ratio of  $w_L$  to the surface bond frequency  $w_S$ , and the ratio of the surface-bond reduced mass  $m_S$  to the lattice atom mass,

$$m_S/m = m_a/(m_a+m).$$

We will publish the result and its derivation shortly. As a function of increasing  $w_L/w_D$ ,  $I/I_0$  varies downward from unity, has a minimum, and then increases without bound. An examination of the expression for  $I/I_0$  reveals that it has a zero for a minimum if and only if

$$w_S/w_D > (m_S/m+1)^{-1/2}.$$

This is similar to the condition derived by Goodman [2] and the interpretation of the quantities appears simpler to us. In other words the surface mode must lie above the lattice cutoff and be pumped by the field at that surface mode frequency which is shifted from the isolated bond frequency of A-S as given by  $w_S$ .

Evidently the procedure of MG for solving the steady state problem did not easily reveal the presence of a true zero in the  $I/I_0$  function when near the minimum. Goodman's choice of a different bond energy is not very crucial overall because his result agrees with the present in the neighborhood of the zero. The solution is of practical importance only near the true zero of  $I/I_0$  because of the very intense field represented by  $I_0$ .

It is important to emphasize that all of these closed-form results pertain to the steady state and depend crucially on the assumption that the surface bond is harmonic and that it has only one degree of freedom. In reality, the surface-bond potential energy must vanish with large separation and consequently is highly anharmonic. Even if the ground state of the A-S bond satisfies the condition for a zero in the  $I/I_0$  function and is pumped at that frequency, the excited bond will shift in frequency to the red and eventually drop into the sub-Debye-cutoff region where it is rapidly quenched into the lattice modes. Thus, while one might expect efficient pumping of certain types of high frequency adatom-surface bonds up to low bond energies, desorption is not predicted to occur unless the laser intensity approaches the order of  $I_0$ .

[1] W.C.Murphy and T.F.George, *Surface Sci.* 102, L46, (1981).

[2] F.O.Goodman, *Surface Sci.* 109, 341 (1981).

Second Harmonic Generation Spectroscopy of  
Molecules Adsorbed on Oxide Surfaces

N. E. Van Wyck, E. W. Koenig, J. D. Byers, Z. Z. Ho and W. M. Hetherington  
Department of Chemistry, University of Arizona, Tucson, Arizona 87521

The observation and analysis of surface second harmonic generation (SHG) phenomena by Shen and coworkers (1) suggest that SHG spectroscopy is an effective interface - specific approach to detecting electronic spectra of surface and interfacial species. Since SHG is only possible in regions lacking inversion symmetry, the interface between two such materials will be the only source of an SHG signal. If a dye laser beam at frequency  $\omega$  is focused upon this interface and the harmonic at  $2\omega$  is monitored as the laser is scanned in frequency, then an electronic spectrum of interfacial species can be generated because of the great enhancement of the second order susceptibility,  $\chi^{(2)}$ , when  $2\omega$  concides with an electronic transition. In this way, spectra of species at solid-solid, solid-liquid, solid-vapor, liquid-liquid and liquid-vapor interfaces can be considered.

A surface SHG spectrometer has been constructed based upon a dye laser synchronously pumped by a frequency-doubled, mode-locked and Q-switched Nd:YAG laser. An important feature of the apparatus is a computer-controlled KDP crystal which is used to frequency double a small portion of each dye laser pulse for accurate normalization purposes. For studies of vapor phase molecules adsorbed onto solid surfaces and of chemically modified surfaces, a high vacuum environment is maintained. Surfaces are cleaned by ion sputtering and examined with Auger spectroscopy. Better resolution of the vibrational structure of electronic transitions is achieved by cooling samples to 77K.

A number of aromatic molecules such as fluorene, carbazole and benzene derivatives have been studied on  $\text{SiO}_2$ ,  $\text{ZnO}$ ,  $\text{TiO}_2$  and  $\text{Al}_2\text{O}_3$  surfaces. SHG spectra in the UV region of small metal clusters on  $\text{SiO}_2$  surfaces have also been observed.

1. C. K. Chan, T. F. Heinz, D. Ricard and Y. R. Shen, Phys. Rev. B., 27, 1965 (1983).

PHOTOCHEMICAL DEPOSITION OF Sn FOR IN-SITU SELECTED AREA DOPING  
OF MBE GaAs (001)Steven P. Kowalczyk and D.L. Miller  
Rockwell International Corporation  
Microelectronics Research and Development Center  
Thousand Oaks, CA 91360

Ultraviolet (UV) initiated microchemistry has recently emerged as a possible new technique in microfabrication for solid-state electronic applications.<sup>1-3</sup> Much of the recent research has centered on delineated deposition of metals by UV photolysis.<sup>4</sup> One intriguing possibility that this capability opens up is that of selected area doping in conjunction with molecular beam epitaxy (MBE) technology.

In brief, the proposed selected area doping scheme consists of (1) MBE growth of GaAs epilayer on a cleaned GaAs (001) substrate, (2) adsorption of several monolayers of a dopant containing molecule on the epilayer surface, (3) UV irradiation of selected areas of the wafer for photolytic decomposition of the dopant molecule, (4) thermal desorption of the nondecomposed doping containing molecule from the unirradiated areas of the wafer, and (5) regrowth of GaAs for incorporation of the dopant.

However, before such a process can be implemented many fundamental aspects relating to basic mechanisms of the above steps must be clarified. In this paper we investigate the possibility of Sn doping of MBE GaAs (001) by UV photolytic deposition. The Sn sources evaluated were tetramethyltin Sn (CH<sub>3</sub>)<sub>4</sub> and stannic chloride SnCl<sub>4</sub>. The adsorption and desorption properties of these molecules on GaAs (001) were studied in-situ in the MBE system by Auger electron spectroscopy (AES). The Sn dopant incorporation was determined by electrolytic capacitance-voltage (C-V) carrier and secondary ion mass spectrometry (SIMS) profiling. The UV photodeposition of Sn was studied by x-ray photo-electron spectroscopy (XPS).

The AES studies of the room temperature adsorption of tetramethyltin on GaAs (001) showed that several monolayers of the molecule were adsorbed. Thermal treatment up to ~ 300°C did not have much effect on the adsorbate. At temperatures above this, the tetramethyltin began to pyrolytically decompose such that above ~ 520°C, the C/Sn ratio as determined by AES had decreased by a factor of ~ 4 while the Ga/As and Sn/Ga ratios remained essentially constant. GaAs was regrown on this surface and the C-V carrier profile exhibited the exponential profile for the carrier concentration expected from Sn incorporation from the surface. In separate experiments, UV photolysis of Sn(CH<sub>3</sub>)<sub>4</sub> with either Xe or Hg radiation over etched GaAs surfaces was studied ex-situ by XPS. XPS showed that tin films which were highly contaminated with carbon were deposited.

The experiments with stannic chloride yielded somewhat different results. The in-situ AES measurements also showed several monolayer adsorption at room temperature, but with no carbon or oxygen contamination. The Sn/Ga ratio at ~ 100°C decreased by a factor of ~ 3 from the initial room temperature value and then remained constant to ~ 580°C. At ~ 300°C the SnCl<sub>4</sub> had been pyrolyzed with no Cl detected. Dopant profiles from GaAs regrowth

over this surface showed that Sn was incorporated as a dopant. XPS measurements showed the formation of tin films from the UV photolysis with Hg irradiation. Preliminary measurements from thin tin films indicate that some photochemical etching may occur at the interface with excited chlorine reacting at the surface to form  $\text{GaCl}_3$ .

These results have shown that (1) MBE GaAs can be doped with a vapor phase source, (2) Sn can be UV photolytically deposited from  $\text{Sn}(\text{CH}_3)_4$  and  $\text{SnCl}_4$ , (3)  $\text{Sn}(\text{CH}_3)_4$  and  $\text{SnCl}_4$  to a lesser extent, pyrolyze before desorption, which may limit their practical usefulness in a selected area doping process and (4) complicated interface interactions occur upon adsorption, desorption and pyrolysis which must be understood before practical applications can be undertaken.

#### Acknowledgment

This work was supported by the Army Research Office, Research Triangle, N.C.

#### References

1. D.J. Ehrlich, R.M. Osgood and T.F. Deutsch, IEEE QE 16, 1233 (1980).
2. R.M. Osgood, Ann. Rev. Phys. Chem. 34, 77 (1983).
3. D.J. Ehrlich and J.Y. Tsao, J. Vac. Sci. Technol. B1, 969 (1983).
4. e.g., see references in 1-3.

"LARGE MODIFICATION OF THE SURFACE ENHANCED RAMAN SCATTERING OF PYRIDINE ON Ag SURFACES BY Pd SUBMONOLAYERS".

T. Lopez-Ríos, Y. Gao

Laboratoire d'Optique des Solides, ERA CNRS n° 462,  
4 place Jussieu 75230 Paris Cedex 05, France.

It is known that SERS is partially due to localized surface plasmons and consequently can be only observed on metals supporting this electromagnetic excitation. It is also known that the surface chemical bonding of the molecule involved on the Raman process is relevant for SERS.

In this communication we investigate, in ultra hight vacuum, the modifications induced by Pd submonolayers on the SERS of pyridine on quenched or island Ag films. The Pd superficial deposits do not modify the electromagnetic properties of the surface but only the chemical environment. By coadsorbing Pd with pyridine we get information about the chemical part of SERS. We found that the SERS of pyridine on Ag surfaces is strongly reduced by very thin Pd deposits. For quenched Ag films exposed to 3 Langmuirs (uncorrected) of pyridine, the SERS intensity is reduced by a factor of 30 when one half monolayer of Pd is deposited on the surface. Not appreciable increasing of the Raman signal is observed when the surface is reexposed to pyridine. We present results showing unambiguously that Pd deposits prior to pyridine exposures destroy the surface enhacement characteristics of the free Ag surface. Complementary Auger and optical investigations will be also presented and the nature of the active sites discussed. Discussion of equivalent experiments for fluorescence of dye molecules will be also presented.

Doppler Shift Laser Fluorescence Spectroscopy of  
Sputtered and Evaporated Atoms under Argon Ion Bombardment.

W. Husinsky, G. Betz and I. Gergis

Institut für Allgemeine Physik, Technische Universität Wien,  
Karlsplatz 13, A-1040 Wien, Austria

Doppler Shift Laser Fluorescence Spectroscopy DSLFS with cw., single mode, tunable dye lasers is an excellent tool to study particles released from surfaces during the interaction of atoms and ions with solids /1,2/. From energy distributions of sputtered particles obtained by DSLFS, the mechanism for the particle release can be derived in many cases /2,3/. In particular, nonlinear and inelastic effects in sputtering have been investigated extensively in recent publications /2,4,5/. In this paper we present measurements of energy and state distributions of Ca, Cr and Zr atoms released from the respective metal targets under 15 keV Argon ion bombardment. The influence of the target temperature and the oxygen concentration on the surface has been studied.

Recently the problem of nonlinear effects in sputtering at high target temperatures has caused some discussion /6,7/. In particular the question has been raised, whether Ion Beam Enhanced Evaporation exists and can lead to (in some cases quite reasonable) enhanced sputtering yields. If existing, additional thermal contributions to the sputtering yield can easily be identified in the energy spectra of the sputtered atoms as low energy peaks. We have measured the energy distribution of Ca atoms from room temperature up to about 250°C and for Cr atoms from room temperature up to 600°C for Argon ion bombardment. Atoms evaporated at higher temperatures could be discriminated against those due to ion beam bombardment by using a Lock-In technique. In both cases no increased sputtering yields at high temperatures could be observed. The energy distributions do not show any sputtering contributions but elastic cascades. However, at 200°C for Ca and at about 500°C for Cr strong evaporation can be observed. The energy distribution of these atoms is Maxwellian.

The influence of the surface composition can be very drastic in regard to the type, energy and state distribution of sputtered products /2,4,5,8/.

Impurity free surfaces in general yield sputtered atoms in the electronic ground state. The contribution of excited atoms and ions is below 5%. For surfaces with oxygen impurities the yield of excited atoms and ions can be enhanced up to one order of magnitude. Furthermore, for many target materials the amount of sputtered ground state atoms is strongly reduced.

Measurements of Cr and Zr ground state atoms are presented. Up to a certain oxygen concentration the yield of sputtered ground state atoms is relatively constant. Then for increasing oxygen concentration a drastic decrease is observed. For Cr this decrease is greater than a factor 100. For Zr we have measured the ground state and the first excited level of the ground state multiplet. Both levels show a decreased population at increased oxygen concentrations during sputtering. The results for the sputtering yields of these discrete levels are compared with measurements of the total sputtering yield of the metals for different oxygen concentrations on the target surface.

- /1/ W. Husinsky, R. Bruckmüller and P. Blum, Nucl. Instr. Meth. 170 (1980) 199
- /2/ W. Husinsky, G. Betz and I. Gergis, Phys. Rev Lett. 50,21 (1983) 1689
- /3/ W. Husinsky, and R. Bruckmüller, Surf. Sci. 80 (1979) 637
- /4/ W. Husinsky, G. Betz and I. Gergis, J. Vac. Sci. Technol. A2 (2) Apr.-June 1984
- /5/ D. Grischkowsky, M.L. Yu and A.C. Balant, Surf. Sci. 127 (1983) 315
- /6/ K. Besocke, S. Berger, W.O. Hofer and U. Littmark, Rad. Eff. 66 (1982) 383
- /7/ M. Szymonski, Nucl. Instr. Meth. B2 (1984) 583
- /8/ W. Husinsky, G. Betz, I. Gergis and F. Viehböck, to be published in Nucl. Mat.(Dec. 1984)

## **SESSION IX**

**E. Wolfe, *Presider***  
**Cornell University**

## ATOMIC-RESOLUTION DYNAMICS BY ELECTRON MICROSCOPY

David J. Smith, Center for Solid State Science and Department of Physics, Arizona State University, Tempe, AZ 85287, USA.

Latest developments in high-resolution electron microscopes (HREMs) have made it possible to obtain localised real-space information on the atomic scale which has resulted in major insights into many important materials problems [1]. The HREM technique has also recently been shown to be applicable to the characterisation of surfaces in profile and initial surface studies of gold, catalysts and semiconductors have been very interesting.

Novel and unexpected information about the morphology of gold surfaces, including atomic arrangements and rearrangements has been obtained. After removal of a carbonaceous surface layer by electron-beam-induced etching in the presence of water vapour, the (111) surface was found to expand outwards, developing a hill-and-valley morphology with surface dislocations also visible [2]. In contrast, the (110) surfaces were generally observed to be microscopically rough whereas surface features on (100), including dislocations, were highly mobile, particularly in the presence of surface steps which markedly influenced the overall direction of surface diffusion [3].

The projection method has also been applied to small metal particles (akin to those found in heterogeneous catalysts) and direct atomic imaging of a reconstructed metal surface has been achieved for the first time in a TEM [4]. Surface features

including steps, facetting and surface reordering have been imaged in catalytically active ferrite spinels [5] and surface decoration of alumina particles by columns of aluminum atoms and other ruthenium metal clusters has also been demonstrated [6].

Extensive surface rearrangements were also observed during studies of the semiconductor material cadmium telluride [7]. Although these studies were limited in resolution to about  $3\frac{1}{2}\text{\AA}$ , the results again confirmed that the profile imaging technique has great potential for characterising the surfaces of semiconductors. Note that these are of particular interest since it is already known from other techniques that, compared to bulk structure, many semiconductors have different, or "reconstructed" surface structures. However, it should be appreciated that improvements in specimen cleanliness and general EM vacuum will probably be required before useful quantitative information can be obtained.

#### REFERENCES

- [1] D.J. Smith (1983), *Helvetica Physica Acta* 56, 463.
- [2] L.D. Marks & D.J. Smith (1984), *Surface Science* 143, 495.
- [3] D.J. Smith & L.D. Marks (1984), *Ultramicroscopy*, in press.
- [4] L.D. Marks & D.J. Smith (1983), *Nature* 303, 316.
- [5] N.A. Briscoe & J.L. Hutchison (1984), *Proc EMAG 1983*, p. 249.
- [6] S. Iijima (1984), *Japan. J. Appl. Phys.* 23, L347.
- [7] R. Sinclair, T. Yamashita & F.A. Ponce (1982), *Nature* 290, 386.

## Excimer Laser Etching and Oxidation of Silicon

Y.HORIIKE, M.SEKINE, K.HORIOKA, T.ARIKADO, M.NAKASE AND H.OKANO  
Toshiba VLSI Research Center,  
Komukai-Toshibacho 1, Saiwaiku, Kawasaki, Japan

In previous report, an anisotropic etching of undoped poly-Si by a Hg-Xe lamp or a XeCl excimer laser in a  $\text{Cl}_2$  gas was demonstrated. However,  $n^+$  Poly-Si, which is currently used as a gate material in MOS devices, is etched isotropically by photo-dissociated Cl radicals(1). For the LSI application, the anisotropic etching for  $n^+$  Poly-Si should be also achieved.

A XeCl excimer laser (308nm) is irradiated normally to the  $n^+$  poly-Si sample which is set in a vacuum chamber introduced by a  $\text{Cl}_2 + \text{Si}(\text{CH}_3)_4$  mixture gas. The collisional reaction between  $\text{Cl}^*$  and  $\text{Si}(\text{CH}_3)_4$  dissociates the  $\text{Si}(\text{CH}_3)_4$  gas to deposit a nonvolatile film on the surface. On the other hand, the surface consisting of the film over the poly-Si is etched by the laser irradiation. Thus, the film remains on the etched sidewall to protect the Cl radical attack. Figure 1 shows variations of etch rates, deposition rates and etched features as a function of  $\text{Cl}_2 + \text{Si}(\text{CH}_3)_4$  total pressure. With increasing total pressure, both rates increase and the undercutting is reduced. At 30 torr, the anisotropic feature is attained successfully. Then, the deposition occurs rapidly, in contrast with the etch rate drop. The etch rate ratio of poly-Si to underlying  $\text{SiO}_2$  is infinite in this method. It offers an advantage for submicron VLSI with very thin gate oxide(2).

The radiation damages induced by ArF and XeCl laser irradiations were also investigated using MOS capacitors. The ArF laser was irradiated only after the down-flow type plasma etching (CDE) of  $n^+$  poly-Si. The ArF irradiation indicates considerably larger flat-band voltage shift after the charge injection than that in both XeCl and CDE. The ArF(6eV) damage may be due to the O-H bond breaking by a light invading into the oxide from the periphery. Hence, various higher energy photon effects to the devices have to be noted.

In the course of the single-Si etching study under the XeCl excimer laser in a  $\text{Cl}_2$  gas, the oxide film growth on the Si surface has been found when a  $\text{O}_2$  gas is added to the  $\text{Cl}_2$  gas. The photo-oxidation does not take place until the native oxide is removed by a BHF solution. Therefore, the Si surface, which is not masked by the thermally grown oxide, is easily oxidized. The Auger analysis of this film demonstrates a stoichiometric  $\text{SiO}_2$ .

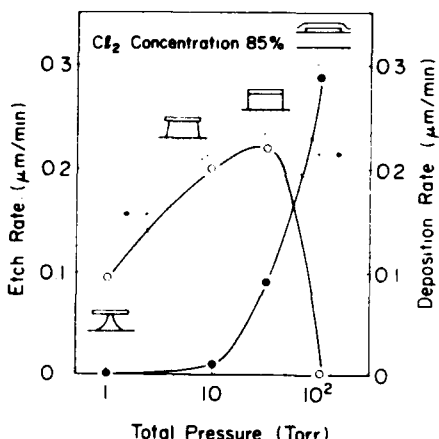


Fig.1  $n^+$  poly-Si etch rate and deposition rate vs.  $\text{Cl}_2 + \text{Si}(\text{CH}_3)_4$  total pressure.

Figure 2 shows variations of Si(100) etched depth,  $\text{SiO}_2$  growing thickness and photo-oxidized features as a function of  $\text{O}_2$  pressure at  $250^\circ\text{C}$ . With increasing  $\text{O}_2$  pressure, the Si etch rates decrease, while the Si substrate is photo-oxidized rapidly. The result suggests that the Si etching products become the  $\text{SiO}_2$  source. On the other hand, although the photo-oxidation was tried employing  $\text{SiCl}_4 + \text{O}_2 + \text{Cl}_2$ , the oxidation rate more than  $5\text{A}/\text{min}$  was not obtained. Thus, the unsaturated Si chlorides of  $\text{SiCl}_x$  ( $x=1\sim 3$ ) are presumed to have more active chemical reactivity than the stable  $\text{SiCl}_4$ . Since the adequate oxygen pressure leads to the successfully buried oxide to the Si substrate, the method is expected as a new field isolation technique. However, the BHF etch rate for the present oxide even after  $800^\circ\text{C}$  annealing is 4 times faster than that for the thermal  $\text{SiO}_2$ . The film structure, which is assumed to be porous, should be improved (3).

Recently, in order to realize the pattern transfer(4), the small-scaled reflective type optical system has been developed as shown in Fig.3. The NA value of this system is 0.17. A  $\text{XeCl}$  laser coherency is reduced by a flyeye lens. The image pattern is not scanned. In the resist patterning, the  $1.2\mu\text{m}$  resolution can be attained at 10 sec. exposure time (80 pulses). At present, a fine resistless etching of poly-Si is not be obtained. Problems related to the optical system and the low contrast due to the present low reaction rate are still remain.

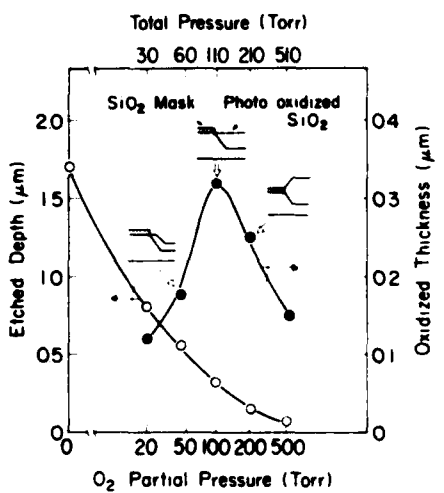


Fig.2 Si(100) etched depth, Si photo-oxidized thickness and their crosssections vs.  $\text{O}_2$  partial pressure.

Recently, in order to realize the pattern transfer(4), the small-scaled reflective type optical system has been developed as shown in Fig.3. The NA value of this system is 0.17. A  $\text{XeCl}$  laser coherency is reduced by a flyeye lens. The image pattern is not scanned. In the resist patterning, the  $1.2\mu\text{m}$  resolution can be attained at 10 sec. exposure time (80 pulses). At present, a fine resistless etching of poly-Si is not be obtained. Problems related to the optical system and the low contrast due to the present low reaction rate are still remain.

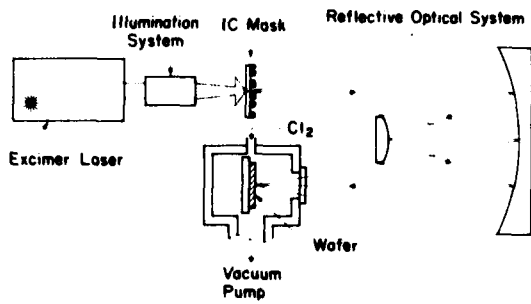


Fig.3 Perkin-Elmer type reflective optical pattern transfer system.

#### Reference

- (1) M.Sekine, H.Okano and Y.Horiike; Proc. 5th Symp. Dry Precesses. Inst. Electr. Eng., Tokyo, p.97 (1983)
- (2) H.Okano, M.Sekine and Y.Horiike; Digest of Tech. Papers 1984 Symp. on VLSI Technol., p.74 (1984)
- (3) K.Horioka, H.Okano and Y.Horiike; 16th Conf. on Sol. St. Device and Materials (Kobe), Late News Abstr. LD-7-1, p.50 (1984)
- (4) T.Arikado, M.Sekine, H.Okano and Y.Horiike, Mat. Res. Soc. Fall Meeting Abs. I9.5, 408 (1983)

## EFFECTS OF OPTICAL PROPERTIES ON WET ETCHING OF SEMICONDUCTORS

D.V.Podlesnik, H.H.Gilgen, C.J.Chen and R.M.Osgood Jr.

Department of Electrical Engineering  
Columbia University ,New York, N.Y. 10027

Many laser microchemical processes, for example, metal photodeposition and semiconductor annealing, are influenced by a surface electromagnetic field which results from the interaction of the incident light with the surface. This effect has not been extensively documented in laser etching of semiconductors. In this talk, we will show that such effects can play an important role in determining the etch profile and surface structure obtained from wet etching of semiconductors. In particular, the formation of surface ripples and the fabrication of high- aspect-ratio via holes will be discussed.

As reported earlier<sup>1</sup>, 257-nm light initiates a rapid etching of GaAs by generating nonthermalized holes in the semiconductor. The UV photon induces an electron transition in the X-band edge of the Brillouin zone which creates the hot holes. This transition also changes the optical properties of the crystal; at this wavelength the GaAs surface then acts like a metal<sup>2</sup>. A similar optical behavior has been observed for other semiconductors with zinc-blende and diamond crystal structure, e.g. Si and InP.

Ripple morphologies have been observed in many laser-driven processes. We observed the formation of surface ripples on Si , GaAs and InP during laser-induced wet etching, at a power density  $< 1\text{ kW/cm}^2$ . As Fig. 1 demonstrates for Si etched in a dilute HF solution, the ripples are well-defined and pronounced. In all cases, including the ripples in GaAs and InP, the characteristic grating structure of  $0.2\text{ }\mu\text{m}$  is aligned perpendicular to the direction of laser polarization. The ripple formation can be explained by the plasma oscillation model<sup>3</sup>.

In the second part of this talk, we will discuss the influence of the optical characteristics of the semiconductor on the formation of via holes in GaAs and Si. Deep-UV laser etching permits micrometer-wide vias through a  $100\text{-}200\mu\text{m}$  wafer. The remarkable feature of these vias is their high aspect ratio and perfectly vertical walls. Study of the via hole

development during etching showed that the etch rate increases  $\sim 4$  times at a depth of  $\sim 5\mu\text{m}$ . Experiments which include measurements of the polarization and intensity of the transmitted light as a function of the hole diameter indicate that the vias behave like a metallic hollow waveguide. This effect can be related to the ultraviolet optical properties of GaAs and Si.

- 1) D.V. Podlesnik, H.H. Gilgen, and R.M. Osgood, Jr., *Appl. Phys. Lett.* **45**, 563 (1984).
- 2) H.R. Phillip and H. Ehrenreich, *Phys. Rev.* **129**, 1550 (1963).
- 3) S.R.J. Brueck and D.J. Ehrlich, *Phys. Rev. Lett.* **48**, 1678 (1982).

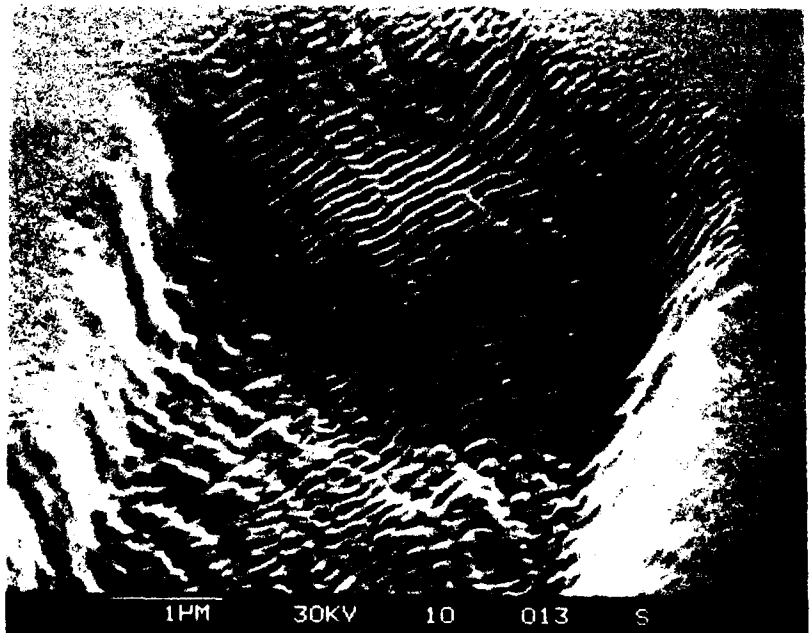


Fig. 1. Scanning electron micrograph of a surface ripple produced during wet etching of Si in a dilute HF solution.

## TRANSIENT NONLINEAR LASER HEATING AND DEPOSITION: A COMPARISON OF THEORY AND EXPERIMENT

J. A. Goldstone and S. D. Allen  
Center for Laser Studies, University of Southern California  
Los Angeles, CA 90089-1112

The deposition rate and deposit resolution in laser chemical vapor deposition (LCVD) and other laser induced chemical processes at surfaces are a function of a large number of variables including: the laser generated surface temperature profile, the local reactant concentration distribution, the substrate and deposited film characteristics and the reaction kinetics. Most laser generated temperature profile calculations to date have assumed steady state behavior and/or neglected the nonlinear temperature dependent thermal properties of the substrate. In addition, most theoretical models neglect the changing surface reflectivity as the film is deposited. Equilibrium calculations, while useful for high thermal conductivity materials such as Si and metals, are inadequate for low thermal conductivity materials such as fused quartz where characteristic reaction times are considerably shorter than the time necessary to reach thermal equilibrium.

We have created a numerical integration scheme which treats the dynamic behavior of thermally driven laser processes such as laser CVD, etching, damage and annealing. Included in the model are a substantial number of experimentally significant parameters. The input intensity distribution may have an arbitrary spatial variation and the substrate may have either a finite or semi-infinite thickness. Substrate thermal parameters are locally temperature dependent and are modeled to match experimentally determined substrate characteristics. The surface reflectivity and, therefore, the energy absorbed from the laser, is a function of the locally deposited film thickness. The deposition thickness profile, in turn, is obtained by integration of the temperature dependent deposition rate.

The model produces surface and depth temperature distributions as well film thickness profiles as functions of time. An example of our results for the temperature distribution obtained in Ni LCVD from  $\text{Ni}(\text{CO})_4$  on fused quartz substrates with a cw gaussian input beam is given in Fig. 1. The flattening of the surface temperature distribution is due to the increase in reflectivity of the central portion of the irradiated area as the film is deposited. As shown in the Fig 1b., the on-axis temperature ultimately declines. The effects of a spatially dependent reactant concentration, which would tend to decrease and broaden the deposition thickness profile, have been neglected in these initial results.

Experimental deposition initiation time and rate were determined as a function of irradiation time and intensity using optical monitoring. The thickness of metal films deposited on fused quartz substrates using a  $\text{CO}_2$  laser heat source was

measured using a collinear He-Ne beam as a thickness monitor. Using the Fresnell equations, the deposition rate as a function of time was calculated from the measured transmission curves. After the laser is turned on, no deposition takes place until the surface reaches the minimum deposition temperature. The deposition rate increases up to a film thickness of approximately 50 Å, where significant laser energy is being reflected.

A comparison of theoretical and experimental results will be presented for a number of substrates and film/substrate combinations. In addition to the prediction of deposition rates and deposit or etching resolution, such comparisons should allow a more accurate determination of material parameters, e.g., substrate absorptivity and heterogeneous reaction kinetics.

This work was funded in part by the Department of Energy (Basic Energy Sciences) and Kodak Corporation.

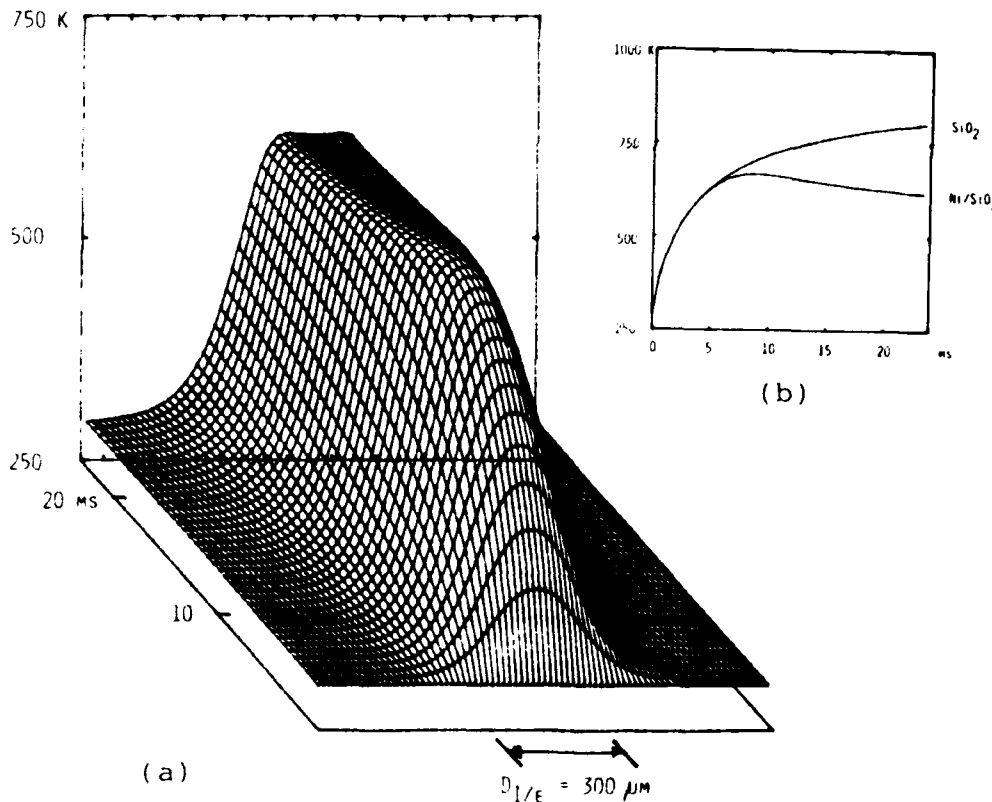


Fig. 1. Temperature of  $\text{Ni/SiO}_2$  surface for an incident laser power,  $P = 1 \text{ W}$ ;  $D_{1/e} = 300 \mu\text{m}$ . a) Surface temperature distribution as a function of irradiation time with Ni deposition. b) Axial surface temperature with  $(\text{Ni/SiO}_2)$  and without  $(\text{SiO}_2)$  deposition.

## KEY TO AUTHORS AND PAPERS

Ai, C. F. — TuA3  
Allen, S. D. — WD4  
Ameen, M. S. — MA1  
Arikado, T. — WD2  
Aspnes, D. E. — WC2  
Avouris, Ph. — MB1  
Avouris, Phaedon — WB4  
Baiker, A. — MC1  
Balooch, M. — MB2  
Bares, S. J. — TuB2  
Barish, E. L. — MA1  
Beri, A. C. — WC8  
Betz, G. — WC13  
Bjorkholm, J. E. — MB6  
Brewer, Peter D. — TuC5  
Bunding, K. A. — WA3  
Burgess, D. R., Jr. — WC6  
Byers, J. D. — WC10  
Campion, Alan — MC2  
Casassa, M. P. — WA4  
Cavanagh, R. R. — WA4  
Chen, C. J. — WD3  
Chu, Jack O. — TuC5  
Chuang, T. J. — TuA1, WC4  
Coburn, John W. — MA2  
Cole, H. C. — TuC4  
Craighead, H. G. — MB6  
Deckman, H. W. — WC1  
Dickinson, J. T. — MB3  
Diestler, Dennis J. — WC9  
Drake, J. M. — WB3, MC5  
Dreyfus, R. W. — MB5  
Dulcey, C. S. — WC5  
Ehrlich, D. J. — WC3, TuB4  
Eichner, L. — MB6  
Fleming, C. G. — TuC3  
Fluhr, W. — MC1  
Flynn, George W. — TuC5  
Fortenberry, R. M. — MC3  
Gao, Y. — WC12  
Garoff, S. — WC1  
Garrison, Barbara J. — MB4  
George, Thomas F. — WC8, WC7  
Gilgen, H. H. — WD3  
Girgis, I. — WC13  
Goldberg, L. S. — WA3  
Goldstone, J. A. — WD4  
Haigh, J. — TuC2  
Hall, R. B. — WC1, TuB2  
Heilwell, E. J. — WA4  
Heinz, T. F. — WA2  
Hetherington, W. M. — WC10, MC3  
Higashi, G. S. — TuC3  
Hirose, Masataka — TuB5  
Ho, Z. Z. — MC3, WC10  
Hoffmann, F. M. — MC4  
Horike, Y. — WD2  
Horloka, K. — WD2  
Howard, R. E. — MB6  
Huang, Xi-Yi — WC7  
Husinsky, W. — WC13  
Irvine, Stuart — TuC1  
Jasinski, J. M. — MB5  
Jedrzejek, C. — TuB1  
Klafter, J. — WB3  
Koenig, E. W. — MC3, WC10  
Kowalczyk, Steven P. — WC11  
Lambert, D. K. — WB2  
Levinson, L. M. — TuC4  
Lin, Jui-teng — WC7, TuB3  
Lin, M. C. — WC5  
Liu, Wu — TuA3  
Liu, Y. S. — TuC4  
Lopez-Rios, T. — WC12  
Loudiana, M. A. — MB3  
Loy, M. M. T. — WA2, WB1  
Mayer, T. M. — MA1  
Meier, M. — MC1  
Miller, D. L. — WC11  
Miller, S. K. — MC1  
Misewich, J. — WB1  
Mizutani, T. — MA1  
Moshrefzadi, R. — MC3  
Nagumo, M. — WA3  
Nakase, M. — WD2  
Okano, H. — WD2  
Olander, D. R. — MB2  
Osgood, Richard M., Jr. — TuC5, WD3  
Philipp, H. R. — TuC4  
Podlesnik, D. V. — WD3  
Pons, B. Stanley — TuA2  
Riley, Merle E. — WC9  
Rothberg, L. J. — TuC3  
Sanders, F. H. M. — MA3  
Sekine, M. — WD2  
Sesselmann, W. — WC4  
Shen, Y. R. — WA1  
Siekhams, W. J. — MB2  
Smith, David — WD1  
Squire, D. W. — WC5  
Srinivasan, R. — MB4  
Stair, P. C. — WC6  
Stegeman, G. I. — MC3  
Stephenson, J. C. — WA4  
Thompson, W. A. — WA2  
Tsao, J. Y. — WC3, TuB4  
Tsong, T. T. — TuA3  
Van Wyck, N. E. — WC10, MC3  
Viswanathan, R. — WC6  
Vitkavage, D. J. — MA1  
Voss, D. F. — WA3  
Walkup, R. — MB1, MB5  
Walther, H. — WB5  
Weitz, E. — WC6  
White, J. C. — MB6  
Winters, Harold F. — MA2  
Wokaun, A. — MC1  
Yakymyshyn, C. P. — TuC4  
Zacharias, H. — WB1  
Zeiger, H. J. — TuB4



D T T C

7 - 86